Universidad de Navarra

Facultad de Medicina

Identification of novel therapeutic strategies for Alzheimer's disease

Marta Pérez González

Pamplona, 2019

Universidad de Navarra

Facultad de Medicina

Identification of novel therapeutic strategies for Alzheimer's disease

Memoria presentada por Dª Marta Pérez González para aspirar al grado de Doctor por la Universidad de Navarra.

VºBº de las directoras del trabajo:

Dra. Mar Cuadrado Tejedor **Dra. Ana García Osta**

Pamplona, Septiembre 2019

There is no darkness but ignorance

William Shakespeare

A mamá y Salva

A Josh

Hace poco tiempo, recordaba con mi madre mi llegada a Pamplona, nos acordábamos del abrazo que nos dimos fuera del portal del que iba a ser mi nuevo hogar y cómo me quedaba ahí llorando mientras veía como se volvían a casa dejándome ahí sola. Lloraba porque no sabía que iba a ser de mi lejos de mi Asturias del alma, de mi familia, de mis amigos…Lloraba sin saber que ese día comenzaba una de las mejores etapas de mi vida. El año del máster se convirtió finalmente en 5 años en Pamplona, 5 años que van llegando a su final y de los que es el momento de despedirse y agradecer a todas las personas que en mayor o menor medida han formado parte de esta importante etapa de mi vida.

Ante todo, me gustaría agradecer a la Asociación de Amigos de la Universidad de Navarra por haberme dado la oportunidad económica de realizar esta tesis doctoral. Así mismo, agradecer al CIMA y la Universidad de Navarra que me hayan permitido no solo desarrollarme como científica sino también iniciarme como docente.

Y todo esto no hubiese sido lo mismo si no hubiese decidido realizar el TFM en el laboratorio de "Neurobiología de la Enfermedad de Alzheimer", ya que, aunque ahora le hayan cambiado el nombre, para mí siempre se va a llamar así. No me cabe la menor duda de que no pude haber elegido mejores jefas: Mar y Ana, el dúo perfecto. Podría decir que además de jefas, gracias a vuestra infinita cercanía, os habéis vuelto como mi familia de Pamplona, siendo un referente y apoyo para mí. No puedo más que agradeceros todo lo que me habéis ayudado a crecer, no solo como profesional sino también como persona. Mar, a ti quiero agradecerte que siempre estés con esa sonrisa en la cara, dándome la tranquilidad de que pase lo que pase te lo puedo contar con la certeza de que no voy a recibir más que calidez y comprensión de tu parte. Gracias además por haber confiado en mí y haberme impulsado a implicarme más en las clases de anatomía, algún día me gustaría ser capaz de hacer lo que tú haces. Ana, muchísimas gracias por haberme enseñado tanto, por incitarme a leer más y a tratar de pensar por mí misma, haciéndome comprender que uno no se puede conformar y debe dar el máximo de sí. Gracias por todas esas tardes en el laboratorio mano a mano, donde una pregunta se convierte en media hora buscando información en tu ordenador. Aunque sé que estás mucho más tranquila sola, echaré de menos esos momentos. A las dos, me gustaría además agradeceros que me hayáis dado este magnífico proyecto que, aunque tortuoso en algunos momentos, me ha recordado que me encanta la ciencia por más ingrata que sea a veces. Por más que consiga participar en nuevos proyectos, la PLA2G4E siempre estará en mi corazón, al igual que vosotras. Por último, también os quiero pedir perdón y agradeceros la paciencia que estáis teniendo estos últimos meses conmigo, ya que el estrés que me está generando esta tesis le está jugando malas pasadas a mi carácter. ¡MIL GRACIAS JEFAS!

No me olvido del resto de miembros del laboratorio. Gracias mi Susi, tanto por tu infinita paciencia en el labo, como por tu amistad, por esas comidas en el Dublin, en fin, por todo. Gracias María, gracias por estar siempre dispuesta a enseñar y ayudar. A ti Alberto, decirte que se echará de menos tu buen humor y tus estornudos escandalosos. A los que ya no están, especialmente Elenit. Gracias por ayudarme a todo y sobre todo por ser tan dulce como eres, te echo de menos. A Carol, gracias por iniciarme en el mundo del comportamiento y enseñarme todo lo que sabías, al igual que Cristina y Damián, que se molestaron en ayudarme cuando llegue al labo sin saber apenas nada. Gracias también a Sara, Dani y todos los alumnos que han pasado por el laboratorio dejando pequeños granitos de arena en esta tesis.

Me gustaría agradecer especialmente a dos compañeros del CIMA, Diego e Iván, siempre dispuestos a ayudar y colaborar con nosotras. Gracias Diego, tu ayuda con los virus ha

sido de un valor incalculable para esta tesis. Y a ti Iván, gracias por ayudarme, escucharme y aconsejarme en todo lo que puedes.

Gracias al laboratorio de Julen Oyarzabal: Obdulia, Juan…sin su colaboración el proyecto de los duales no sería posible.

A special acknowledgement is for Professor Marina Lynch and her team. She kindly hosted me in her lab and helped me with everything I need. She offers me the amazing opportunity to learn a lot about research in neuroinflammation, to improve my English and to meet amazing people. I would like to specially thank Ana, who nicely teach me everything I needed. And also Virginia, who became a friend outside the lab. Thank you very much!

Gracias también al Dr. Rafael Luján y a su equipo por ayudarnos con la microscopía electrónica.

Todo este camino no habría sido lo mismo sin vosotros, los amigos que Pamplona ha puesto en mi camino, empezando por los del máster y terminando por huérfanos. No os podéis imaginar lo importantes que habéis sido para mí y lo mucho que os voy a echar de menos. Las tardes con vosotros en Pío siempre estarán en mi corazón. ¡Os quiero!

No podía olvidarme de las mejores compañeras de piso que se puede tener. Sil, ¿qué nos deparará el futuro? Seguro que será algo de lo que ya hayamos hablado en nuestras reuniones improvisadas en la mesa de la cocina. Gracias por estar siempre dispuesta a escuchar mis comederos de cabeza y gracias por tus tantos consejos. ¡Te adoro! Y a ti, mi Marti, si algo bueno me llevo de Pamplona eso eres tú sin duda. Mi amiga, mi compañera. Quién me iba a decir después de aquel incómodo apretón de manos que te convertirías en alguien tan especial para mí. No tengo siquiera palabras para agradecerte todo lo que haces por mí, y la paciencia que tienes conmigo. Te quiero mucho y estemos donde estemos siempre voy a estar aquí para ti.

David, aunque has llegado a mitad de este camino, espero que continúes recorriéndolo conmigo día a día, creciendo y evolucionando juntos. No puedo más que agradecerte tu infinito cariño y paciencia. ¡Te quiero!

A mis amig@s de toda la vida, gracias por estar siempre ahí para mí, por preguntarme constantemente cómo me va en la tesis, esa que no tenéis muy claro ni siquiera de que va. Gracias, ¡os quiero!

Pero sobre todo gracias a mi familia y mi círculo más cercano. Gracias por ser ese ancla, por recordarme siempre quién soy y de dónde vengo. Por estar en las buenas y en las malas, os quiero mucho.

Gracias a ti mamá, gracias y perdón, gracias por habérmelo dado todo sin importar el sacrificio que eso suponía para ti, gracias por ayudarme con cosas que no te corresponden simplemente para que no sean una carga para mí, en definitiva, gracias por ser mi inspiración y ejemplo a seguir. Y perdón, perdón todos los sufrimientos y quebraderos de cabeza que te he dado a lo largo de los años. No tendré suficiente vida para pedirte perdón, pero espero que sí para hacer que te sientas orgullosa de mí y, aunque nuestros carácteres nunca vayan a ser compatibles, no tengas duda de que has criado una buena hija. ¡Te quiero más que a nada!

Salva, a ti tengo que agradecerte más que a nadie. Porque, aunque no tienes ninguna obligación conmigo, nunca has dejado de estar ahí para mí. Siempre me has ayudado en todo y te has sacrificado por mí como si de una hija más se tratase. Sabes que eres un pilar fundamental en mi vida ya que aparte de guiarme e inculcarme valores, siendo como un segundo padre para mí, también eres mi amigo. Gracias por todo y no me faltes nunca. ¡Te quiero!

Papá, muchas gracias por apoyarme constantemente, por estar ahí siempre para mí. Gracias por darme la tranquilidad de saber que mi abuelo está en buenas manos y permitirme hablar con el día tras día. ¡Te quiero mucho!

Abuelito, estar lejos de ti es una de las cosas que más duras se me hacen de estar aquí. Espero que, aunque no comprendas del todo mi decisión de estar lejos de casa, te sientas orgulloso de mí. Te quiero.

Lo mismo para ti abuelita, aunque te hayas ido sin haberme visto crecer y madurar, espero que puedas sentir orgullo de tu nieta. Siempre te querré.

A ti güela, muchas gracias por todo lo que haces por mí. Gracias por no quejarte nunca cuando te pido que me hagas más tupes o algún que otro capricho. Te quiero mucho.

Y a ti piqui, tú no te enteras y pasas de esto, pero espero que esta etapa me ayude a encontrar un buen trabajo para que el día de mañana te pueda ofrecer lo mismo que me han ofrecido a mi tus padres. ¡Te quiero!

Pero sobre todo, esta tesis quiero dedicártela y agradecértela a ti Joshlin. Esta vida a veces nos pone a prueba y se lleva a las mejores personas de nuestro lado antes de tiempo. Te fuiste en la recta final y no sé cómo va salir esto sin ti. No te puedes imaginar cómo echo de menos tus ¡qué quieres ya pesada! y aunque aún no soy del todo consciente de que ya no vas a estar ahí para mí nunca más, sé que me vas a estar guiando desde arriba. Sabes que no habría llegado hasta aquí sin tu ayuda, mi graduado en Biotecnología te lo debo en gran parte a ti, ya que sin tu sabiduría en informática nunca habría aprobado bioinformática. Y qué decir de las innumerables horas juntos al volante, en las que me demostrarte una y mil veces tu infinita paciencia; sabes que no sería capaz de coger un coche si no hubiese sido por ti. Gracias, gracias y gracias. Me quedo con todos los buenos momentos pasados a tu lado: las numerosas comidas, viajes y demás momentos vividos juntos. Espero que allí donde estés, puedas sentirte orgulloso de mí. Te quiero mucho y no dudes que siempre estarás presente en cada paso que dé Josh.

Con todo esto, solo me queda recordar esta maravillosa etapa y esperar a ver que nos deparará el futuro.

INDEX

ABBREVIATIONS

A

Aa: amino acids

Aβ: amyloid beta

AAV: adeno-associated virus

AC: adenilate cyclase

AD: Alzheimer's disease

AAD: asymptomatic Alzheimer's disease

AcH3K9: acetylated histone 3 at lysine 9

Ac-tubulin: acetylated tubulin

AICD: APP intracellular domain

AIDS: acquired immune deficiency syndrome

ALS: amyotrophic lateral sclerosis

AMP: adenosine monophosphate

APH-1: anterior pharynx defective 1

ApoE: apolipoprotein E

APP: amyloid precursor protein

APP_{swe}: APP containing the Swedish double mutation

Arg1: arginase 1

B

BBB: blood brain barrier

bp: base pairs

C

CAMKII: Ca^{2+}/calmodulin dependent kinase type II

cAMP: cyclic adenosine monophosphate

CDK5: cyclin-dependent kinase 5

CD11b: cluster of differentiation 11b

cDNA: complementary DNA

cGMP: cyclic guanosine monophosphate

CIMA: Center for Applied Medical Research

Cm: centimeter

CNS: central nervous system

COX2: cyclooxygenase 2

CREB: cAMP response element-binding

CSF: cerebrospinal fluid

C-terminal: carboxi-terminal

D

DEPC: diethilpirocarbonate

DMEM: Eagle's medium modified by Dulbecco

DMSO: dimethylsulfoxide

DNA: deoxyribonucleic acid

dpi: dots per inch

DTT: dithiothreitol

E

EDTA: ethylenediaminetetraacetic Acid

EOAD: early onset Alzheimer's disease

ELISA: enzyme-linked immunosorbent assay

ER: endoplasmic reticulum

ERK: extracellular signal-regulated kinase

F

FAD: familial Alzheimer's disease

FC: fear conditioning

FDR: false discovery rate

G

GC: guanylate cyclase

GEO: gene expression omnibus

GFAP: gliar fibrillary acidic protein

GL: good-learner

GMP: guanosine monophosphate

GSK3β: glycogen synthase kinase-3

H

HAT: histone acetyl transferase

HDAC: histone deacetylase

Hsp70: heat-shock protein 70

Hsp90: heat-shock protein 90

HSF1: heat shock transcription factor 1

HRP: horseradish peroxidase

h: hour/s

I

iHDACs: histone deacetylases inhibitors

IL: interleukine

iNOS: inducible nitric oxide synthase

i.p: intraperitoneal

iPSCs: induced pluripotent stem cells

ITRs: inverted terminal repeats

J

JNK: c-Jun amino-terminal kinase

L

LIMMA: linear models for microarray data

LTP: long-term potentiation

M

m:meter

mA: milliamp

mAbs: monoclonal antibodies

MAPs: microtubule-associated proteins

MARK: microtubule affinity regulatory kinase

mm: millimeter/s

Min: minute/s

MRC1: mannose receptor C-type 1

MWM: Morris water maze

N

NAE: N-acyl ethanolamine

NAPEs: N-acyl phosphatidylethanolamines

NCE: novel chemical entity

NCSTN: nicastrin

NFTs: neurofibrillary tangles

NGS: normal goat serum

NMDA: N-methyl-D-aspartate

NMDARs: NMDA receptors

N-terminal: amino-terminal

P

pAkt: phosphorylated Akt

PB: phosphate buffer

PBS: phosphate buffer saline

PCR: polymerase chain reaction

PDE: phosphodiesterase

PEN-2: presenilin enhancer 2

PI3K/Akt: phosphatidylinositol 3-kinase pathway

PFA: paraformaldehyde

PHF: paired helical filaments

PKA: protein kinase A

PKC: protein kinase C

PKG: protein kinase G

PL: poor learner

PLA2: phospholipase A2

PLA2G4E: phospholipase A2 group IVE

PP1: protein phosphatase 1

PP2A: protein phosphatase 2A

PP5: protein phosphatase 5

PS: phosphatidylserine

PS1: presenilin 1

PS2: presenilin 2

ptau: (hyper)phosphorylated tau

Q

qPCR: quantitative PCR

R

RNA: ribonucleic acid

rSAP: recombinant shrimp alkaline phosphatase

RT: room temperature

RT-PCR: real time PCR

S

sAPPα: soluble APP alpha

sAPPβ: soluble APP beta

s: second/s

SEM: standard error of the mean

siRNA: small interfering RNA

SNP: single nucleotide variant

T

TGS: Tris-Glycine-SDS

V

vp: viral particles

W

WT: wild-type

ABSTRACT

Alzheimer's disease (AD) is a progressive and irreversible neurodegenerative disorder that constitutes nowadays the main form of dementia in the elderly, affecting about 50 million people all over the world. The lack of an effective treatment, linked with the high failure rate of AD clinical trials highlights the urgent need to search novel therapeutic strategies for this devastating disease.

Several authors have suggested that, due to its multifactorial origin, multi-target therapies may represent a promising strategy to treat AD. However, it is possible that a more drastic approach would be needed to achieve it.

Here, a novel therapeutic strategy, based on concomitant HDAC6 and PDE9 inhibition have demonstrated to be effective on reversing memory impairment and ameliorating amyloid pathology in a well-established mouse model of AD. Its effect seems to be mediated by the augmentation of the chaperones GRP78 and Hsp70.

Moreover, a new target for AD, the phospholipase A2 group IVE (PLA2G4E) has been identified by a newfangled strategy: identification and deep study of cognitive resilient AD mice. An adeno-associated viral vector-mediated overexpression of this enzyme in hippocampal neurons has been able to completely restore cognitive deficits in elderly APP/PS1 mice, an established model of AD, without affecting amyloid or tau pathology thus, suggesting its potentiality for AD treatment. In the same line, its overexpression has also improved memory retention in wild-type elderly mice. Both results pointed out to the promising use of this novel strategy not only for AD but also for other diseases coursing with cognitive deficits.

INTRODUCTION

1. Alzheimer's disease, epidemiology and social impact

Alzheimer´s disease (AD) is a progressive an irreversible neurodegenerative disorder that was first described in 1906 by Dr. Alois Alzheimer (1864-1915) when he analyzed the brain of a 56-year-old patient named Auguste Deter, finding senile plaques and neurofibrillary tangles (NFTs)(Hippius & Neundörfer, 2003). The patient presented an unusual mental illness characterized by memory loss, language problems and unpredictable behavior.

However, the term "Alzheimer's disease" was not used until the psychiatrist Emil Kraepelin (1856-1926) introduced it in the 8th edition of his Manual of Psychiatry in 1910, and it currently refers to a clinical picture characterized in its initial phases by disorders in short-term memory, disorientation and inability to perform daily-life skills. The disease progresses towards a complete deterioration of cognitive functions altering patients' personality and making them completely dependent (Mielke *et al.* 2014).

The incidence of neurodegenerative diseases, including dementia, is rising due to the increase in life expectancy and the consequent population aging (Martin Prince *et al.*, 2014). This increase in dementia cases constitutes a major public health issue because it exacts a heavy toll on not just family life and health and social services, but also on the national economy (Cotter, 2007).

AD constitutes nowadays the main form of dementia in the elderly (60-70% of all cases), affecting about 50 million people all over the world (Alzheimer's association, 2018). Moreover, it is believed that AD cases will nearly quadruple in the next 50 years if the current trend continues (Cummings & Cole, 2002). In Spain, it has been estimated that there are about 1.2 million people affected with AD, which has an associated average expense of 32000 € *per* patient each year (Confederación Española de Familiares de personas con Alzheimer y otras demencias (CEAFA)).

The highly cost associated with AD, linked to the lack of an effective treatment, makes essential to investigate AD with the aim of finding new therapies to cure or at least slow down the progression of the disease.

2. Pathological features of Alzheimer's disease

Macroscopically, AD brains typically present a deep atrophy that principally affects brain areas related to learning and memory, such as the temporal, parietal and frontal cortex, hippocampus and amygdala. This atrophy, that causes a reduction of the cerebral volume, is manifested as a sulcal widening and ventricular expansion and it is mainly due to the important synaptic loss and neuronal degeneration that occurs during AD development (Mattson, 2004; Liu *et al.*, 2012)(Figure 1).

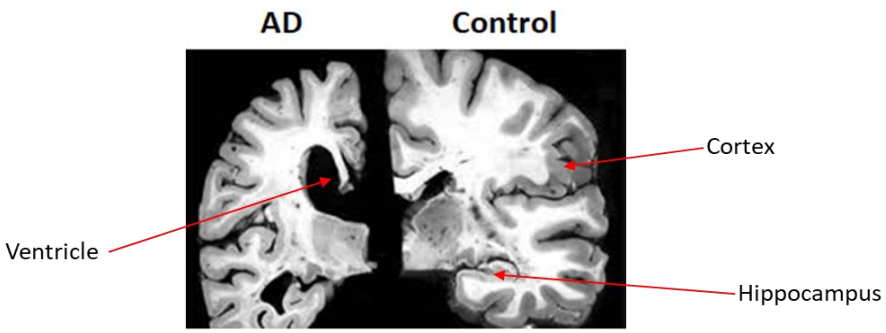

Figure 1. Neuroanatomical comparison of Alzheimer´s disease (AD) and normal brain (control). Note the cortical and hippocampal atrophy, the sulcal widening and the ventricular expansion characteristic of AD. Adapted from Andrea Alce.

The histopathological characterization of AD is mainly focus on the presence of two elements (Hardy, 2006; Selkoe, 2004; Small *et al.* 1997)(Figure 2):

- Senile or amyloid plaques: extracellular deposits composed of diverse amyloid beta (Aβ) peptides derived from the proteolytic processing of amyloid precursor protein (APP), associated molecules such as heparin sulfate, complement proteins, proteases inhibitors and apolipoproteins, degenerating neuronal processes and reactive glia (Dickson, 1997).
- Neurofibrillary tangles: intraneuronal filamentous aggregates of hyperphosphorylated tau protein (ptau)(Kosik *et al.* 1986).

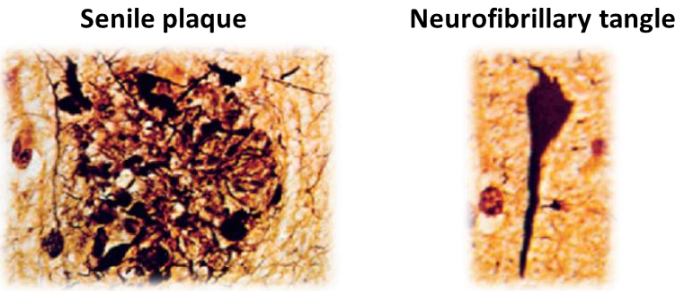

Figure 2. Histopathological hallmarks of Alzheimer's disease: senile plaque (left) and neurofibrillary tangle (right). Adapted from Harald J Hampel.

Whereas in the brain of AD patients senile plaques present a random distribution with no correlation between the density of the amyloid plaques and the progression of the disease, NFTs has a defined pattern and temporality. The initial phases of the disease are characterized by the appearance of this histopathological hallmark in a group of neurons located in the entorhinal cortex and the hippocampus, thus affecting cognitive function. Subsequently, as the disease progresses, the presence of NFTs extends to associative areas and subcortical structures, which produces an accentuation of the deterioration of the patients. Motor areas are only affected in the final stages of the disease (Braak & Braak, 1991, 1995). Thus, it can be consider that the distribution of NFTs correlates better with AD clinical alterations than that of senile plaques (Arriagada *et al.*, 1992)(Figure 3). In fact, Braak scale, which is commonly used for staging AD, considers tau pathology and

its anatomical distribution for histopathological correlation of dementia in AD (Braak *et al.*, 2006). Nevertheless, some studies have suggested that soluble oligomeric forms of Aβ could be triggering elements of the neurodegenerative processes that occur in this disease (Selkoe & Hardy, 2016; Brinkmalm *et al.*, 2019). In any case, evidence suggests that Aβ and tau contribute to the synaptic loss that precedes neuronal death in AD, being synapse loss the factor that better correlates temporally with cognitive impairment (Terry *et al.*, 1991)(Figure 3).

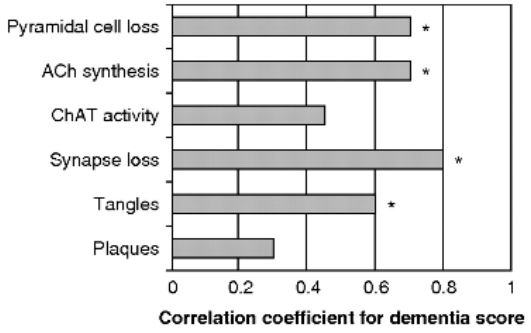

Figure 3. Correlation coefficient of different pathological hallmarks of Alzheimer's disease for dementia score ($^{*}p \leq 0.05$). Adapted from Terry *et al.* 1991.

Apart from the previously mentioned hallmarks of AD, there are other characteristic alterations that occur during the progression of the disease. Among all of them, it can be highlighted an increased state of neuroinflammation and oxidative stress, changes in gene expression processes and a reduction in cerebral glucose uptake (Cummings, 2004).

3. Etiology

Although the etiology of AD is not fully understood, it is believed that it is a multifactorial disease in which both genetic and environmental factors are implicated. Two types of AD can be distinguished regarding the onset and causal factors of the disease: familiar and sporadic AD. However, both are clinically similar.

- **Familial Alzheimer's disease (FAD)**

Familiar or early onset AD (EOAD) represents a 1-5% of all AD cases. It is usually developed before 65 years of age and can be characterized by the Mendelian inheritance pattern (Bird, 2008). So far, it have been pointed out that mutations in three specific genes are directly implicated in familiar AD:

-Amyloid precursor protein gene: this gene is located on chromosome 21. Al least 50 familiar AD-related mutations have been identified in this gene, which are responsible of around a 10% of all EOAD cases. These mutations are located in specific regions that are critical to the APP physiological processing thus increasing the amyloidogenic processing and, in consequence, causing an overproduction of Aβ. The Swedish mutation, which produces the substitution of the amino acids lysine (K) and methionine (M) by Asparagine

(N) and Leucine (L)(K670N/M671L) immediately before the amino-terminal domain of the Aβ peptide is one of the most well-known mutations in this gene (Mullan *et al.*, 1992).

-Presenilin 1 gene: it is located on chromosome 14. More than 180 mutations associated with FAD were found in this gene, which are the causers of about a 30-50% of all EOAD cases (Sherrington *et al.*, 1995). Some of these mutations increase the production of $A\beta_{40}$ and $A\beta_{42}$ (Campion *et al.*, 1999).

-Presenilin 2 gene: PS2 gene is located on chromosome 1. Only about 15 EOAD-related mutations have been described for this gene, which constitute just a 1% of all FAD cases (Levy-Lahad *et al.*, 1995).

Apart from the mentioned mutations, duplications of a chromosomal segment that contains the APP gene have also been described in patients with familial AD. These cases would approximately account for a 8% of all EOAD cases (Rovelet-Lecrux *et al.*, 2006). Despite the different origin, in both FAD cases increase the production of Aβ peptide which subsequently leads to its accumulation in the brain.

The discovery of the genetic mutations that cause FAD has allowed the generation of numerous AD animal models that constitute a fundamental tool to study AD although currently, none of them is able to recapitulate all AD hallmarks (Janus & Westaway, 2001).

- **Sporadic Alzheimer's disease**

Sporadic or late-onset AD represents a 95-99% of all AD cases and it is usually developed after 65 years of age. It is consider a multifactorial disease with unknown etiology in which the interaction of different elements leads to the development of the pathology. Lately, several epidemiological studies have been conducted to identify the predisposing factors of the disease, being the main risk factors identified:

-Age: it is the main risk factor of sporadic AD. As mentioned above, most cases are developed over 65 years of age. Moreover, it has been described that the risk of suffering from dementia duplicates every 5 years from this age (Alzheimer's association).

-Sex: women present a higher prevalence of sporadic AD than men. The cause of this fact may be partially explained by a higher incidence among older women and partially by differential survival rates (Ferri, 2005).

-Genetic factors: it has been described polymorphisms in several genes able to modulate the risk of suffering from sporadic AD. The most studied one is the allele ε4 of the Apolipoprotein E (ApoE) gene. This gene presents a polymorphism determined by the change of an amino acid at codons 112 and 158 that give rise to three isoforms: ApoE-ε2, ApoE-ε3 and ApoE-ε4. Individuals carrying the ApoE-ε4 allele have increased risk of suffering from AD compared with those carrying the more common ApoE-ε3 allele while the ones carrying ApoE-ε2 allele have been associated with a decreased risk of developing AD (Kim *et al.*, 2009). In recent years, other genes such as BIN1, CLU, ABCA7, CR1, PICALM, TOMM40, DYRK1A, GSK3β, APOC1, CAMK1D, FBXL13,

PLC62, ABI3, TREM2 among others have also been associated with late-onset AD although its influence on sporadic AD is much lower than those of APOE gene (Ballard *et al.*, 2011a; Floudas *et al.*, 2014; Sims *et al.*, 2017).

-Environmental factors: several environmental factors can also increase the risk of suffering from sporadic AD. These factors include some treatable medical conditions such as stroke (Purandare *et al.*, 2006), hypertension (Qiu *et al.*, 2005), hypercholesterolemia (Whitmer *et al.*, 2005), depression (Wilson *et al.*, 2003), diabetes (Xu *et al.*, 2009), obesity (Gustafson, 2006) and head trauma (Plassman *et al.*, 2000), together with some life-style related factors like alcohol intake (Anttila *et al.*, 2004) and smoking (Aggarwal *et al.*, 2006).

Nevertheless, there are also some neuroprotective factors that could reduce the susceptibility of developing AD. The most important ones are cognitive reserve (concept that combines the benefits of education, occupation, and mental activities), physical activity, some kind of "healthy diet" and social interaction (Ballard *et al.*, 2011a; Karp *et al.*, 2006)

4. Pathogenesis of Alzheimer's disease

Despite recent advances in the study of AD, the causes and mechanisms that lead to the development of the disease remain unknown. However, it has been postulated several theories which try to explain them.

4.1. Amyloid cascade hypothesis

It was the first hypothesis proposed to explain AD development. It postulates that an imbalance between the synthesis and the clearance of Aβ peptide is produced in AD. As a result, Aβ is accumulated in the brain in form of senile plaques and this deposition finally provokes neurodegeneration by triggering several events such as the formation of NFTs, glutamatergic excitotoxicity, oxidative stress, inflammation and cell apoptosis (Evin *et al.*, 2006; Hardy & Selkoe, 2002).

Amyloid precursor protein processing

APP is a type I transmembrane protein that contains a large amino-terminal (N-terminal) extracellular domain and a short carboxi-terminal (C-terminal) intracellular domain. Its ubiquitous distribution in the cell includes the plasmatic membrane, the Golgi reticulum, the endoplasmic reticulum and the membrane of the endosomes, lysosomes and mitochondria (Lammich *et al.*, 1999).

Although its function has not been well established yet, in the brain it is believed to play an important role in preserving axonal structure (Zhang *et al.*, 2011), in iron transportation (Duce *et al.*, 2010), in the maintenance of calcium homeostasis (Octave *et al.*, 2013), in the regulation of synapse formation (Priller *et al.*, 2006), in neuronal plasticity (Turner *et al.*, 2003) and in the neurogenesis of the dentate gyrus (Wang *et al.*, 2014).

The amyloid precursor protein can be cleavage at different recognition sites by several enzymes:

- **α-secretase:** the α-secretase activity has been found in several members of the ADAM family, which is a family of metalloproteinases with a disintegrin domain. Specifically, this activity has been found in three transmembrane members of the ADAM family: ADAM9, ADAM10 and ADAM17.
- **β-secretase:** this enzyme, also known as BACE1, is a transmembrane protein that presents aspartic protease activity.
- **γ-secretase:** it is a multi-subunit protease complex, itself an integral membrane protein, formed by presenilin 1 (PS1), presenilin 2 (PS2), nicastrin (NCSTN), APH-1 (anterior pharynx defective 1) and PEN-2 (presenilin enhancer-2). PS1 and PS2 constitute the catalytic center of this complex.

The sequential action of these enzymes gives rise to two alternative processing pathways of the APP: the non-amyloidogenic and the amyloidogenic pathway (Figure 4).

-Non-amyloidogenic pathway: this pathway takes place under physiological conditions and does not lead to the production of Aβ peptide. Through this pathway, APP is firstly cleaved by α-secretase in Lys16 position generating a soluble shard that contains the N-terminal fragment of APP (sAPPα) and a peptide of 83 amino acids (C83) that includes the C-terminal fragment of APP (Lammich *et al.*, 1999). C83 is retained in the membrane, where it is cleaved again by γ-secretase to release a soluble N-terminal fragment (p3), that is secreted to the extracellular medium, and a membrane-bound C-terminal fragment called APP intracellular domain (AICD), that goes to the nucleus where it acts as a transcriptional regulator of several genes such as APP, BACE1 and neprilysin (Aβ degrading enzyme)(von Rotz *et al.*, 2004; Belyaev *et al.*, 2009). It has been described that both sAPPα and C83 have beneficial effects in neuronal cultures associated with cell survival, interaction cell-interstitial matrix, neurite outgrowth, synaptic formation and neuronal plasticity (Shivers *et al.*, 1988; Jin *et al.*, 1994; Perez *et al.*, 1997; Meziane *et al.*, 1998).

-Amyloidogenic pathway: this metabolic pathway is mainly produced during AD and finally leads to Aβ production. The initial cleavage of APP is mediated by β-secretase, which cut at the N-terminal fragment of APP to generate a distal fragment that is secreted into the extracellular medium (sAPPβ) and a 99 amino acids peptide (C99) that contains the Aβ peptide and the C-terminal fragment of APP (Vassar *et al.*, 1999). C99 fragment is subsequently cleavage by γ-secretase inside the lysosomes to produce full-length Aβ and a 55-57 amino acids peptide called AICD. γ-secretase can cleave APP at different sites, leading to Aβ peptides of 39-40 or 42-43 amino acids ($A\beta_{40}$ or $A\beta_{42}$ respectively). $A\beta_{40}$ is the form mainly produced under normal conditions (Evin *et al.*, 2006), however, $A\beta_{42}$ presents a greater hydrophobicity which leads to a higher tendency to form fibers (Jarrett *et al.*, 1993). Moreover, $A\beta_{42}$ is also the predominant form in senile plaques (Iwatsubo *et al.*, 1994).

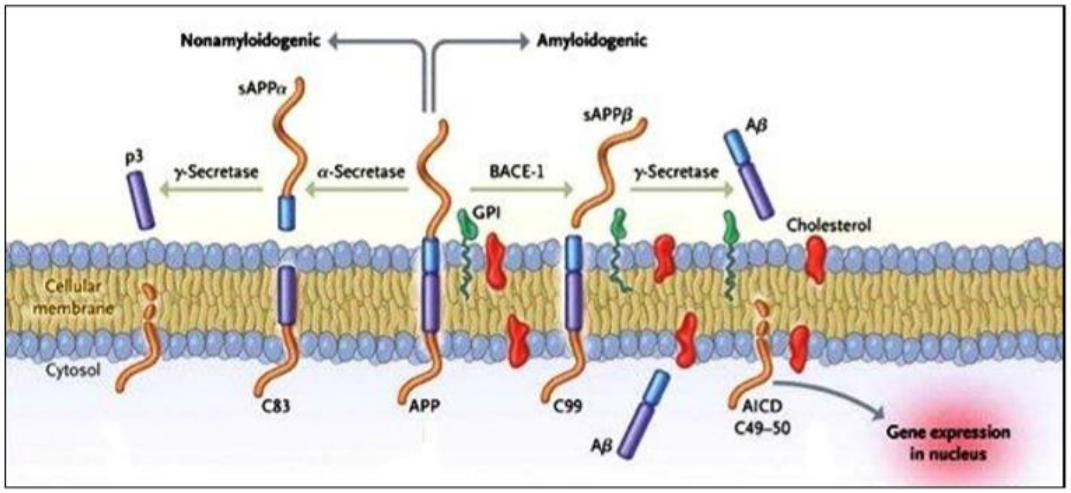

Figure 4. Alternative APP processing: non-amyloidogenic and amyloidogenic pathway. Querfurth and Laferla, 2010.

The amyloid cascade hypothesis is mainly based on the genetic component of AD as it has been observed that mutations presented by patients with familiar AD lead to an overproduction of the $A\beta_{42}$ peptide. In addition, the APP locus is duplicate in some cases of EOAD (Rovelet-Lecrux *et al.*, 2006) and, in the same line, it is widely known that people with Down syndrome, who have a trisomy on chromosome 21 (where APP gene is located), present a higher prevalence of EOAD with Aβ deposition (Masters *et al.*, 1985). In the case of sporadic AD, this hypothesis argues that the accumulation of Aβ is not due to an increase in its production, but a reduction in the capacity to clear it (Hama & Saido, 2005). However, in both cases the hypothesis postulates that the accumulated Aβ undergoes conformational changes that facilitate its aggregation in soluble oligomers, which subsequently give rise to the formation of insoluble fibers that are deposited in the form of senile plaques within the brain.

Nowadays, it is widely accepted that the accumulation of Aβ peptide in brain regions related with learning and memory significantly contributes to AD development. However, the biochemical mechanism by which Aβ-aggregates produce cellular dysfunction and finally neuronal death remains unknown (Mucke & Selkoe, 2012). Although it was initially postulated that the neurodegeneration present in AD was caused by the accumulation of insoluble fibers of Aβ in form of amyloid plaques (Hardy & Higgins, 1992), it is now known that soluble oligomers of Aβ are the main triggers of the pathological processes that take place in AD (Hardy & Selkoe, 2002). Specifically, it has been postulated that 7 kDa-Aβ dimers, which molecular composition has been recently elucidated (Brinkmalm *et al.*, 2019), impair LTP and consequently memory (Shankar *et al.*, 2008) and induce aberrant tau phosphorylation and neuritic degeneration (Jin *et al.*, 2011).

4.2. Tau pathology

The second theory postulates that an aberrant phosphorylation of tau initiates the pathological cascade of events in AD.

Tau protein belongs to the microtubule-associated proteins (MAPs) family and it presents a cytosolic location within the neurons. It binds to other proteins such as tubulin to allow microtubules stabilization, so it plays an important role maintaining neuronal structures, such as dendrites and axons, and allowing axonal proteins-transportation (Drubin & Kirschner, 1986; Iqbal *et al.*, 2009).

The function of tau as a stabilizing protein is regulated by its phosphorylation state. In consequence, when it is hyperphosphorylated, as occurs in AD, tau losses its physiological role producing a collapse of the cellular transport system and a dysfunctional interneuronal communication. Hyperphosphorylated tau is able to sequester its physiological form and proteins of its family such as MAP1 and MAP2 contributing to the disassembly of the microtubules (Iqbal *et al.*, 2010). Moreover, this hyperphosphorylation increases its auto-adhesion producing its aggregation in paired helical filaments (PHF) that join together to produce NFTs. All of this results in a disintegration of the microtubules and a rupture of the cytoskeleton that ultimately lead to neuronal death (Chun & Johnson, 2007)(Figure 5). It is also noteworthy that ptau presents a greater resistance to proteolysis than tau, thus facilitating its accumulation in the neurons with the consequent toxic effect (Shimura *et al.*, 2004).

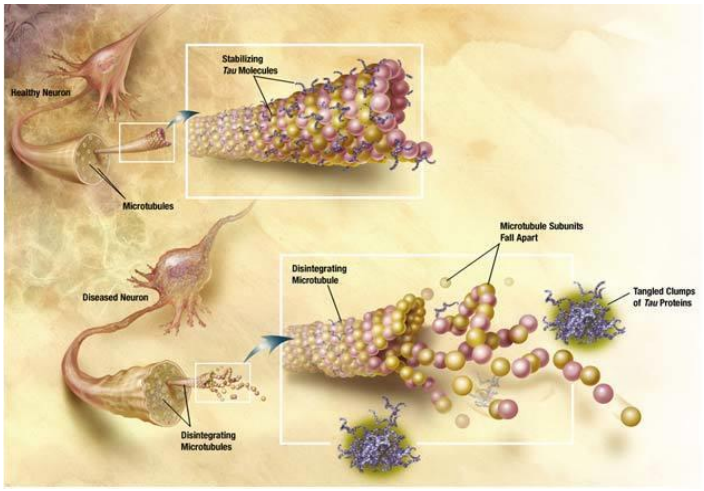

Figure 5. Disintegration of microtubules caused by tau hyperphosphorylation during AD. De Castro, A.K, 2010.

It has been shown that there is a high correlation between the number of NFTs in the extracellular space and the number of neurons damaged in the hippocampus, supporting the idea that intraneuronal ptau accumulation induces the formation of NFTs that would cause a global failure in cellular functioning and subsequent neuronal death (Braak *et al.*, 1994).

The tau phosphorylation state is determined by the balance between the activity of different kinases and phosphatases over about 79 different phosphorylation sites present in the protein (Goedert *et al.*, 1989). At least 30 of these residues are phosphorylated in AD, mainly by two types of kinases: kinases directed to proline or proline-serine/threonine motifs, such as the glycogen synthase kinase-3 (GSK3β), cyclin-

dependent kinase 5 (CDK5), p38 and c-Jun amino-terminal kinase (JNK) or by those directed to other residues such as Ca^{2+}/calmodulin dependent kinase type II (CAMKII), the microtubule affinity regulatory kinase (MARK) and the protein kinases A and C (PKA and PKC)(Morishima-Kawashima *et al.*, 1995; Gong *et al.*, 2005). The main phosphatases involved in tau dephosphorylation are protein phosphatase 2A (PP2A), protein phosphatase 1 (PP1) and protein phosphatase 5 (PP5), being its activity decreased by 50 %, 20 %, and 20 % respectively in AD (Martin *et al.*, 2013).

As mentioned above, one of the most important kinases involved in tau phosphorylation and therefore, in AD pathogenesis, is GSK3β (Hanger *et al.*, 1992; Lovestone *et al.*, 1994; Avila & Hernández, 2007). Among all the pathways implicated in GSK3β regulation, the phosphatidylinositol 3-kinase pathway (PI3K/Akt) is the most studied. The activation of PI3K gives rise to the production of phosphatidyl-inositol-3-phosphate, which binds to the protein Akt promoting its phosphorylation and consequent activation. Phospho-Akt (pAkt) in turn, phosphorylates GSK3β in the residue Ser-9 causing its inactivation (Yang *et al.*, 2004) and therefore, preventing the pathological tau phosphorylation. It is extensively accepted that during AD, the amyloidogenic processing of APP and consequent Aβ increase produces GSK3β activation (Ma *et al.*, 2006; De Felice *et al.*, 2007)(Figure 6).

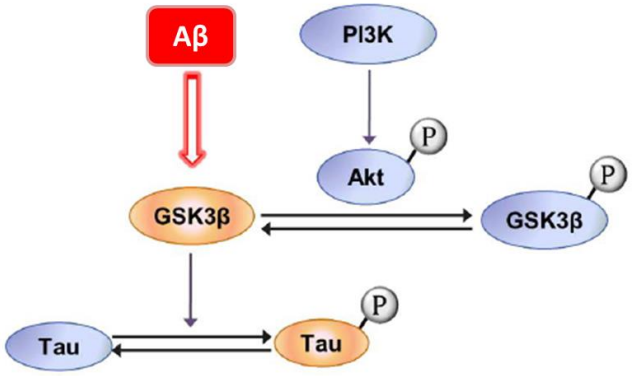

Figure 6. Signaling pathway PI3K/pAkt. Adapted from Schloesser et al., 2008.

The important implication of GSK3β in AD, acting as a link between the amyloid cascade and tau pathology hypothesis, has led to postulate the "GSK3β hypothesis". It has been demonstrated that this kinase interacts with PS1 and that it forms part of the regulatory complex of tau phosphorylation (Baki *et al.*, 2004). Moreover, it is known that its overexpression impairs memory and learning (Hernández *et al.*, 2002; Hooper *et al.*, 2007; Avila & Hernández, 2007), exacerbates the inflammatory response induced by the microglia around the senile plaques (Rodionova *et al.*, 2007) and induces pro-apoptotic processes that would finally lead to neuronal loss (Turenne & Price, 2001).

Nowadays, it is widely accepted that the accumulation of Aβ causes alterations in tau and that, although both contribute to the pathophysiology of the disease, is the latter the main responsible for the structural and functional deterioration that takes place in AD brains. In fact, it has been observed that elevated amounts of Aβ increase the formation of lesions

mediated by fibrillar tau in AD animal models (Lewis *et al.*, 2001; Oddo *et al.*, 2003; Pérez *et al.*, 2005; Selkoe & Hardy, 2016) supporting the idea that amyloid and tau pathologies appear chronologically in this order. However, although GSK3β could be the link between both pathological events, further studies would be needed to completely elucidate how these two markers interact.

4.3. Synaptic pathology

As previously mentioned, the synaptic loss that precedes neuronal death in AD is the factor that better correlates with the cognitive impairment observed in AD patients during disease development (Terry *et al.*, 1991).

The synaptic pathology that occurs during AD is characterized by a progressive loss of axon terminals (Scheff *et al.*, 2007), a decrease in the expression of presynaptic and postsynaptic proteins (Almeida *et al.*, 2005), alterations in the dendritic spines structure (Knobloch & Mansuy, 2008) and even their loss (Blanpied & Ehlers, 2004). The observed synaptic degeneration starts in neurons of the entorhinal cortex and the hippocampus and finally extends to cortical areas (Selkoe, 2002).

Although the pathological mechanisms that lead to synaptic damage in AD have not been fully elucidated, it is extensively believe that Aβ peptide plays a key role in this process. The accumulation of intraneuronal Aβ peptide seems to be one of the main responsible factors for the synaptic dysfunction that occurs in AD as it correlates with the learning and memory deficits observed in different animal models of AD (Westerman *et al.*, 2002).

5. Treatment

Despite all the efforts employed to find a cure or a treatment that would slow down the development of AD, the reality is that nowadays there is not an effective treatment for this devastating disease. There are only some symptomatic treatments available since the mid-1990s (Ballard *et al.*, 2011a).

5.1. Pharmacological treatment

Currently, there are only 4 drugs approved for AD treatment. They modulate cholinergic or glutamatergic neurotransmission with the aim of delay the decline of cognitive and behavioral functions in the patients. However, as mentioned above its effect is only symptomatic showing a temporary mild improvement in cognitive functions and other symptoms over the first 12 months approximately (Yiannopoulou & Papageorgiou, 2013).

Specifically, commercialized drugs for AD treatment are:

-Cholinesterase inhibitors

The first demonstration of cholinergic deficiency in AD brains (Whitehouse *et al.*, 1982) gave rise to the development of anti-cholinesterase therapies for AD (Farlow & Cummings, 2007).

Tacrine was the first neurotransmitter-based drug approved for AD treatment. It had a short effective half-life, so it needed to be administered four times *per* day. Moreover, it presented common side-effects such as hepatic toxicity, which made patients to require attendant for monitoring liver function. As a consequence, and due to the commercialization of new cholinesterase inhibitors with a more safety profile, it was withdrawn from the market in 2013 (Honig & Boyd, 2013).

Nowadays, donepezil, rivastigmine and galantamine constitute the first line pharmacotherapy for AD, being licensed for mild-to-moderate AD. Although they have slightly different pharmacological properties, they all inhibit the breakdown of acetylcholine by blocking the enzyme acetylcholinesterase. This blockage produces an increase in cholinergic function which results in a modest and temporal enhancement of memory and cognitive status in AD patients (Birks, 2006).

-NMDA receptor antagonist

Although the neurotransmitter glutamate and the N-methyl-D-aspartate (NMDA) receptor play an important role in learning and memory under physiological conditions, during AD occurs an increase of glutamatergic activity which leads to a massive NMDA receptors activation that finally produces neuronal dysfunction. In consequence, it arose the idea of partially inactivate these receptors to improve memory function in AD patients, which was manifested in the drug memantine (Bannerman *et al.*, 2004).

Memantine is an uncompetitive antagonist of NMDA receptors which was approved for moderate-to-severe AD in 2003. This activity-dependent NMDA antagonist is able to dampen the excitatory activity in the brain when it is excessive. It has been probe that short-term use of this compound can modestly improve cognition, behavior, and daily-life skills in AD patients (Winslow *et al.*, 2011). It can also decrease delusions and agitation/aggression in this patients (Gauthier *et al.*, 2008). Note that this compound can be also administered in combination with cholinesterase inhibitors. In fact, the combination of donepezil and memantine has been recently approved for AD treatment under the commercial name Namzaric (FDA U.S. Food and Drug Administration, 2014).

-Treatments for neuropsychiatric symptoms

In order to improve other symptoms of AD such as apathy and depression, the drugs mentioned above can be combined with another therapies such as atypical antipsychotics, antidepressants and/or anticonvulsants (Ballard *et al.*, 2011a).

5.2. Non-pharmacological treatment

Due to the lack of an effective pharmacological treatment for AD, non-pharmacological approaches have arisen as promising strategies to improve cognition in these patients. They are mainly focus on the stimulation of patient's intellectual and/or physical faculties. For example, cognitive training or stimulation has proven to be effective at early stages of the disease improving patient's life-quality (Ballard *et al.*, 2011b).

6. Alzheimer's disease clinical trials: causes of the high failure rate

Apart from the previously mentioned commercialized drugs for AD, that have minimal to non-clinical symptomatic benefit, the 40-year search for effective disease-modifying therapeutics to treat AD has resulted in a clinical failure rate of 100% (Mullane & Williams, 2019).

Nowadays, the development of new drugs for AD is mainly focus on the amyloid cascade hypothesis, trying to reduce Aβ production or address its degradation. β-secretase inhibitors, inhibitors and modulators of the γ-secretase, immunotherapy against Aβ peptide and antiplatelet Aβ agents can be found among the explored strategies. At this moment, the most extensively developed anti-Aβ approach is immunotherapy, specifically, passive immunization through administration of exogenous monoclonal antibodies (mAbs) binding different epitopes and conformations of Aβ. Recently, Biogen and Eisai have discontinued phase III clinical trials ENGAGE and EMERGE with the drug adecanumab, a high-affinity, fully human IgG1 mAb against a conformational epitope found on Aβ (Biogen, 2019). However, despite the failure of these AD clinical trials, the results obtained are being really useful to understand better the pathogenesis of the disease and to get important clues to improve future therapeutic approaches, for example, initiate clinical trials earlier in the course of AD (van Dyck, 2018).

Regarding tau pathology, the efficacy of several inhibitors of tau phosphorylation have also been tested, however, until now, none of them have been translated into clinical practice. Likewise, due to the aggregating nature of tau protein, antiaggregants and/or microtubule stabilizing agents have also been tested although, unfortunately, none of them have been able to stop the dementia or decrease the progression of the disease. In consequence, they have failed in clinical trials, most of them even before reaching clinical phase III (Mangialasche *et al.*, 2010)(Figure 7).

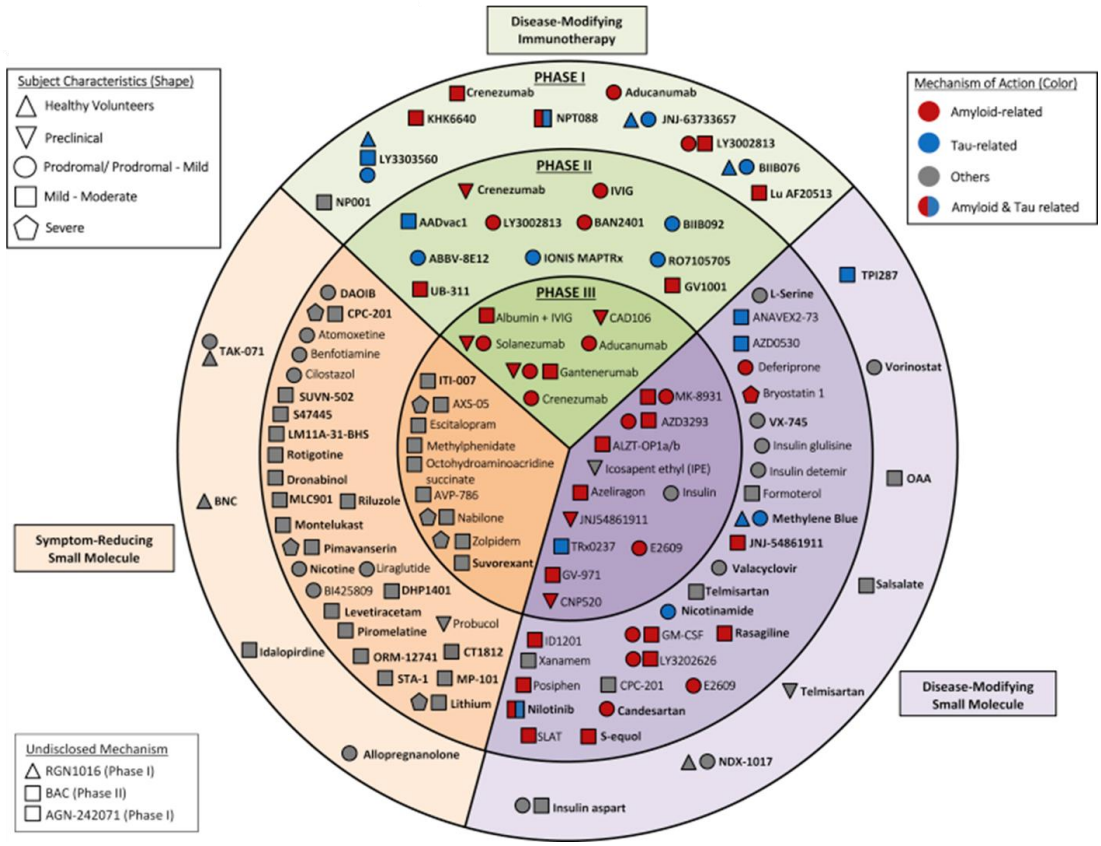

Figure 7. Drug development in Alzheimer's disease (2018). Adapted from Cummings *et al*., 2018.

The inability to find a disease-modifying therapy to treat AD can be explained by the conjunction of several factors.

The heterogeneity of AD and its clinical similarity with another kind of dementias, has pointed out at the selection of the patients enrolled in clinical trials as one of the critical factors of AD drug development; although the increasing use of Aβ imaging, cerebrospinal fluid (CSF) and/or blood-based biomarkers (Altuna-Azkargorta & Mendioroz-Iriarte, 2018) to document AD pathology before the initio of the clinical trials is helping to defray the problem (Golde *et al.*, 2018).

Moreover, efforts are now focus on testing agents at earlier stages of the disease, where efficacy may be more likely. In consequence, the identification of novel biomarkers that allow AD early detection would be a really valuable tool to achieve it (Golde *et al.*, 2018).

Another important factor is the existing poor-understanding of the complex mechanism involved in AD pathogenesis, which has led to an overarching focus on the amyloid cascade hypothesis (Mullane & Williams, 2019), fact that can be subjectively precluding the discovery of new therapeutic targets for AD.

Other serious handicap is the inefficient translation from the preclinical studies performed in AD animal models to patients. Although AD animal models are a valuable tool to

investigate and test new therapies for the disease, they are not able to fully reproduce human pathogenesis. Most of these models have amyloid metabolism abnormalities but generally lack other aspects of human AD such as the formation of NFTs or neuronal loss. The reason could be that they are based on the genetics of EOAD, so they are not a good animal model for sporadic AD, which represents the 95-99% of all AD cases. However, as there are not better models available, it is necessary to execute all the experiments rigorously to facilitate their reproducibility and translation (Cummings, 2018; Mullane & Williams, 2019).

The complex nature of AD is also generating a rejection of the dominant hypothesis "one protein, one drug, one disease" that postulates that the aim of drug development is to find a selective compound that acts on a single specific disease target to produce the desired clinical effects. Several authors have suggested that, as occurs in other complex diseases such as cancer or acquired immune deficiency syndrome (AIDS), multi-target approaches would be required for AD (Mangialasche *et al.*, 2010; Cummings *et al.*, 2018).

7. New perspectives in Alzheimer's disease treatment

Nowadays, there is an urgent need of investigating AD with the scope of finding effective therapies for this devastating disease. However, the high failure rate in clinical trials suggests the importance of changing the way scientists are focusing Alzheimer's research.

The use of multimodal action drugs, directed against several targets at once, has been proposed as a promising strategy to get a disease-modifying therapy (Mangialasche *et al.*, 2010; Cummings *et al.*, 2018) but perhaps, a more drastic change in the way of approaching the study of AD, starting from preclinical stages, would be needed to achieve it.

7.1. Novel multi-target approach for Alzheimer's disease treatment: HDAC and PDE inhibition

7.1.1. Epigenetics and Alzheimer's disease: HDACs

C.H. Waddington conceived in 1942 the term epigenetics to explain the phenotypic changes that cells experiment during their lifetime (Bard, 2008). Nowadays, this term refers to acquired and heritable modifications to DNA that regulate the expression and functions of genes without affecting the DNA nucleotide sequence (Adwan & Zawia, 2013).

The basic unit of the chromatin is the nucleosome, a protein octamer comprised of four core histones (H3, H4, H2A and H2B) around which DNA winds (Figure 8). Post-translational modifications can regulate gene expression by remodeling chromatin structure thus facilitating or avoiding the recruitment of the transcriptional machinery to the DNA (Bannister & Kouzarides, 2011). These modifications include DNA methylation and hydroxymethylation, histone modifications and non-coding RNA regulation (Adwan & Zawia, 2013).

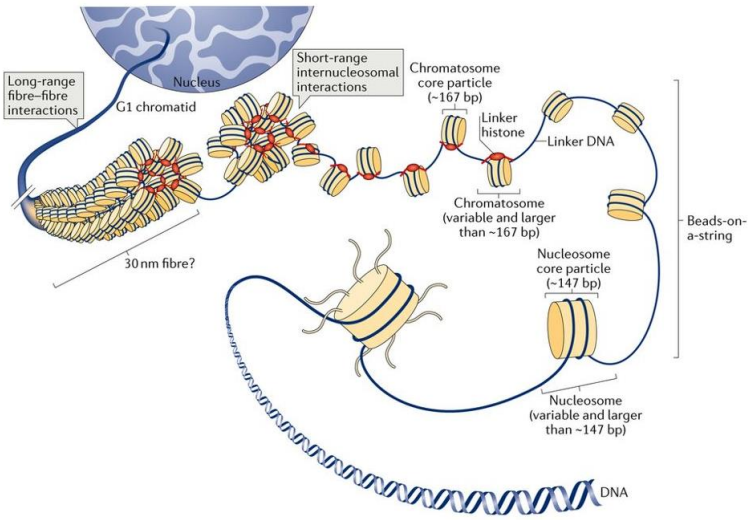

Figure 8. Stages of chromatin compaction. *Fyodorov et al.*, 2018.

Several epigenetic modifications have been associated with cognitive functions, being histone acetylation the most robustly associated with the promotion of memory formation. Histone acetylation is a reversible process that consists on the addition of acetyl groups to lysine amino acids located at the N-terminal tails of histones. It induces a less tightly packaged chromatin structure that allows the accession of the transcriptional machinery to the DNA thus facilitating gene transcription (Di Cerbo *et al.*, 2014). It has been described that histone acetylation improves learning and memory processes by facilitating the transcription of memory-related genes (Levenson *et al.*, 2004).

Histone acetylation is regulated by the antagonistic activity of two types of proteins: histone acetyl transferases (HATs) and histone deacetylases (HDACs). The first ones are responsible of the addition of acetyl groups to histones whereas the second catalyzed their removal (Figure 9).

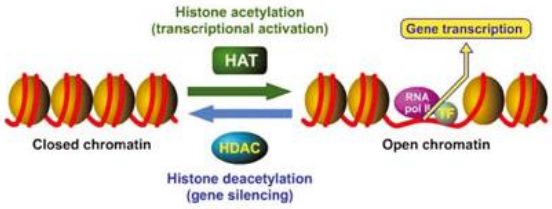

Figure 9. Chromatin remodeling mediated by histone acetylation. Shonka and Gilbert, 2010.

Histone deacetylases can be divided in four groups: class I (HDAC 1, 2, 3 and 8), class II, that is subdivided in class IIa (HDAC 4, 5, 7 and 9) and class IIb (HDAC 6 and 10), class III (sirtruins 1-7) and class IV (HDAC 11).

All members of HDACs class I, II and IV are expressed in the brain, most abundantly in neurons (Gräff & Tsai, 2013; Yun *et al.*, 2011).

It has been demonstrated that class I HDACs, particularly HDAC2 and HDAC3, negatively regulate learning and memory (Guan *et al.*, 2009; McQuown *et al.*, 2011).

Mice overexpressing HDAC2 showed impaired LTP and decreased associative and spatial memory whereas HDAC2 knockout mice presented an enhanced synaptic density and neuroplasticity (Guan *et al.*, 2009). Moreover, it has been reported that HDAC2 was increased in the hippocampus and entorhinal cortex of AD patients from the earliest stages of the disease, suggesting that an increase in this enzyme, and consequent chromatin compaction, might be an early pathological event in AD (Gräff *et al.*, 2012). However, other groups have found this enzyme unchanged in the prefrontal cortex (Mahady *et al.*, 2018) or even reduced in the nucleus basalis of Meynert (Mahady *et al.*, 2019) during AD progression.

Regarding AD, it is also extensively believed that HDAC6, a cytoplasmic HDAC class IIb isoform, is overexpressed in the brain of AD animal models and in AD patients, although its role in AD remains controversial (Mahady *et al.* 2018; Zhang *et al.* 2012). This enzyme, that regulates microtubule behavior and stability via α-tubulin acetylation (Hubbert *et al.*, 2002), plays an important role in protein clearance in the cell (Moreno-Gonzalo *et al.*, 2018). In fact, its reduction seems to promote tau and Aβ clearance, thereby ameliorating the memory deficits in AD models (Cook *et al.*, 2012; Sung *et al.*, 2013; Govindarajan *et al.*, 2013; Zhang *et al.*, 2014). Furthermore, its inhibition rescued the reduced mitochondrial axonal transport and mitochondrial length in hippocampal neurons treated with Aβ (Kim *et al.*, 2012) and in induced pluripotent stem cells (iPSCs) from amyotrophic lateral sclerosis (ALS) patients (Guo *et al.*, 2017).

In consequence, the involvement of different epigenetic processes in aging and in the detriment of cognitive functions point to HDAC inhibitors (iHDACs) as potential therapeutic tools for AD treatment (Rodriguez-Rodero *et al.* 2010; Peixoto and Abel 2012). This strategy has been pre-clinically validated by demonstrating that pan-iHDACs administration enhances learning ability in animal models through the promotion of synaptic plasticity-related genes transcription (Ricobaraza *et al.*, 2009; Fischer *et al.*, 2007; Guan *et al.*, 2009; Abel & Zukin, 2008; Zhao *et al.*, 2018; Benito *et al.*, 2015). HDAC2 and HDAC6 have been proposed as the main responsible targets of pan-iHDACs-mediated memory improvement as HDAC2 inhibition would contribute to counteract cognitive deficits by enhancing memory related genes while HDAC6 inhibition would help to restore microtubule stability and cellular transport, thereby decreasing the accumulation of misfolded proteins (Cuadrado-Tejedor *et al.*, 2013). Although, using a specific HDAC3 inhibitor in a mouse model of AD, it has been recently demonstrated that this isoform is also implicated in tau and amyloid pathology amelioration, as well as in memory function improvement (Janczura *et al.*, 2018).

However, the main problem with pan-iHDACs is that HDAC class I inhibition (including HDAC2) has been associated with cytotoxicity, precluding its chronic use (Subramanian *et al.*, 2010). Accordingly, as HDAC6 inhibition presents a more safety profile, this isoform is currently being considered as one of the most promising epigenetic targets in AD.

7.1.2. Phosphodiesterases in Alzheimer's disease: PDEs

Phosphodiesterases (PDEs) are enzymes that catalyze the hydrolysis of cyclic guanosine monophosphate (cGMP) and/or cyclic adenosine monophosphate (cAMP) nucleotides to their corresponding 5'-nucleoside monophosphate forms (GMP and AMP respectively).

cAMP and cGMP are important second messengers that regulate signal transduction in different biological systems. They are of special interest in the central nervous system (CNS), where they respond to extracellular signals (neurotransmitters, hormones, olfactory and light signals) and activate intracellular targets such as ion channels, kinases and transcription factors provoking a specific cellular response. The extracellular signal is transferred by cyclical nucleotides to the effector proteins, being protein kinase A (PKA) and protein kinase G (PKG) two of the most important. These kinases in turn, phosphorylate other enzymes or transcription factors to finally produce the desired response (Puzzo *et al.*, 2008)(Figure 10).

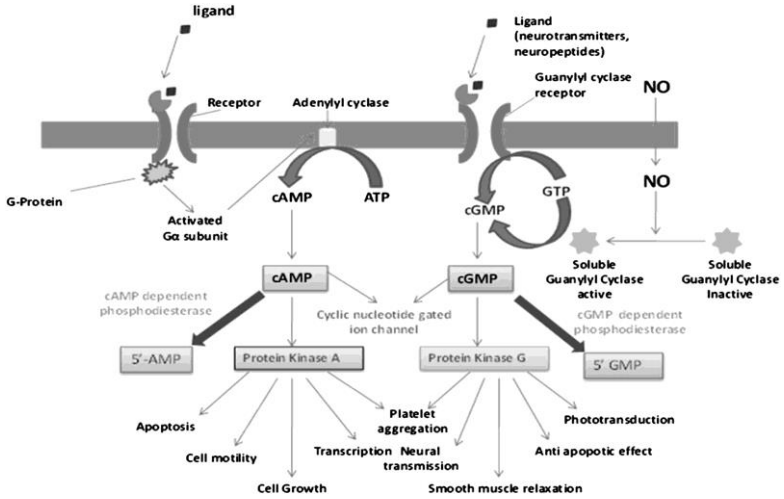

Figure 10. Pathway of signal transduction in the cell. Singh and Patra, 2014.

Cellular levels of cAMP and cGMP are maintained by a balance between their production and degradation. The enzymes adenylate cyclase (AC) and guanylate cyclase (GC) mediate its production while PDEs provoke its destruction. The temporal and spatial regulation of these signal nucleotides modulates the communication between several second messengers within the cell.

Phosphodiesterases can be classified into 11 families attending to different characteristics such as their subcellular distribution, structural similarities, regulatory mechanisms, sequence homology and enzymatic properties including substrate specificity, kinetic and sensitivity to endogenous regulators and inhibitors (Beavo, 1995). The main PDEs classification is based on their affinity for the substrate. Attending to this criteria three categories can be distinguished: PDEs specific for cAMP (PDE4, PDE7, PDE8), PDEs with exclusive affinity for cGMP (PDE5, PDE6, PDE9) and those with mixed specificity (PDE1, PDE2, PDE3, PDE10)(Omori & Kotera, 2007)(Figure 11).

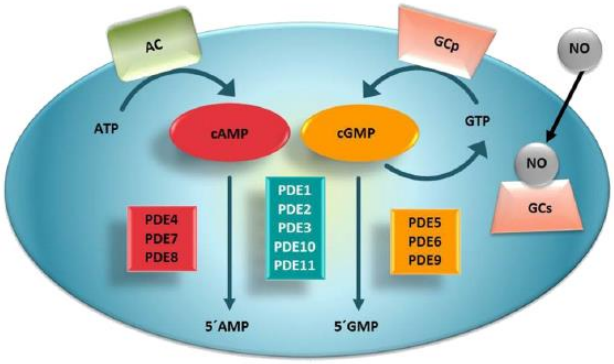

Figure 11. Phosphodiesterases classification according to their affinity for the substrate. AC: adenylate cyclase; GCp: guanylate cyclase particles; GCs, soluble guanylate cyclase; NO, nitric oxide.

Several studies have pointed out at PDEs as potential drug targets for a wide variety of diseases. In fact, inhibitors of PDE 3, 4 and 5 have been approved for medical conditions such as congestive heart failure, chronic obstructive pulmonary disease, erectile dysfunction and pulmonary hypertension (Zewail *et al.*, 2003; Setter *et al.*, 2005; Ahmad *et al.*, 2015). In the same line, various studies in the past years have been focus on elucidating the role of PDEs in the CNS and have proposed the use of PDEs inhibitors for CNS disorders (Kleppisch, 2009).

Most PDEs families are expressed in the brain although their level of expression varies among regions and, in some cases, even neurons of the same region. The expression of the different PDEs isoforms in the CNS is especially marked in brain areas involved in memory and learning (Xu *et al.*, 2011). PDE6 is the only isoform not detected in the CNS, being its expression mainly restricted to the ocular retina (Lagman *et al.*, 2016).

The activation of the cAMP/PKA pathway triggers the activation of transcription factors, such as cAMP response element-binding (CREB), which facilitates the transcription of genes necessary for learning and memory consolidation (Bernabeu *et al.*, 1997; Abel *et al.*, 1997). Alike, cGMP has also been linked with cognition. It indirectly enhances CREB phosphorylation due to increases in intracellular Ca^{2+} levels thus stimulating synaptic plasticity (Impey *et al.*, 1996; Lu *et al.*, 1999). It has been demonstrated that cGMP is able to regulate functions such as learning, memory and nerve regeneration (Houslay *et al.*, 2005; Teng & Tang, 2006; Tanis & Duman, 2007).

In consequence, the use of PDEs inhibitors has been pointed out as a potential therapeutic target for AD (García-Osta *et al.*, 2012). Previous studies in our laboratory have shown enhanced hippocampal PDE5 mRNA expression and decreased cGMP in the CSF of AD patients compared to control individuals (Ugarte *et al.*, 2015). Consequently, the efficacy of PDE5 inhibition for AD was tested after a chronic treatment with two different PDE5 inhibitors, sildenafil and tadalafil, in the Tg2576 and J20 AD mice respectively. In both cases, cognitive deficits were reversed and the observed memory restoration was independent of amyloid pathology. However, the beneficial effect was accompanied by a significant decrease of hippocampal and cortical ptau levels, a significant increase in

hippocampal BDNF, as well as an increase in dendritic spine density (Cuadrado-Tejedor *et al.*, 2011; García-Barroso *et al.*, 2013).

Within the brain, PDE9 is located in the cortex and hippocampus, two brain areas implicated in memory and learning processes (Xu *et al.*, 2011). Moreover, it is known that it plays a role in NO/cGMP/PKG signaling, pathway which is implicated in synaptic plasticity and cognition. All of these points out to a possible role for PDE9 in cognitive function and, consequently, as a therapeutic target for cognitive dysfunction in AD (Domek-Łopacińska & Strosznajder, 2010). It has been demonstrated that PDE9 inhibition improved rodent natural forgetting in social and object recognition, reversed scopolamine-induced impairments in passive avoidance and facilitated long-term potentiation (LTP) in hippocampal slices of aged-rats (van der Staay *et al.*, 2008). In the same line, a novel PDE9 inhibitor was able to reverse LTP impaired by $A\beta_{42}$ oligomers in rat hippocampal slices, enhance hippocampal cGMP levels and improve memory performance in the AD Tg2576 mice (Kroker *et al.*, 2014). Nowadays, a phase 2 clinical trial is being carried out to determine the effects of a PDE9 inhibitor (PF-04447943; ClinicalTrials.gov identifier: NCT00930059) in AD, although there are still no results available. And recently, the PDE9A inhibitor BI 409306 (Boehringer Ingelheim) failed to meet the primary outcome in phase 2 clinical trials, so the company decided to abort the study (Boehringer Ingelheim, 2018).

These evidences support the use of PDE5 and PDE9 inhibitors as therapeutic candidates for AD.

7.1.3. Dual HDAC and PDE inhibition for Alzheimer's disease treatment

Nowadays, it is widely believed that successful AD treatment will involve a "multi-therapy" based on a cocktail of medications directed at several targets (Mangialasche *et al.*, 2010; Cummings *et al.*, 2018). Moreover, it has been demonstrated that the combination of different drugs can produce synergistic effects that allow dose reduction and consequently, toxicity and side-effects minimization (Lehár *et al.*, 2009).

Accordingly, in our laboratory, a new approach that targets different pathways involved in AD pathology (Figure 12) has been proposed as a possible therapy for AD.

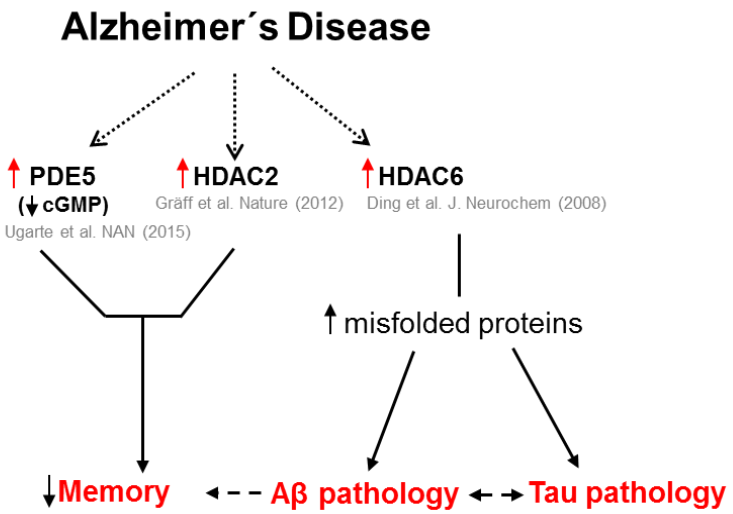

Figure 12. Relationship of PDE5, HDAC2 and HDAC6 with Alzheimer's disease pathology.

The novel multi-target therapy proposed is based on the concomitant inhibition of HDACs and PDE5, enzymes that are up-regulated in AD (Ding *et al.*, 2008; Gräff *et al.*, 2012; Ugarte *et al.*, 2015)(Figure 12) and that has been recently validated using the reference compounds vorinostat (pan-HDAC1 inhibitor) and tadalafil (PDE inhibitor). The combination of subeffective concentrations of vorinostat and tadalafil rescued LTP impairment in slices from APP/PS1 mice. Moreover, when it was administered *in vivo*, improved memory deficits, ameliorated amyloid and tau pathology and increased dendritic spine density on hippocampal neurons of Tg2576 mice. Interestingly, a synergistic effect was observed with the combination of vorinostat and tadalafil since it lead to a more efficacious effect than when each drug was separately administered (Cuadrado-Tejedor *et al.*, 2015)(Figure 13).

The efficacy of this therapeutic approach was then confirmed using a new drug and novel chemical entity (NCE), CM-414, that acts as a dual inhibitor of PDE5 and HDACs with a moderate activity against class I HDAC and potent activity against HDAC6 and PDE5 (Rabal *et al.*, 2016; Cuadrado-Tejedor *et al.*, 2017). As occurred with the combination, a chronic treatment of Tg2576 mice with CM-414 diminished the accumulation of Aβ and ptau in the brain, reversing the decrease in dendritic spine density on hippocampal neurons and the cognitive deficits in these mice. These effects were, at least in part, produced by an induction in the expression of synaptic transmission-related genes (Cuadrado-Tejedor *et al.*, 2017). It is also interesting that the therapeutic effects with both therapies, the combination of vorinostat and tadalafil and the compound CM-414, persisted one month after the completion of a 4-week treatment period (Cuadrado-Tejedor *et al.*, 2015, 2017)(Figure 13).

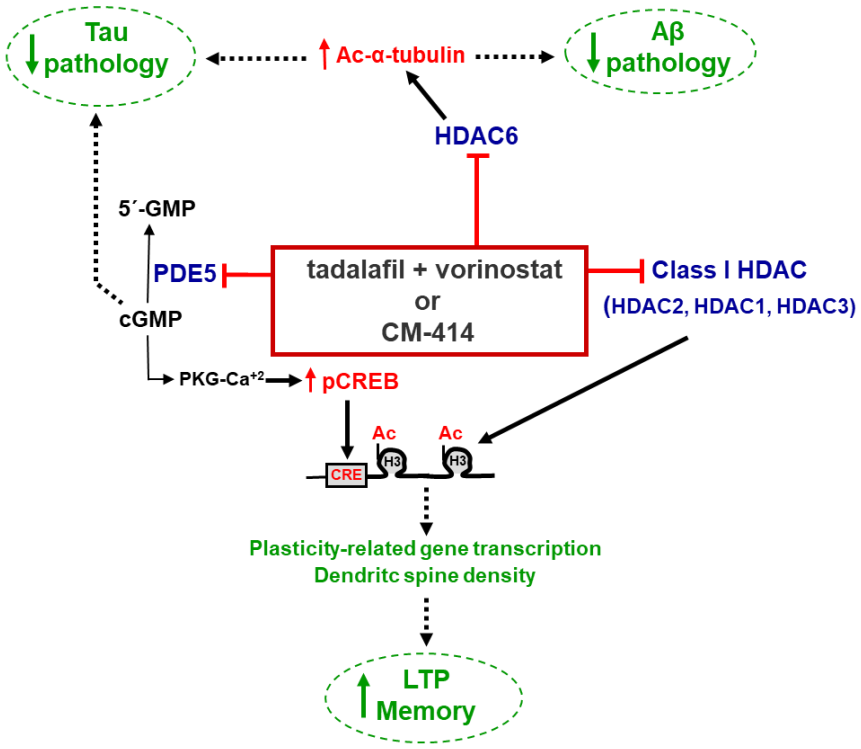

Figure 13. Proposed mechanism of action for the combination tadalafil and vorinostat or for the compound CM-414 over AD pathological hallmarks. HDAC: histone deacetylases; Ac: acetyl; PDE: phosphodiesterases; PKG: protein kinase G.

Due to the synergistic effect observed when inhibiting HDAC and PDE5, that directs the transcription through CREB-dependent genes, a strong inhibition of HDAC class I is not necessary to trigger the transcription of memory-related genes. In this sense, as HDAC inhibitors are not the best option for chronic treatments due to their known associated-cytotoxicity (Subramanian *et al.*, 2010), the use of therapeutic strategies combining HDAC and PDE inhibition may be a good option to reduce toxicity and increase efficacy. However, it would be interesting to find similar strategies avoiding HDAC class I inhibition, as it could preclude their clinical use.

7.2. Study of cognitive resilient subjects to identify new therapeutic targets for AD

Studying AD is becoming really complex as sometimes, there is discordance between the appearance of the classic AD markers (amyloid plaques and NFTs) and the symptoms of dementia.

Substantial AD lesions have been observed in the brain of cognitively normal elderly subjects in several longitudinal studies. For example, in the known as the Nun Study, a 12% of the participants with normal cognition showed significant amounts of Aβ and NFTs (Riley *et al.*, 2005). Similarly, in the 90+ Study, Aβ accumulation was found in about ¼ - ½ of the elderlies that did not shown any kind of cognitive deficit (Balasubramanian *et al.*, 2012).

These findings suggest that classical AD hallmarks are not enough to produce dementia and open the possibility of study this AD resilient patients in order to find new targets for AD treatment. It should be noted that, in the world of AD research, the term resilience applies to people who live into old age without apparent symptoms of dementia despite having high burden of AD pathology in their brains. These people would be expected to develop dementia and never do (Wanucha, 2018).

Most of the studies about cognitive resilient individuals pointed out a combination of some genetic and environmental factors as causes of the resilience (Iacono *et al.*, 2009; Legdeur *et al.*, 2018).

It is widely accepted that subjects with higher brain and/or cognitive reserve tolerate better the age- and AD- related pathological brain changes. The term "brain reserve" constitutes a passive model of reserve and refers to actual differences in the brain itself, such as intracranial and brain volume, that correlate with the number of neurons and synapsis. In contrast, the term "cognitive reserve" suggests that in some way, the brain actively attempts to cope with damage by using pre-existing cognitive processing approaches or by enlisting compensatory approaches. For example, it has been reported that individuals with higher education have greater cognitive reserve (Stern, 2012; Negash *et al.*, 2013; Arnold *et al.*, 2013).

On the other hand, several studies suggest that some lifestyle related factors such as physical performance or specific diets can modulate the individual's capacity to deal with age- or disease- related neuronal problems, either promoting or avoiding them (Bullain *et al.*, 2013; Shlisky *et al.*, 2017).

Regarding AD-related biomarkers, lower amounts of mature senile plaques have also been linked with cognitive resilience in elderly subjects (Perez-Nievas *et al.*, 2013) and, in the same line, differences in astrogliosis and/or microglial activation have been pointed out as possible causes of resilience, despite the obtaining of controversial results (Arnold *et al.*, 2013; Perez-Nievas *et al.*, 2013).

However, the molecular mechanisms underlying cognitive resilience have not been studied. Iacono *et al.* observed neuronal hypertrophy in AD resilient patients and suggested that it may constitute a compensatory mechanism against dementia through the augmentation of the transcription of memory-related genes, indicating that differences in gene expression may also play a role in the protection against AD-associated cognitive deterioration (Iacono *et al.*, 2009), although further studies would be needed to confirm it.

Nevertheless, the chance of identifying the factors responsible of the observed protection against dementia in these subjects is hindered by the intrinsic limitations of using postmortem brain samples (Ferrer *et al.*, 2008) and by its variability (Caspers *et al.*, 2014). Accordingly, the use of transgenic mice would facilitate the identification of the resilient causal factors through the minimization of the environmental and genetic variability present in human patients. Interestingly, as it occurs in humans, it has been reported that

at 8 month-old (mo), a 30% of the AD 5XFAD model showed intact fear contextual memory (Neuner *et al.*, 2017).

In fact, the identification of resilient individuals had also been reported while using animal models for other diseases such as Duchenne Muscular Dystrophy, where a mutation in the dystrophin gene causes muscular dysfunction in these patients. A recent study had identified two Golden Retriever Muscular Dystrophy dogs that, despite the complete absence of dystrophin, were mildly affected and had functional muscle and normal lifespan (Zucconi *et al.*, 2010). The study of these resilient dogs allowed the identification of Jagged1 as a new target for Duchenne Muscular Dystrophy therapy (Vieira *et al.*, 2015).

Therefore, studying cognitive resilient mice could be a really valuable tool to find new targets and therapeutic approaches for AD treatment thus giving new hope to AD patients.

HYPOTHESIS AND OBJECTIVES

The lack of an effective treatment for AD, together with the high failure rate in AD clinical trials, suggests the necessity to change the way of approaching the study of this pathology.

Taking into account the multifactorial nature of this disease, several authors have pointed out that treatments targeting a single cause of the disease may lead to limited benefits. In this regard, the use of combined therapies or multi-modal action drugs has been proposed as a promising strategy for AD treatment (Mangialasche *et al.*, 2010; Cummings *et al.*, 2018).

For this reason, a novel multitarget therapy for AD focused on the concomitant inhibition of HDACs and a PDE5 has been recently validated in our laboratory using reference compounds (tadalafil and vorinostat) and a NCE, CM-414. This compound acts as a dual inhibitor of PDE5 and HDACs with moderate activity against class I HDAC and potent activity against HDAC6 and PDE5. This approach was able to ameliorate AD histopathological hallmarks and reverse cognitive impairment in the Tg2576 mouse model of AD (Cuadrado-Tejedor *et al.*, 2015, 2017).

In order to avoid the side effects related to class I HDAC inhibition (Subramanian *et al.*, 2010) a new NCE, CM-695, able to simultaneously inhibit HDAC6 and PDE9 was synthesized to be tested *in vivo*. Note that it inhibits PDE9 instead of PDE5 as it has been described that PDE9 is the PDE most highly expressed in the brain (Andreeva *et al.*, 2001).

However, the use of multi-modal action drugs may be not enough to treat efficiently AD so, it is possible that a more drastic change in the way of studying this disease would be needed to achieve it. Consequently, in the present thesis, apart from testing this novel multi-target approach for AD treatment, it has been proposed to identify new targets for AD by studying cognitive resilient subjects (from AD mouse models) that present normal cognition despite having elevated amounts of amyloid and tau pathology. As it happened in Duchenne Muscular Dystrophy, the study of resilient subjects could allow the identification of novel targets for AD (Vieira *et al.*, 2015).

Thus, the main objective of the present thesis is to validate novel therapeutic strategies for AD, being the specific objectives:

1. To test the efficacy of a chronic treatment with CM-695, a dual HDAC6 and PDE9 inhibitor, on a well-established mouse model of AD, the Tg2576. Being the concrete aims:

    1.1. To analyze its effect on cognitive function by two behavioral tests: the fear conditioning and the Morris Water Maze.
    1.2. To check its effect on amyloid pathology by measuring $A\beta_{42}$ levels using an ELISA assay.
    1.3. To test its effect on synaptic plasticity thought the determination of synaptic spine density using the Golgi-Cox method.

1.4. To elucidate its mode of action taking into account the pathways differentially expressed with the treatment in an Affymetrix Microarray Hybridization assay.

2. To identify and validate novel targets for AD by studying cognitive resilient AD mice, specifically:

2.1. To identify, through the MWM test, cognitive resilient aged-Tg2576 mice.
2.2. To neuropathologically characterize these cognitive resilient AD mice using different biochemical tools.
2.3. To identify gene(s) involved in cognitive resilience using an Affymetrix Microarray Hybridization assay.
2.4. To validate selected gene(s) as therapeutic targets for AD modulating its hippocampal expression though adeno-associated viral vectors.

MATERIALS AND METHODS

1. Experimental animals

Two different AD *murine* models, the Tg2576 and the APP/PS1, were used in the present thesis together with their respective negative littermates (WT mice).

The Tg2576 model express human 695-aa isoform of the amyloid precursor protein (APP) containing the Swedish double mutation (APPswe) [(APP695)Lys670→Asn, Met671→Leu] under the control of a hamster prion promoter. These mice are on an inbred C57BL/6/SJL genetic background and present Aβ accumulation from 7 months, amyloid burden, memory impairment (fear-memory deficits from 6 months and spatial-memory impairment from 12 months), synaptic pathology, tau hyper-phosphorylation and increased neuroinflammation (Hsiao *et al.*, 1996; Chapman *et al.*, 1999; Westerman *et al.*, 2002). Only female Tg2576 mice (and their negative female littermates) were used in this thesis as they present a more advanced AD phenotype (Callahan *et al.*, 2001) and are less aggressive than males.

The APP/PS1 model expresses human transgenes for the APP bearing the Swedish mutation and for the PSEN1 containing a L166P mutation, both driven by the Thy1 promoter. These mice are on an inbred C57BL/6J genetic background. The AD *murine* model APP/PS1 is a more accelerated amyloidosis model than the Tg2576. In this model, the expression of human APP transgene is approximately three times higher than that of endogenous murine APP and human $A\beta_{42}$ is preferentially generated over $A\beta_{40}$. Moreover, amyloid plaque deposition starts in the hippocampus at 3-4 months *(Maia et al.,* 2013; Radde *et al.,* 2006) and cognitive impairment is presented from 7 months (Serneels *et al.,* 2009). In the case of APP/PS1 and their correspondent negative littermates, both male and female mice were used for the experiments in the present thesis.

Animals were bred and housed in the animal facility at Center for Applied Medical Research (CIMA) in Pamplona. They were housed 3-6 per cage with free access to food and water and maintained in a temperature and humidity controlled environment on a 12 hours light-dark cycle. Behavioral tests were always conducted between 8:00 and 15:00 to minimize the influence of circadian rhythms.

All procedures developed in the present work were in agreement with the European and Spanish regulations (2010/63/EU; RD52/2013) and the study was approved by the Ethical Committee for the Animal Experimentation of the University of Navarra (protocols no. 079-14, 040-17 and 113-18).

2. Animal genotyping

2.1. DNA extraction

Genotyping was carried out at postnatal day 21 by polymerase chain reaction (PCR) from mice genomic DNA obtained of ear fibroblasts. After anesthetizing the animals with a combination of ketamine/xylazine (80/10 mg/kg) injected intraperitoneally, a punch of ear was taken to subsequently extract DNA by using the DNeasy Tissue commercial kit (Qiagen).

2.2. Conventional PCR

In the case of Tg2576 mice, the primers used (Table 1) enabled the determination of the presence or absence of the APP_{swe} transgene.

For APP/PS1 mice genotyping two PCRs, each with a different couple of primers (Table 2), were needed to determine the presence or absence of both the APP_{swe} transgene and the one for PS1 with the L166P mutation.

Table 1. Primers used for Tg2576 mice genotyping by conventional PCR.

Name	Sequence	Complementarity
1501	5' AAGCGGCCAAAGCCTGGAGGGTG 3'	3' murine PrP promoter
1502	5' GTGGATAACCCCTCCCCCAGCCTAGACCA 3'	5' murine PrP promoter
APPx1501	5' GTTGAGCCTGTTGATGCCCG 3'	APP_{swe}

Table 2. Primers used for APP/PS1 mice genotyping by conventional PCR.

Name	Sequence	Complementarity
APP1597	5' GACTGACCACTCGACCAGGTTCTG 3'	APP_{swe}
APP1598	5' CTTGTAAGTTGGATTCTCTCATATCCG 3'	APP_{swe}
PSEN1644	5' AATAGAGAACGGCAGGAGCA 3'	PS1 (L166P mutation)
PSEN1645	5' GCCATGAGGGCACTAATCAT 3'	PS1 (L166P mutation)

To carry out the PCR, 5 µl of 5x buffer (Promega), 2 µl of 2.5 mM dNTPs (Invitrogen), 1.5 µl of 25 mM $MgCl_2$, 1 µl of each primer at 5µM, 0.2 µl of 5 U/µl GoTaq DNA Polymerase (Promega), 2 µl of genomic DNA and sterile distilled water q.s. 25 µl were mixed and then submitted to the PCR cycles depicted in figure 14 through the GeneAmp PCR System 2400 (Applied Biosystems).

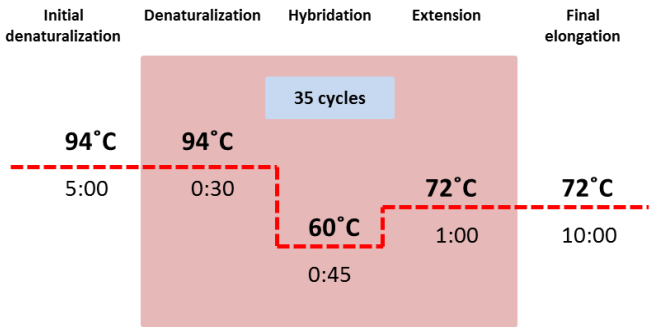

Figure 14. Temperature cycles used to genotype Tg2576 and APP/PS1 mice by conventional PCR.

2.3. DNA electrophoresis in agarose gels

One percent agarose gels were prepared in 1x TAE buffered solution [40 mM Tris-Acetate and 1 mM EDTA (pH 8.0)]. SYBR Safe DNA Gel Stain (Life Technologies, dilution 1:25000) was also added to the liquid agarose solution to enable DNA bands visualization under ultraviolet light.

The products obtained by conventional PCR as described in section 2.2 were loaded onto the agarose gels and they underwent an electrophoresis at 100 V to achieve the separation of the bands.

In the case of Tg2576 genotyping, the presence of the transgene was manifested by a fragment of 470 base pairs (bp), product of the amplification carried out by the oligonucleotides 1501 and APPx1501. PrP promoter, that was used as internal control, was detected as a single band of 760 bp amplified by the primers 1501 and 1502.

For APP/PS1 genotyping, the presence of the APP_{swe} transgene was detected by a band of 350 bp correspondent to the amplification product of the primers APP1597 and APP1598 in a first PCR and the presence of the transgene for PS1 with the L166P mutation by another band (608 bp) resultant of the amplification with the oligonucleotides PSEN1644 and PSEN1645 in other PCR.

3. *In vitro* studies

3.1. Human neuroblastoma SH-SY5Y cell line culture

Cells of the human neuroblastoma SH-SY5Y cell line were plated in 6-wells plates and incubated at 37 °C in a humid atmosphere with 5% CO_2, until reaching a confluence of 80-90%. They were cultivated in Eagle's medium modified by Dulbecco (DMEM, Gibco) supplemented with 1% non-essential amino acids solution (Gibco), penicillin/ streptomycin 100 U/ml (Gibco) and 10% fetal bovine serum (Gibco).

3.2. Treatments

To determine the functional activity of the compound CM-695, cells at 90% of confluence were incubated with different concentrations of CM-695 (0, 1 nM, 10 nM, 100 nM, 500 nM and 1μM) during 2 hours. After incubation, the medium was removed and the cells were washed twice with PBS. Then, they were lysed in 150 μL of a buffer containing 2% SDS, 10 mM Tris-HCl (pH=7.5), phosphatases inhibitors (1 mM NaF and 0.1 mM Na_3VO_4) and the Complete Protease Inhibitor Cocktail (Roche). Protein was extracted from these homogenates as described in section 10.1.1 to subsequently carry out a western blot to analyze the acetylated histone 3 at lysine 9 (AcH3K9), pCREB, acetylated tubulin and β-actin.

3.3. Transfection

Murine PLA2G4E was overexpressed *in vitro* by transfection of SH-SY5Y cells with the pRK5-PLA2G4E plasmid, that was kindly ceded by Dr.Cravatt's (Ogura *et al.*, 2016). To check the specificity of the *murine* PLA2G4E overexpression, a parallel transfection was done using the same plasmid combined with an interference RNA for the mentioned enzyme, specifically a siRNA (sense m-PLA2G4E: GGUCUAUGGUCUCCUUGUA[dT][dT] and anti-sense m-PLA2G4E UACAAGGAGACCAUAGACC[dT][dT], SIGMA).

Transfection was carried out in cells at 80% of confluence using 3 µl/well Lipofectamine (Invitrogen) transfection reagent in Opti-MEM medium (Gibco). Plasmid pRK5-PLA2G4E and siRNA final concentrations were 0.125 µg/ml and 100 nM respectively. Transfection with siRNA was carried out 2 h after the transfection with pRK5-PLA2G4E plasmid in the correspondent wells. Culture medium was renewed 6 h after the transfection with pRK5-PLA2G4E plasmid and cells were maintained 48 h in culture. After that, medium was removed and cells were washed twice with PBS. Then, they were lysed in 150 µL of a buffer containing 2% SDS, 10 mM HCl (pH=7.5), phosphatases inhibitors (1 mM NaF and 0.1 mM Na_3VO_4) and the Complete Protease Inhibitor Cocktail (Roche) and protein was extracted from the homogenates as described in section 10.1.1. Subsequently, an immunoblot was carried out as described in section 10.2 for PLA2G4E analysis.

4. Human samples

Brain samples from the Biobank of the Navarre Health Service-Osasunbidea were used in the present work. The samples came from patients which met the criteria for the diagnosis of dementia type AD with severe cognitive impairment (AD; n=9)(Table 3) proposed by the National Institute on Aging (NIA) of the United States and the Alzheimer's Association (McKhann *et al.*, 2011), from asymptomatic AD patients (AAD; n=10)(Table4), that presented amyloid and/or tau pathology in their brains but did not develop cognitive impairment, and from age-matched healthy people (controls; n=8) (Table 5).

Table 3. Relevant information about Alzheimer's disease (AD) cases.

Case	Age	Sex	Clinical diagnosis	Neuropathological diagnosis
BCN62	79	Female	Vascular mild cognitive impairment vs probable AD	AD-III B
BCN112	77	Female	Cognitive impairment due to primary cortical affectation	AD-V B
BCN267	78	Male	AD	AD-VI
BCN277	71	Male	AD	AD-VI
BCN288	73	Male	Probable AD	AD-VI C
BCN291	83	Male	AD	AD-VI C
BCN341	61	Male	Cortical degenerative disease. AD	AD-VI C
BCN369	86	Male	Senile dementia	AD-VI C
BCN549	81	Female	AD	AD-VI C

AD: Alzheimer's disease; AD-III B, AD-V B, AD-VI, AD-VI C: Alzheimer's disease patient with Braak stage III B, V B, VI and VI C respectively.

Table 4. Relevant information about asymptomatic Alzheimer's disease (AAD) cases.

Case	Age	Sex	Clinical diagnosis	Neuropathological diagnosis
BCN66	69	Female	Cognitive impairment not mentioned in the clinical report	AD-III B
BCN162	79	Male	Without cognitive impairment	AD-IV B
BCN181	83	Male	Without antecedents of cognitive impairment	AD- IV B
BCN207	87	Male	Familiars reported no cognitive impairment	AD-V B
BCN238	85	Female	Without cognitive impairment	AD-III C
BCN241	98	Female	Without cognitive impairment	AD-II C
BCN302	99	Female	Without cognitive impairment	AD-II A
BCN438	86	Female	Without cognitive impairment	AD-II A
BCN442	71	Male	Without cognitive impairment	AD-II A
BCN446	79	Male	Without cognitive impairment	AD-II only NFTs

AD: Alzheimer's disease; AD-II, AD-II A, AD-II C, AD-III B, AD-III C, AD-IV B, AD-V B: Alzheimer's disease patient with Braak stage II, II A, II C, III B, III C, IV B and V respectively; NFTs: neurofibrillary tangles.

Table 5. Relevant information about control cases.

Case	Age	Sex	Clinical diagnosis	Neuropathological diagnosis
BCN251	53	Male	Without cognitive impairment	CNS with light hypoxia
BCN256	80	Male	Without cognitive impairment	Subdural, subarachnoid and intraparenchymal hemorrhage in the left hemisphere
BCN283	103	Male	Without cognitive impairment	Mild demyelination of the white matter
BCN362	72	Male	Without cognitive impairment	Signs of cerebral anoxia
BCN382	66	Male	Without cognitive impairment	Signs of cerebral anoxia
BCN473	65	Male	Without cognitive impairment	Left cerebellar hemisphere infarction
BCN600	72	Male	Without cognitive impairment	Control
BCN618	68	Female	Without cognitive impairment	Arteriovenous angioma of 6 mm in the cerebellum

CNS: Central nervous system

In all cases, an informed consent was obtained from the subject's relatives prior to the extraction of brain tissue. Once temporal cortex samples were acquired during the autopsy, they were stored at -80 ºC until processing. This study was carried out in agreement with the Ethics Committee of the University of Navarra (protocol no. 2018.020).

5. Generation of the virus AAV2/9-hsynapsin-PLA2G4E

5.1. Viral vector construction

5.1.1. Cloning of PLA2G4E under the control of human synapsin promoter in AAV genome

Full-length mouse phospholipase A2 group IVE (PLA2G4E) was cloned into the pRK5 vector with C-terminal FLAG tag using Sal I and Not I sites by Dr.Cravatt's team (Ogura *et al.*, 2016), who kindly ceded the pRK5-PLA2G4E plasmid to our laboratory. To allow the subsequent cloning into the adeno-associated virus (AAV) genome, this plasmid was digested with XmnI and Sac I, both in CutSmart Buffer, to create a blunt and a sticky end respectively. An electrophoresis in 1% agarose gels, that allows the separation of DNA fragments, was then carried out thus enabling the obtaining of a 3108 bp fragment. This fragment, that contains the PLA2G4E and FLAG sequences, was extracted from the gel using the commercial system QIAquick Gel Extraction kit (Qiagen) and purified through QIAquick PCR Purification kit (Qiagen) before its sequencing. It was then ligated in a rAAV2-hsynapsin vector obtained from the rAAV2-hsynapsin-hα-synucleinA53T plasmid (kindly gifted by Dr. J. Gerez), which contains AAV2 inverted terminal repeats (ITRs), an improved neuronal promoter based on human synapsin and which confers ampicillin resistance. The rAAV2-hsynapsin-hα-synucleinA53T was subjected to several steps to eliminate the α-synuclein sequence before the ligation procedure. It was digested with Xhol (in CutSmart Buffer) and treated with Klenow polymerase, dNTPs and NEB2.1 buffer, which allows the generation of blunt ends. After being purify, this new fragment was digested with SacI (in CutSmart Buffer) and dephosphorylated using the Shrimp Alkaline Phosphatase (rSAP) to avoid vector re-ligation. As mentioned before, the DNA obtained was subjected to an electrophoresis in 1% agarose gel and the fragment of 4163 bp generated was then extracted from the gel, purified and sequenced.

Once both fragments (3108 bp from pRK5-PLA2G4E and 4163 from rAAV2-hsynapsin vector) were isolated, they were ligated though a T4 DNA ligase (Invitrogen). The amount of viral vector used was 100 ng and, to obtain a high efficiency, two molecular ratios insert:vector were tested, 1:1 and 3:1.

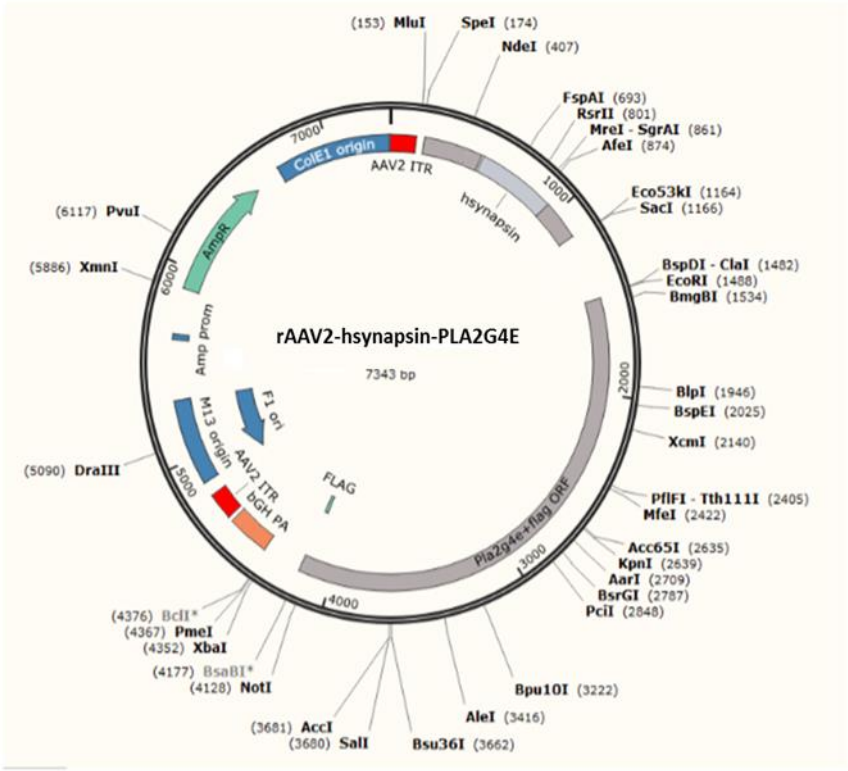

Figure 15. Sequence map of rAAV2-hsynapsin-PLA2G4E plasmid containing a neuronal hybrid promoter composed of the CMV immediate-early enhancer fused to human synapsin promoter, the coding sequence for PLA2G4E and the tag FLAG, the bovine growth hormone poly A signal and the AAV2 inverted terminal repeats (ITRs) among other elements.

5.1.2. Amplification of the rAAV2-hsynapsin-PLA2G4E

Once the desired construct was produced (Figure 15), it was subjected to several steps to generate an appropriate amount of plasmid for final virus production.

Firstly, *E.coli* chemically-competent bacteria were transformed with the plasmid using TOP10 electro-competent cells (Invitrogen) and the bacteria that had incorporated the plasmid were selected by plating on LB medium with ampicillin (50µg/ml). Then, the plasmid was obtained and purified from the bacteria using a QIAprep Spin Miniprep kit (Qiagen). After checking the presence and correct orientation of the insert, as well as the presence of the AAV2 ITRs, a commercial QIAGEN Plasmid Maxi kit (Qiagen) was used to obtain and purify the desired amount of plasmid from the ampicillin resistant clones.

5.2. AAV2/9-hsynapsin-PLA2G4E virus production

Recombinant single-stranded AAV2/9 vectors were obtained and purified from HEK-293T cells that had been previously co-transfected using 25 kDa linear polyethylenimine (Polysciences) with two different plasmids: one containing ITR-flanked transgene constructs (rAAV2-hsynapsin-PLA2G4E) and the other (pDP9) containing the adenoviral helper genes plus AAV2 rep and AAV9 cap as described by Dr. Kamen's laboratory (Durocher *et al.*, 2002). Supernatant was treated with polyethylene glycol

solution (PEG8000, 8% v/v final concentration) for 72 h at 4°C and centrifuged at 1734 g for 15 min. Pellet containing particles from the supernatant was resuspended in lysis buffer (50 mM Tris-Cl, 150 mM NaCl, 2 mM MgCl2, 0.1% Triton X-100) and kept at −80°C. In the same way, cells containing AAV particles were also collected, treated with lysis buffer and maintained at -80ºC. Then, both lysates were subjected to three cycles of freezing and thawing to allow viral liberation. They were also treated with DNaseI/RNaseA for 30 min at 37 ºC and centrifuged again at 1445 g for 10 min. The viral particles obtained from supernatants were then purified by ultracentrifugation in an iodixanol gradient according to Zolotukhin's method (Zolotukhin *et al.*, 1999). To further concentrate the viral batches, they were passed through Centricon tubes (YM-100, Millipore) and kept at -80ºC.

Viral titration, expressed as viral particles (vp)/ml, was obtained through quantitative PCR (qPCR) using primers for mouse PLA2G4E: forward 5′-ATGGTGACAGACTCCTTCGAG -3′ and reverse 5′- CCTCTGCGTAAAGCTGTGG -3′. The viral title obtained was 2.6 x 10^{11} vp/ml.

6. Stereotactic surgery for viral administration

To overexpress PLA2G4E in hippocampal neurons, mice were administered with the adeno-associated virus AAV2/9-hsynapsin-PLA2G4E (called from now AAV9-PLA2G4E to simplify) in the CA1 region of the hippocampus through a stereotactic surgery. This procedure is based on a three-dimensional system of axes and spatial coordinates that allows the localization of specific points in the mouse brain (given as three-dimensional distances in millimeters (mm)) taking bregma or lambda, two easily identifiable points in the brain, as reference. In the present work, with the help of a mouse atlas (Paxinos & Franklin, 1997), the coordinates chosen for hippocampal CA1 injection were: antero-posterior -2.0 mm; half-side ± 1.7 mm; dorso-ventral -2.0 mm using bregma point (formed by the intersection between the sagittal and coronal suture) as reference.

Before viral administration or sham-procedure (only the surgery), animals were anesthetized with an intraperitoneal (i.p) dose of 80/10 mg/Kg of ketamine/xylazine and treated with the analgesic buprenorphine (Buprex) at a dose of 0.1 mg/Kg . Once they were fully anesthetized, they were placed in the stereotactic device with the head completely immobilized. After disinfecting the area with 96º alcohol, an antero-posterior cut was made in the skin using a scalpel, releasing thus the skull from its periosteum and leaving visible the bregma and lambda reference points. Next, with the help of a drill bill, a hole was made in the skull and a 5 µl Hamilton syringe was placed on the stereotaxic arm loaded with the virus (2.6 x 10^8 genomic copies) or unloaded (for sham procedure). Once positioned on the exact coordinate, 1 µl of the solution was injected at 0.2 µl/min and then, the syringe was maintained there for another 2 min to allow correct diffusion of the virus before withdrawing slowly the syringe. The same procedure was repeated for the other hemisphere. Once animals were bilaterally injected, the wound was sutured and povidone iodine (Betadine) was administered topically. Then, animals were placed on an electric blanket to avoid heat lost until their awakening. Finally, they were stabled in

cages with easy access to softened-in water food to facilitate food intake after surgery. Throughout the intervention, physiological serum was continuously applied in mice eyes to avoid their dryness and consequent loss of vision.

***7. In vivo* treatments**

7.1. Treatment with CM-695

Different groups of mice were administered intraperitoneal (i.p) with CM-695 (40 mg/kg) or vehicle (10% dimethylsulfoxide (DMSO) and 10% Tween-20 in saline solution) along the present thesis. Note that drug solution was prepared daily to avoid precipitation due to their hydrophobic nature.

- Functional response of CM-695 in mouse brain was assessed *in vivo* in a group of 2 months-old WT mice (acute treatment: one single injection).

-The effect of the compound CM-695 on memory function and AD pathology was tested in 16-18 months-old Tg2576 mice (chronic treatment: four weeks).

7.2. AAV9-PLA2G4E administration

Along the present doctoral thesis several groups of mice were treated with the AAV9-PLA2G4E generated:

-A pilot study was performed in 17 months-old WT mice to analyze the effect of hippocampal PLA2G4E overexpression on memory function.

-Another study was realized in 16-19 months-old APP/PS1 mice to test the effect of hippocampal PLA2G4E overexpression on memory function and AD-related physiopathology.

8. Behavioral tests

8.1. Morris Water Maze test

The Morris Water Maze (MWM) is a behavioral test that analyzes both spatial and working memory. It is considered as a consistent test for hippocampal damage evaluation, which is one of the main characteristics of AD in humans (D'Hooge & Deyn, 2001).

This test was carried out in a circular pool (diameter 1.2 m) filled with water at 20 ºC and made opaque by the addition of non-toxic white paint. The pool was divided into four imaginary quadrants, in one of which was located the platform that the mouse must learn to locate in order to escape from water and be safe. In each of the four walls that surround the pool there was a picture of a geometric figure that would serve as a guide for the mouse and that would have been cover or uncover depending on the phase of the test. Throughout the test, mice behavior was monitored by a camera anchored in the ceiling, just above the pool, and recorded with an HVS system to allow the subsequent analysis of escape latencies, swimming speed, path length and percentage of time spent in each quadrant of the pool using the software SMART-LD (Panlab)(Figure 16).

Three different phases can be distinguished in the MWM test (Figure 16):

1) Visible-platform phase: In this phase, the platform was located in the center of one of the quadrants, elevated 1 cm above the water and identified by a piece clearly visible to the animal in order to facilitate its location. Here, mice should became familiar with the pool and learn to go to the platform to escape from water, so the visual clues remain hidden. Mice were trained 8 times *per* day during 3 consecutive days. In each trial, mice had 60 s to locate the platform; if they could not reach it during this period, they were placed on it. Once the animal was on the platform, it was allowed to inspect it for 15 s before being returned to its cage.

2) Hidden-platform phase: In the second phase of the test, the platform was located in the opposite quadrant to that on the visible platform-phase. It was submerged 1 cm below the water level, without any piece above it. In this stage, mice should learn how to locate the platform with the help of the clues presented in the walls, that are now uncovered. For it, mice were trained four times *per* day during 4-9 days (depending on the experiment). As in the previous stage, mice had 60 s to reach the platform. If they could not locate it in 60 s, they were led to it. In both cases, they remained on the platform for 15 s. Three random start positions were established in each of the quadrants not occupied by the platform to avoid the appearance of trajectory preferences in mice.

3) Probe trial: Memory retention was evaluated in probe trials carried out at different days of the hidden-platform phase, before starting the hidden-platform trials of the chosen day. For this test, the platform was removed from the pool and animals were allowed to swim for 60 s. The time that mice spend in the quadrant where the platform was placed during the hidden-platform phase is considered an estimate of memory retention capacity. Retention rates higher than 25% are considered indicative of learning while those lower than 25% are considered random. Time spent in the correct quadrant was analyzed both, during the first 15 s of the test, as it has been suggested that the sensitivity of the MWM test can be increased by giving shorter probe trials (Gerlai, 2001), and during the whole 60 s.

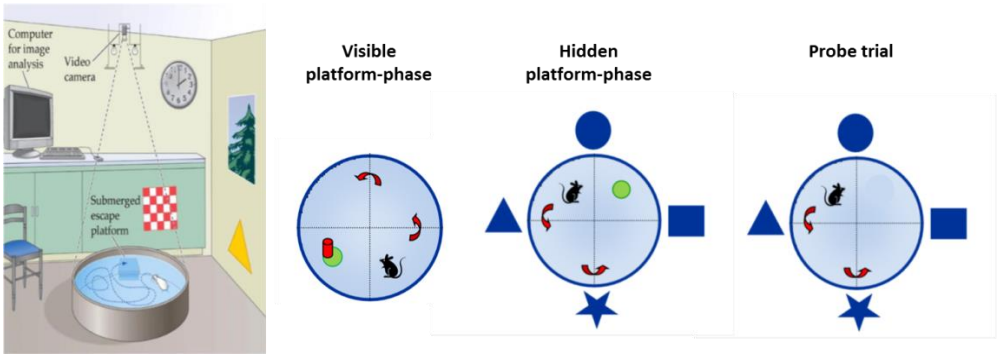

Figure 16. Scheme of the MWM test: devices employed and phases of the test.

Four weeks or two months after the first MWM, the hidden platform phase and the probe trials were performed again changing the location of the platform in a test known as reversal MWM.

8.2. Fear conditioning test

The fear conditioning (FC) test is a highly hippocampal dependent behavioral test that allows studying long-term memory consolidation by assessing the association between two stimuli, one conditioned (context) and another unconditioned (an electric shock) (Maren, 2008). It is a type of classical or Pavlovian conditioning where the mouse receives a brief electric shock (unconditioned stimulus) after staying a while in a conditioning chamber (conditioned fear context). The strength of the association between both stimuli is measured by the freezing time that is the time that the rodent remains immobile, just with a residual movement caused by its normal breathing, when it is re-exposed to the same conditioning chamber. A StartFear Combined system (Panlab) (Figure 17), which transmits the analog signal toward the software FREEZING and STARTLE, was used to carry out this test.

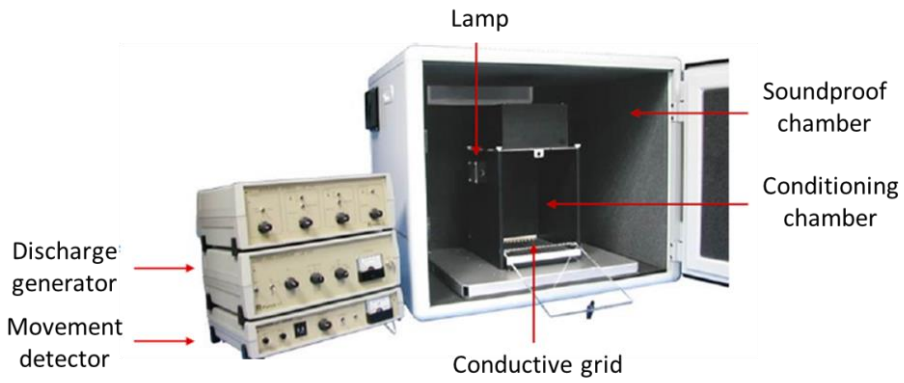

Figure 17. Equipment employed to perform the fear conditioning test (StartFear, Panlab).

The StartFear combined system consist of a conditioning chamber supported on four motion transducers that record any oscillation inside its interior. The floor of this room is formed by 36 stainless steel rods connected to an electric discharge generator. There is a bigger soundproof chamber or box surrounding the conditioning chamber to guarantee that the animal only hears the background noise of the context during the test, not exterior noises. There is also a discharge generator coupled to the steel rods in the conditioning room to regulate the intensity of the electric discharge.

As depicted in figure 18, three different phases can be distinguished in the FC test:

1. Habituation: During this phase, animals should familiarize with the context. For it, they were introduced in the conditioning room and left explore freely for 3 min in absence of unconditioned stimuli.
2. Training: This phase took place 24 hours after the habituation. Mice were placed again in the conditioning chamber and they were free to explore it for 2 minutes.

Then, they were exposed to two electrical foot shocks (0.3 mA) of 2 s separated by an interval of 30 s. After another 30 s, they were returned to their home cages.

3. Test: Memory retention was evaluated 24 h after the training. Animals were re-introduced in the conditioning room and allowed to explore for 2 minutes during which freezing time was measured. Freezing scores were expressed as percentages.

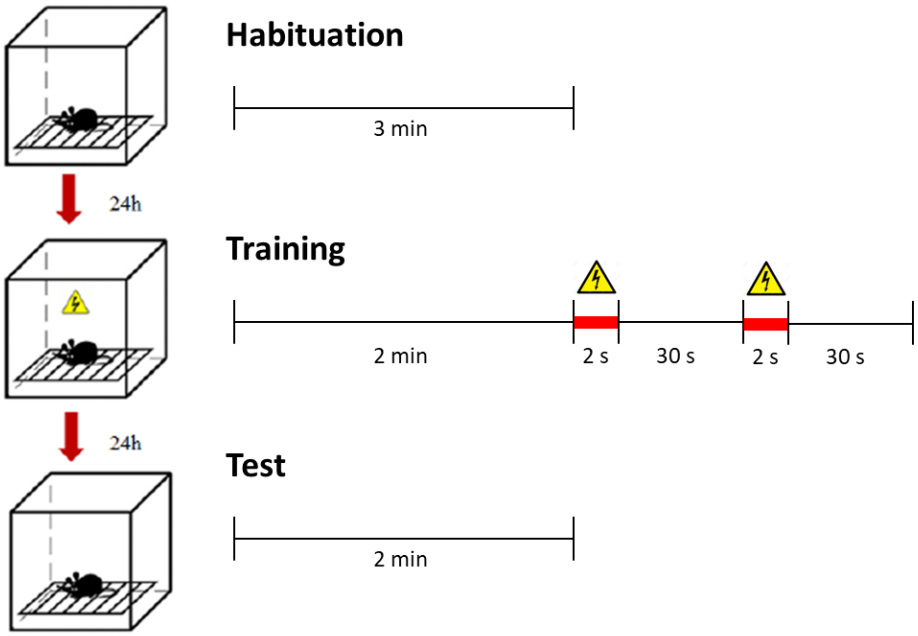

Figure 18. Methodology used for the FC paradigm.

9. Gene expression analysis

9.1. RNA extraction

For RNA extraction, brain tissue was first homogenized in 1 ml TRIzol Reagent (Invitrogen) using an IKA T10 basic ultra-turrax (Sigma-Aldrich) and incubated 5 min at RT. After that, 200 µL of chloroform (Panreac) were added to each sample and they were subsequently mixed and incubated for 10 min at RT. Then, samples were centrifuged for 10 min at 18000 g and 4ºC obtaining three differentiated phases. The aqueous phase (top phase), which contains the RNA, was added to 500 µL of isopropanol (Sigma-Aldrich) and incubated for 10 min at RT. Thereafter, samples were centrifuged for 10 min at 18000 g and 4ºC. The supernatant obtained was discarded and the pellet was washed in 1 ml of ethanol 75% (Panreac) in diethilpirocarbonate (DEPC) (Sigma-Aldrich) water to eliminate impurities. Afterwards, they were centrifuged for 5 min at 18000 g and 4ºC. After discarding the supernatant, the pellet was dried at 37ºC and re-suspended in 30 µL of sterile DEPC water. Then, it was heated at 65ºC for 5 min to facilitate dilution. Finally, RNA concentrations were measured in a NanoDrop 1000 (Thermo Fisher Scientific) and samples were stored at -80ºC until use.

9.2. Affymetrix Microarray Hybridization

RNA was extracted with TRIzol Reagent as describe above and purified with the RNeasy Mini-kit (Qiagen). RNA integrity was then confirmed on Agilent RNA Nano LabChips (Agilent Technologies). The sense cDNA was prepared from 300 ng of total RNA using the Ambion WT Expression Kit. The sense strand cDNA was then fragmented and biotinylated with the Affymetrix GeneChip WT Terminal Labeling Kit (PN 900671). After that, labeled sense cDNA was hybridized to the Affymetrix Mouse Gene 2.0 ST microarray according to the manufacturer's instructions using GeneChip Hybridization, Wash and Stain Kit. Finally, genechips were scanned with the Affymetrix GeneChip Scanner 3000. Microarray data files correspondent to CM-695 treatment were submitted to the GEO (Gene Expression Omnibus) database and are available under accession number GSE128422 (CM-695 treatment).

Background correction and normalization were done using RMA (Robust Multichip Average) algorithm (Irizarry *et al.*, 2003). A filtering process was also performed to eliminate low expression probe sets and R/Bioconductor (Gentleman) was used for preprocessing and statistical analysis.

LIMMA (Linear Models for Microarray Data) (Smyth, 2004) method was used first to find out the probe sets that showed significant differential expression between experimental conditions, selecting genes as significant using p-value<0.01 as threshold. False Discovery Rate (FDR) method was also use to correct for multiple hypotheses testing and finally the Ingenuity Pathway Analysis software (Ingenuity Systems, www.ingenuity.com) was used to check altered metabolic pathways between groups.

9.3. Retro-transcription

Prior to retro-transcription, RNA was treated with DNase to digest unwanted DNA. This reaction was carried out incubating for 30 min at 37ºC the sample (2µg of RNA diluted in DEPC water (e.a. to 8µL)), 1µl of DNase (Invitrogen) and 1 µL of DNase buffer (Invitrogen). Thereafter, 1 µL of EDTA (2.5 mM) was added and samples underwent an incubation of 10 min at 65ºC in order to inactivate the DNase.

Once DNA was inactivated from samples, retro-transcription was performed to obtain complementary DNA (cDNA). RNA samples pre-treated with DNase were mixed with 2 µg of 100 ng/µL random oligo-dT primers (Invitrogen), 1.5 µL of 10 mM dNTPs (Invitrogen) and 5.5 µL of sterile water and incubated for 5 min at 65ºC. Next, 6 µL of 5x FS buffer (Invitrogen), 1.5 µL of 0.1 M DTT (Invitrogen) and 1 µL of RNaseOUT (Invitrogen) were added and mixture was left for 2 min at RT before adding 1 µL of 200 U/µL SuperScript III retrotranscriptase. Finally, samples were incubated for 10 min at RT, 60 min at 42 ºC and 15 min at 70 ºC. They were then stored at -20 ºC.

9.4. Real-time PCR

To perform the real-time PCR assay, 4 µL of cDNA (0.01-0.07µg cDNA) were added per well into a 96-well plate and mixed with 10 µl of a mix containing 7 µl of SYBR™ Green

(Applied Biosystems), 0.5 µl of the correspondent 10 µM forward primer (Table 6) and another 0.5 µl of the 10 µM reverse primer (Table 6). Then, the plate was stirred for 1 min at 1000 g and it was placed in an ABI Prism 7300 Real-Time PCR System (Applied Biosystems) where it was subjected to the temperature cycles shown in figure 19. Each sample was charge by triplicate.

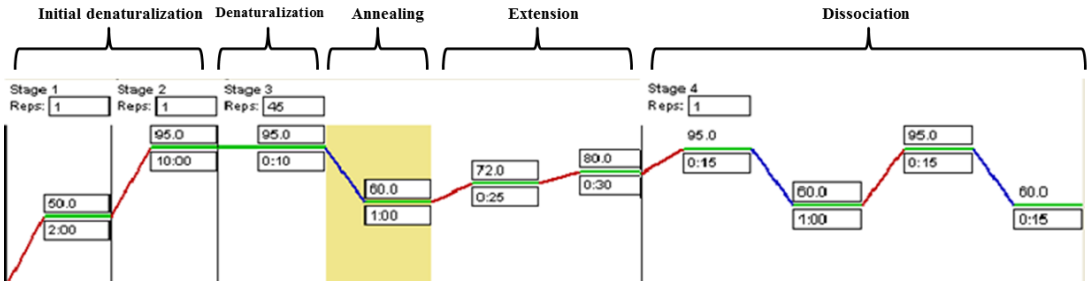

Figure 19. Temperature cycles of the RT-PCR with SYBR™ Green.

The employed reference gene was 36B4, which encodes the acidic ribosomal phosphoprotein P0. This gene is highly conserved among tissues and species, and it has been probe to be a very reliable and consistent standard for use in gene expression analysis among multiple tissues including brain (Akamine *et al.*, 2007).

Results were analyzed using the Sequence Detection Software v.3.0 and relative gene expression was calculated using the $2^{(-\Delta(\Delta Ct))}$ method (Livak & Schmittgen, 2001).

Table 6. Sequence of the primers used in the RT-PCR with SYBR Green.

Gen	Primer Forward	Primer reverse
36B4	5' AACATCTCCCCCTTCTCCTT 3'	5' GAAGGCCTTGACCTTTTCAG 3'
BIP (GRP78)	5' ACCAACTGCTGAATCTTTGGAAT 3'	5' GAGCTGTGCAGAAACTCCGGCG 3'
HSPA1A/B	5' AGCCTTCCAGAAGCAGAGC 3'	5' GGTCGTTGGCGATGATCT 3'
PDE5A	5' ACCGGGACTTTACCTTCTCTT 3'	5' CAAGAGCCTTGAGCACTGGT 3'
PDE9	5' CCACCATCTCCCTTTTAACCAC 3'	5' CAGCACGCCCTGGATAAGT 3'
m-PLA2G4E	5' ATGGTGACAGACTCCTTCGAG 3'	5' CCTCTGCGTAAAGCTGTGG 3'
h-PLA2G4E	5' AGAACGTGCTAGAGTTGAGTGT 3'	5' TGGGTTTTCTTTCGGAACAGAG 3'

The analysis of genes related with neuroinflammation was done in the laboratory of Professor Marina Lynch at Trinity College Dublin so a slightly different RT-PCR protocol was used. In this case, TaqMan probe was employed instead of SYBR Green. Its effect is based on the 5'-3' exonuclease activity of Taq polymerase. This activity allows the cleavage of a dual-labeled probe during hybridization to the complementary target sequence and in consequence, a fluorophore-based detection (Holland *et al.*, 1991). Moreover, β-actin was used as reporter gene instead 36B4. In brief, 17.5 µl of a mix containing 10 µl of taqman polimerase (Applied Biosystems), 1 µl β-actin primer (VIC reporter), 1 µl of the target 20x primer (FAM reporter) and 5.5 µl of water were mixed with 2.5 µl of cDNA in a 96-well plate and subjected to the temperature cycles shown in figure 20. The primers used are commercialized by Applied Biosystems (Applied

Biosystems TaqMan Assays)(Table 7) and they basically consist on a pair of PCR primers and a TaqMan probe with a FAM or VIC dye tag at the 5 ' end.

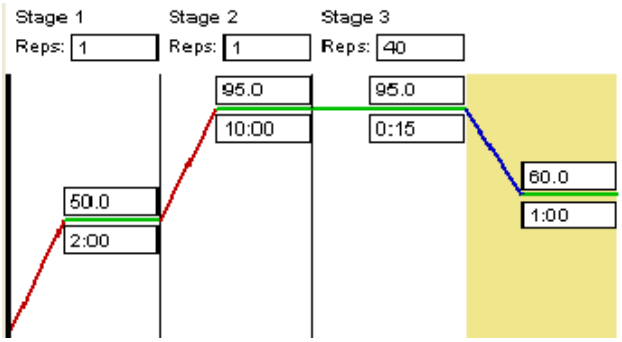

Figure 20. Temperature cycles of the RT-PCR with TaqMan.

Table 7. Reference of the primers from Thermo Fisher Scientific used in the RT-PCR with TaqMan.

Gen	Reference
β-actin	Mm00607939_s1
CD11b	Mm00434455_m1
GFAP	Mm01253023_m1
IL-1β	Mm00434228_m1
TNF-α	Mm00443258_m1
IL-6	Mm00446190_m1
IL-4	Mm00445259_m1
IL-10	Mm00439616_m1
MRC1	Mm00485148_m1
Arg1	Mm00475988_m1
COX2	Mm03294838_g1
iNOS	Mm00440502_m1

10. Protein analysis by immunoblotting

10.1. Protein extracts preparation

10.1.1. Total protein extracts

Brain samples or cells were homogenized in a buffer that allows total protein extraction containing 2% SDS, 10 mM Tris-HCl (pH=7.5), phosphatases inhibitors (1 mM NaF and 0.1 mM Na_3VO_4) and the commercial Complete Protease Inhibitor Cocktail (Roche).

Homogenates were then sonicated for 2 min, left 20 min on ice, vortexed and centrifuged for 13 min at 15700 g and 8ºC. Supernatants were then kept and maintained at -80ºC until use. Protein concentration was determined using the Pierce BCA Protein Assay kit (Thermo Fisher Scientific).

Protein extracts for APP processing analysis were prepared as described above but with a centrifugation of 1 h at 100000 g (Beckman ultracentrifuge, rotor Type 70.1 Ti, Beckman Coulter) instead of the one at 15700 g for 13 min to allow maximal debris elimination.

10.1.2. Synaptosome-enriched protein extracts

Brain tissue was homogenized in a buffer containing Syn-PER (Thermo Fisher Scientific), a commercial proteases inhibitors cocktail (Sigma P8340) and two commercial phosphatases inhibitors (SigmaP5726 and SigmaP0044). Homogenates were then centrifuged for 15 min at 1000 g and 4ºC and the supernatants were kept and centrifuged again for 20 min at 15000 g and 4ºC. The supernatants obtained in this second centrifugation constitute the cytosolic fraction. The pellets were re-suspended in a solution containing 1% sodium deoxycholate, a proteases inhibitors cocktail (Sigma P8340) and phosphatases inhibitors (SigmaP5726 and SigmaP0044) diluted in PBS. Thereafter, they were sonicated in 20 pulses and centrifuged for 20 min at 15000 g and 4ºC. The supernatants obtained constitute the synaptosome-enriched fraction and were kept at -80ºC until used. Protein concentration was obtained using the Pierce BCA Protein Assay kit (Thermo Fisher Scientific).

10.2. Immunoblotting

Western blot technique was used to analyze the levels of different proteins in the desired brain extracts (prepared as describe in section 10.1).

10-30 µg of protein extract (depending on the protein to be quantified) were mixed with the correspondent volume of 6x Laemmli Sample Buffer [For 10 ml: 5 ml glycerol, 1.8 mg bromophenol blue, 0.93 g DTT, 1.2 g SDS and 1.6 ml of upper Tris pH 6.8 (For 1L: 60.6 g Tris and 4 g SDS)] before heating at 95˚C for 5 minutes in order to achieve protein denaturalization. Samples were then loaded onto polyacrylamide gels (8-15% depending on the size of the studied protein) and proteins were electrophoretically separated by the application of a 90 V voltage for 15 minutes followed by one at 120 V for 1 h using 1x Tris-Glycine-SDS (TGS) buffer (Bio-Rad). For APP processing analysis, 50 µg of protein were mixed with 4x XT sample buffer (Bio-Rad) and resolved onto a Criterion XT precast gel 4-12% Bis-Tris (Bio-Rad) using XT MES (Bio-Rad) running buffer. In both cases, once proteins had been separated by electrophoresis they were transferred onto nitrocellulose membranes using the equipment Mini Trans-Blot™ (Bio-Rad) at 340 mA for 2 h and 4ºC or the Trans-Blot Turbo (Bio-Rad) at 1.3 A for 10 min. Membranes were then blocked for 1 h with 5% milk in TBS [0.133 M NaCl, 0.150 M Tris-HCl (pH=7.4)] and incubated overnight with the corresponding primary antibody (Table 8) at 4ºC. Next day, after 3 washes with TTBS [0.05% Tween® 20 in TBS], membranes were incubated

for 1 h at RT with an HRP-conjugated anti-rabbit or anti-mouse antibody (Santa Cruz; dilution 1:5000). After that, they were washed again: twice with TTBS and once with TBS. To detect the complex protein-antibody, an enhanced chemiluminiscence system (ECL, GE Healthcare Bioscience) was used. Finally, an autoradiogram indicative of the signal was obtained using Hyperfilm ECL (GE Healthcare Bioscience) or the ChemiDoc Imaging System (Bio-Rad). Bands' optic density was obtained using the Quantity One software v.4.6.3 (Bio-Rad) and immunoreactivity was calculated as per-unit increase or decrease over the signal obtained from control samples employing β-actin as load control.

Table 8. Antibodies used for immunoblotting.

Antibody	Protein molecular weight	Commercial firm	Dilution (µg/µl)	Secondary antibody
β-actin	44-50 kDa	Sigma-Aldrich	1:100000	Mouse
Acetyl-Histone H3 (K9)	17 kDa	Cell Signaling	1:1000	Rabbit
pCREB-Ser133	43 kDa	Cell Signaling	1:1000	Rabbit
Acetylated-tubulin	50 kDa	Sigma	1:2000	Mouse
6E10 (1-16 aa Aβ)	125 and 13 kDa	Chemicon	1:1000	Mouse
AT8 (pTau Ser-202:Thr-205)	50 kDa	Pierce	1:1000	Mouse
pGSK3β-Ser9	46 kDa	Cell Signaling	1:1000	Rabbit
Synapsin-I	74 kDa	Synaptic Systems	1:4000	Mouse
PSD95	95 kDa	Chemicon	1:1000	Mouse
Synaptophysin	38 kDa	Chemicon	1:1500	Mouse
pCAMKII-T286	50 kDa	Upstate	1:1000	Mouse
Total CAMKII	50 kDa	Chemicon	1:1000	Mouse
pERK(1/2)-Thr202/Tyr204	42 and 44 kDa	Cell Signaling	1:1000	Rabbit
GluN2B	180 kDa	Upstate	1:1000	Rabbit
pGluA1-Ser831	98 kDa	Millipore	1:1000	Rabbit
GluA2/3	110 kDa	Upstate	1:1000	Rabbit
PLA2G4E	100 kDa	Proteintech	1:1000	Rabbit
NeuN	48 kDa	Millipore	1:1000	Mouse
PHF1	62 kDa	Donated by Peter Davis	1:1000	Mouse

11. Determination of Aβ levels by ELISA

$A\beta_{42}$ levels were measured through an enzyme-linked immunosorbent assay (ELISA) kit commercialized by Invitrogen using brain tissue (hippocampus or parieto-temporal cortex) homogenized in two different types of 2% SDS extracts (section a and section b). It allows the detection of a pool containing both intracellular and membrane-associated $A\beta_{42}$ that has been reported to be more closely associated with AD-related symptoms than other $A\beta_{42}$ species (Steinerman *et al.*, 2008).

This kit provides micro-titer strips coated with a monoclonal antibody specific for the amino terminal end of human Aβ. Fifty microliters of the standards (samples prepared as described in the kit with known human $A\beta_{42}$ concentrations), controls, and samples to measure (diluted 1:2000 in the case of mice hippocampus, 1:5000 in mice parieto-temporal cortex and 1:4000 in human samples as mentioned in the kit) were added into the wells and co-incubated overnight at 4ºC with 50 µL of a specific rabbit antibody for the $A\beta_{42}$ carboxyl-terminus, the detection antibody. Next day, after washing to eliminate un-bound antibody, the bound one was detected by co-incubation with 100 µL of a horseradish peroxidase–labeled anti-rabbit antibody for 30 minutes at RT. After washing again, 100 µL of the peroxidase substrate (stabilized chromogen) that acts upon by the bound enzyme to generate color was added and incubated for 30 minutes in darkness at RT. After stopping the reaction by the addition of 100 µL of stop solution (provided by the kit), absorbance at 450 nm was measured in a microplate photometer Multiskan (Thermo Fisher Scientific). As the intensity of the colored product is directly proportional to the concentration of human $A\beta_{42}$ present in the sample, $A\beta_{42}$ concentrations were inferred from the ones of the standards using a standard curve and this value was corrected by the samples concentrations obtained using the Pierce BCA Protein Assay kit (Thermo Fisher Scientific).

12. Dendritic spine density measurement by Golgi-Cox staining

In order to analyze dendritic spine density and morphology, a modified Golgi-Cox method was used (Glaser & Van der Loos, 1981). Firstly, half-brains were incubated in Golgi-Cox solution (1% potassium dichromate, 1% mercury chloride, 0.8% potassium chromate) just after being removed from the skulls for 48h at RT and protected from light. After that time, solution was renewed and tissue was maintained there for another 3 weeks. Thereafter, brains were washed with distilled water and maintained in 90º ethanol for 30 min until they were processed in 200 µm-thick coronal slices using a vibratome. Afterwards, slices were incubated in 70º ethanol, washed with distilled water, reduced in 16% ammonia for one hour and fixed in 1% sodium thiosulfate for 7 min. After another wash, slices were placed in microscope slides, dehydrated in an increasing alcohol graduation and mounted with DPX Mountant (VWR, BDH Prolabo).

Spine density was determined in the secondary apical dendrites of the pyramidal cells located within the CA1 region of the hippocampus. Each selected neuron was captured using a Nikon Eclipse E600 light microscope and images were recorded with a digital camera (Nikon DXM 1200F) at a resolution of 1,000-1,500 dots per inch (dpi). Secondary

dendrites taken between 100-200 μm apart from the soma, where spine density is relatively uniform in CA1 pyramidal neurons (Megías *et al.*, 2001), were used for the quantification. For each mouse (n=3-4 per group), 3 dendrites of 9 different neurons were used for the analysis.

13. Protein analysis by immunofluorescence

13.1. Animal sacrifice and tissue fixation

Animals were first sacrificed by cervical dislocation and half-brains were immersion-fixed in 4% paraformaldehyde (PFA) at 4º C for 24 h and in 2% PFA for another 48 hours. Fixed tissue was cryopreserved at 4ºC in 30% sucrose diluted in PBS until coronal microtome sections of 30 μm thick were obtained and collected in a solution containing 20% glycerol, 2% DMSO and 0.125 M phosphate buffer (pH 7.4) and stored at -20ºC until use.

13.2. Immunofluorescence

Brain slices were incubated with 70% formic acid for 10 minutes to expose the epitope before being blocked in a solution containing 1% Triton-X100 and 0.5% BSA in 0.125 M phosphate buffer for 2 hours at room temperature. They were then incubated overnight at 4ºC with the primary antibody 4G8 (against amino acids 17-24 of Aβ peptide, 1:1000, BioLegend). After washing with 0.125 M phosphate buffer, brain sections were incubated with the secondary anti-mouse 546 antibody (1:200, Alexa Fluor) for 2h at room temperature in darkness. Then, slices were placed on slides and allowed to dry protected from light for at least 24 hours. They were then dehydrated in toluene and mounted with Immu-Mount (Thermo Fisher Scientific). Finally, fluorescence signals were analyzed on an automated microscope (Zeiss Axioplan 2ie).

14. Thioflavin T staining

Compact senile plaques were detected in PFA immersion-fixed half-brains (obtained as described in section 13.1) by Thioflavin T staining. This staining allows the detection of proteins that contain β-pleated sheets in their tertiary structure.

To perform this technique, brain slices were first placed on the slides and dried for 24 h at RT. Afterwards, they were incubated in Mayer's hematoxylin solution (Sigma) for 3 minutes and washed in distilled water. After that, they were treated with 1% Thioflavin for 3 min, washed again with distilled water and incubated for 10 min in 1% acetic acid. Finally, brain slices were dehydrated in toluene and mounted using Immu-Mount ™ (Thermo Fisher Scientific). An automated microscope (Zeiss Axioplan 2ie) was used to analyze fluorescence signals.

15. Protein analysis by immunohistochemistry

Immunohistochemistry was performed in formalin-fixed paraffin-embedded hippocampal sections from human patients.

A rabbit-polyclonal antiserum (Proteintech; diluted 1:100) was used to detect brain PLA2G4E inclusions. Antibody binding was then detected using the EnVision+ System-HRP labeled polymer (Dako) and DAB as chromogen. After immunostaining, sections were counterstained with hematoxylin–eosin and protein immunoreactivity was finally assessed under a light microscope (BX51, Olympus).

16. Single nucleotide polymorfism genotyping

After extracting genomic DNA from human temporal cortex as described in section 2.1, a PCR was performed to determine the presence of specific single-nucleotide variants (SNPs) in the desired genes.

A mix containing 10 µl of TaqMan Fast Advanced Master Mix (Thermo Fisher Scientific), 0.5 µl of the specific probe (rs12232304 for PLA2G4E; rs7412 and rs429358 for APOE; Thermo Fisher Scientific), 7.5 µl of sterile water and 2 µl of genomic cDNA was subjected to the temperature cycles shown in figure 21 using a QuantStudio 3 RT-PCR (Thermo Fisher Scientific).

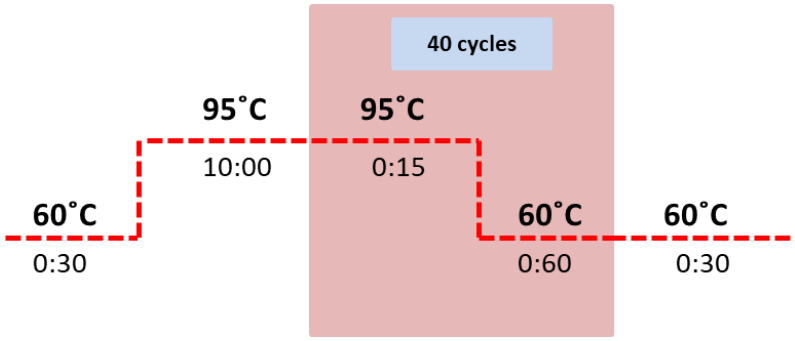

Figure 21. Temperature cycles used for SNP genotyping.

Note that for APOE genotyping, the results obtained with the two mentioned probes need to be taken into account.

17. Synaptic protein location studies by pre-embedding immunogold

17.1. Animal sacrifice and perfusion

Animals were anesthetized with an intraperitoneal injection of ketamine/xylazine (80/10 mg/kg) and perfused through the ascending aorta with 0.9% saline followed by 400 ml of freshly prepared ice-cold fixative solution containing 4% paraformaldehyde and 0.05% glutaraldehyde in 0.1 M phosphate buffer (PB), pH=7.4.

Brains were then removed from the skull and immersed in the same fixative for 2 h. Thereafter, they were washed in 0.1 M PB and processed in 60 µm-thick coronal sections using a vibratome (Leica V1000).

17.2. Pre-embedding immunogold

Brain sections were washed with 0.1 M PB to remove any remaining fixative and they were then rinsed with TBS for 30 min. Thereafter, they were blocked for 1 h in TBS containing 10% normal goat serum (NGS) and incubated with 3-5 μg/ml of the primary antibody PLA2G4E (Proteintech) in TBS containing 1% NGS for 24 h at 4ºC. After being washed with TBS, sections were incubated in goat anti-rabbit IgG coupled to 1.4 nm gold (Nanoprobes Inc.) for 2 h. Sections were then rinsed 4 times in TBS and twice in PBS (15 min each) before being postfixed in PBS containing 1% glutaraldehyde for 10 min. After washing the sections again with PBS and distilled water, silver intensification was carried out using an HQ silver kit (Nanoprobes Inc.). Sections were then treated with 1% osmium tetroxide in 0.1 M PB for 30 min and rinsed in 0.1 M PB and distilled water to remove all traces of osmium. Staining was performed after that incubating the slices in 1% uranyl acetate solution in distilled water for 30 min. Sections were then dehydrated in crescent ethanol concentrations (50%, 70%, 90%, 95% and 100% (10 min/each)) and submerged in 100% dry ethanol for another 10 min. Thereafter, slices were infiltrated in Durcupan (Fluka) resin for 4 h and flat-embedded. Resin was polymerized by heating in an oven at 60 ºC for 48 h. Regions of interest were cut at 70-90 nm on an ultramicrotome (Reichert Ultracut E, Leica) and collected on single slot pioloform-coated copper grids. Staining was then performed on drops of 1% aqueous uranyl acetate followed by Reynold's lead citrate. Ultrastructural analyses were finally performed in a JEOL-1010 electron microscope.

18. Data and statistical analysis

The number of animals and experiments performed, as well as the statistical analysis employed are detailed in the figure legend of the figure containing the correspondent results. Unless otherwise indicated, results are presented as mean ± standard error of the mean (SEM). Normal distribution of data was checked by the Shapiro–Wilk test. Unpaired two-tailed Student's t-test was used to compare two groups and one-way ANOVA followed by Newman-Keuls Multiple comparison post hoc test to compare more than two groups. In the MWM test, latencies to find the platform were analyzed by two-way repeated measures ANOVA test (genotype x trial) followed by the Bonferroni's post hoc test to compare cognitive status among groups. All results were processed for statistical analysis using SPSS for Windows version 15.0 or GraphPad PRISM version 5.03.

RESULTS

NOVEL MULTITARGET APPROACH FOR ALZHEIMER'S DISEASE TREATMENT: DUAL HDAC6 AND PDE9 INHIBITION

Using reference compounds (Cuadrado-Tejedor *et al.*, 2015) and the first-in class CM-414 (Cuadrado-Tejedor *et al.*, 2017), it has been recently validated in this laboratory that the simultaneous inhibition of histone deacetylases (class I HDACs and HDAC6) and phosphodiesterase 5 (PDE5) has a synergistic therapeutic effect in AD models.

In order to avoid the cytotoxicity associated with HDAC class I inhibition (Subramanian *et al.*, 2010) and due to the fact that PDE9 is the PDE most strongly expressed in the brain (Andreeva *et al.*, 2001), result that was corroborated here (Figure 22), the compound CM-695 (HDAC6 and PDE9 inhibitor) was designed and synthetized by the Small Molecule Discovery Platform at CIMA to be tested in AD mice (Cuadrado-Tejedor *et al.*, 2019; Rabal *et al.*, submitted). Its role as a potent HDAC6 and PDE9 inhibitor and a moderate class I HDAC inhibitor was confirmed after analyzing its binding affinity for different targets: HDAC1 (IC_{50}=593 nM), HDAC2 (IC_{50}=3530 nM), HDAC6 (IC_{50}=40 nM), PDE5 (IC_{50}>10 µM) and PDE9 (IC_{50}=107 nM).

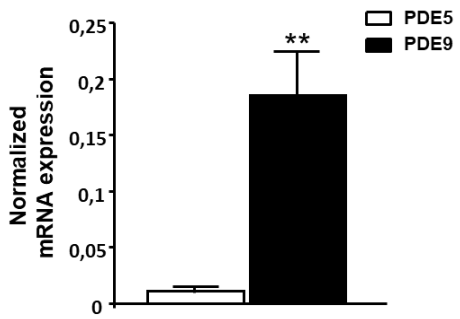

Figure 22. PDE9 and PDE5 mRNA expression levels in mice hippocampi was analyzed by quantitative RT-PCR and normalized with 36B4 (unpaired two-tailed Student's t-test, n=4, **P≤0.01 PDE5 versus PDE9).

1. Biological evaluation of CM-695

The functional activity of the compound CM-695 against its targets: HDAC6, class I HDAC and PDE9 was assessed *in vitro* using SH-SY5Y neuroblastoma cells.

SH-SY5Y cells were exposed to CM-695 at concentrations ranging from 1 nM to 1 µM for 2 hours and its effect on α-tubulin acetylation, histone 3 acetylation (lysine 9 of histone 3, H3K9 mark) and CREB-Ser133 phosphorylation (pCREB) was then analyzed by immunoblotting in SDS 2% extracts.

As depicted in figure 23, there was a significant increase in α-tubulin acetylation but not of AcH3K9 in SH-SY5Y cells exposed to CM-695 at 100 nM, which is consistent with its selective inhibition of HDAC6 (IC50 = 40 nM) as opposed to class I HDACs (IC50 = 593 and 3530 nM for HDAC1 and HDAC2, respectively). However, CM-695 had a significant effect on AcH3K9 at 500 nM, although the increase was much stronger on tubulin acetylation. In addition, at 500 nM CM-695 also increased significantly the levels

of pCREB, indicating that this compound inhibits PDE9 (IC50 = 107 nM) besides HDACs.

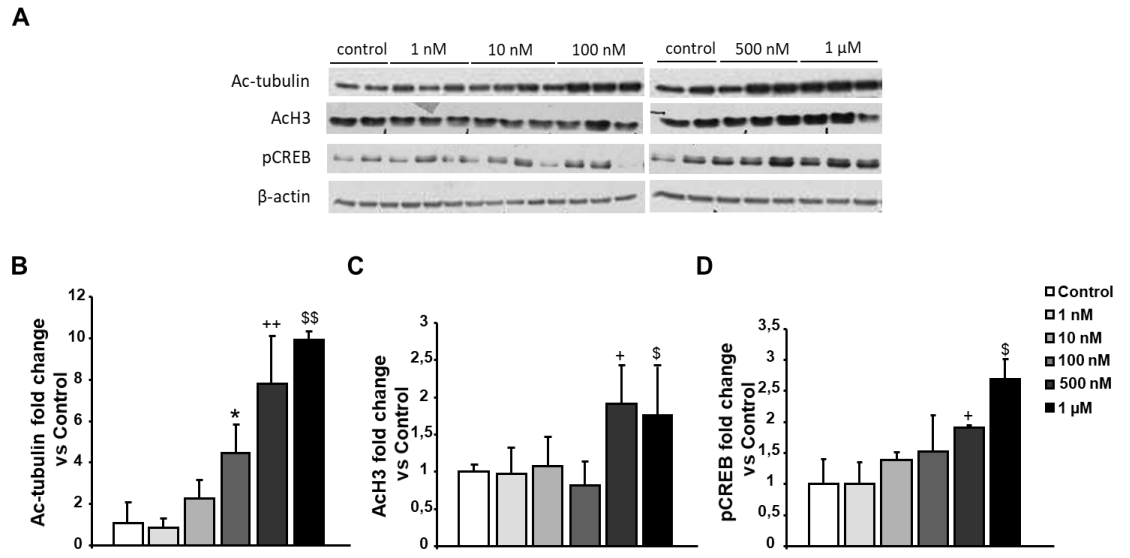

Figure 23. *In vitro* functional activity of CM-695. A) Representative bands of the blots. B) Ac-Tubulin, C) Histone 3 acetylation at lys 9 (AcH3K9) and D) pCREB levels analyzed by immunoblotting in SDS 2% extracts of SH-SY5Y cells treated with CM-695 at different concentrations (1nM to 1µM) for 2 hours and normalized vs β-actin (one-way ANOVA test followed by Newman-Kewls *post hoc* test, n=3, $^{*}p\leq0.05$ Control vs 100 nM, $^{+}p\leq0.05$ Control vs 500 nM, $^{++}p\leq0.01$ Control vs 500 nM, $^{\$}p\leq0.05$ Control vs 1 µM, $^{\$\$}p\leq0.01$ Control vs 1 µM).

These results confirm functional activity of CM-695 *in vitro* against HDAC6 and PDE9.

Pharmacokinetic studies performed by the Small Molecule Discovery Platform team at CIMA indicated that CM-695 reached an acceptable brain concentration (around 100 nM) 15 min after administering a dose of 40 mg/kg (Rabal et al., submitted) concentration that would ensure an effect on HDAC6 and PDE9.

To confirm those data, functional response in mouse brain was assessed *in vivo* in a group of animals to demonstrate the ability of the compound to inhibit HDAC6 and PDE9. Fifteen, 30 and 60 min after i.p. injection of 40 mg/Kg of CM-695 mice were sacrificed by cervical dislocation and their hippocampi were dissected. A western-blot was carried out to analyze Ac-Tubulin and pCREB in the hippocampus. As it shown in figure 24, CM-695 increased pCREB levels. However, as basal levels of this protein are high in the brain of the animals, no significant differences were appreciated in Ac-Tubulin. Likewise, a higher effect would probably be obtained with longer exposure time or in a chronic treatment. Note that AcH3 levels were not analyzed as changes were not expected due to the low selective inhibition of the compound over class I HDACs (IC50 = 593 and 3530 nM for HDAC1 and HDAC2, respectively).

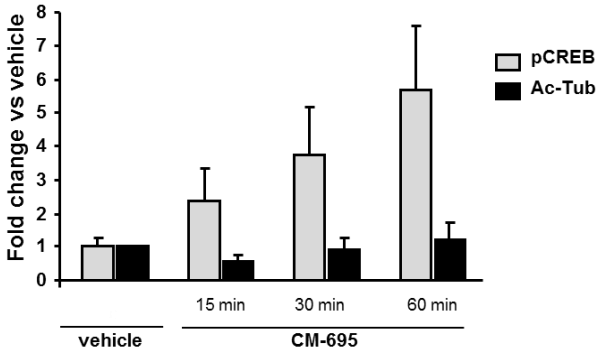

Figure 24. *In vivo* functional activity of CM-695. pCREB and Ac-Tubulin levels were analyzed by immunoblotting in hippocampal SDS 2% extracts of 2 months-old WT mice treated with vehicle or 40 mg/Kg CM-695 and sacrificed at different times (15, 30 and 60 min). Data are normalized vs β-actin (n=3).

These data, demonstrated that CM-695 cross the BBB and reach the brain at a concentration which is enough to inhibit PDE9 (IC50=107 nm), supporting the results obtained in the pharmacokinetic studies performed by the Small Molecule Discovery Platform team at CIMA (Rabal et al., submitted).

2. Effect of CM-695 on reversing Alzheimer's disease phenotype in old-Tg2576 mice

The effect of CM-695 on AD pathology was tested in 16-18 months old female mice of the strain Tg2576. Mice were administered six times a week during four weeks with a 40 mg/kg dose of CM-695 (n=11) or vehicle (10% DMSO, 10% Tween-20 in saline solution; n=10) injected intraperitoneally. Age- and strain-matched negative littermates (WT, n=10) were also used as controls for the behavioral and biochemical studies.

2.1. Effect on memory function

The effect of CM-695 on cognitive function was evaluated after two weeks of treatment using a fear-conditioning paradigm and after three weeks using the Morris Water Maze test. Four animals *per* group were sacrificed for biochemical studies 24 h after the last probe trial of the MWM test and, to see if the effect of the compound was maintained along the time, the remaining animals were subjected to a reversal phase of the MWM after a washout period of 4-weeks. These mice were then sacrificed 24 h the last probe trial of the reversal MWM test for biochemical studies (Figure 25).

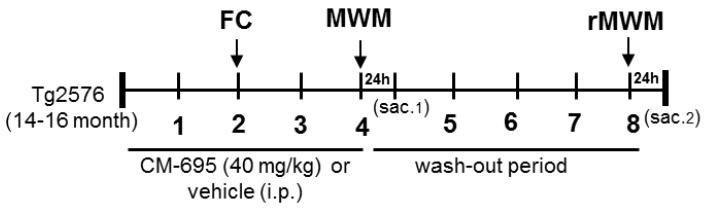

Figure 25. Experimental design carried out to study the effect of CM-695 on AD using elderly Tg2576 mice (FC: fear conditioning; MWM: Morris water maze; rMWM: reversal MWM; Sac: sacrificed).

Note that, although the following experiments were achieved to compare Tg2576 mice treated with vehicle vs CM-695, behavioural data corresponding to vehicle-treated WT

animals were also analyzed to demonstrate that AD-phenotype was well-established (Figure 26).

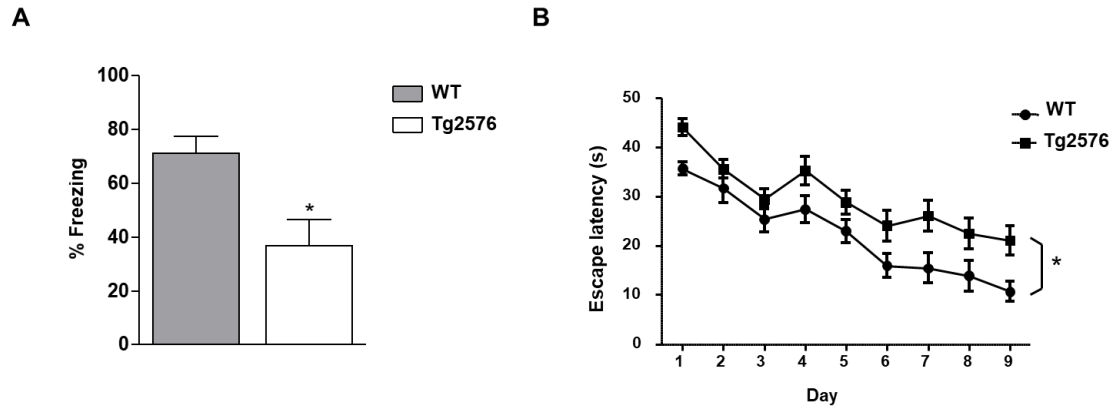

Figure 26. Tg2576 mice showed memory deficits in the FC and MWM test. A) Freezing behavior from 14-16 month old Tg2576 compared to age-matched WT mice (unpaired two-tailed Student's t-test, n=10-12, *p≤0.05). B) Escape latency of the hidden platform in the MWM test for 14-16 month old-Tg2576 and WT mice (two-way ANOVA test followed by Bonferroni's *post hoc* test, n=10, *p≤0.05).

As shown in figure 27, Tg2576 mice treated with CM-695 presented significantly higher freezing rates than those that receive the vehicle in the FC test.

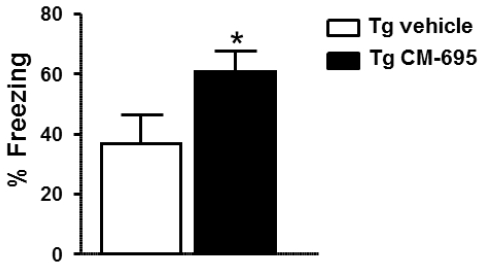

Figure 27. Freezing behavior from Tg2576 (Tg) mice treated with vehicle or CM-695 (unpaired two-tailed Student's t-test, n=10-11, *p≤0.05).

The effect of CM-695 on spatial memory was evaluated one week later using the MWM test. During the hidden platform phase, escape latencies were slightly shorter in the Tg2576 mice that received the compound compared to transgenic mice receiving the vehicle (Figure 28A). Similarly, the Tg2576 mice treated with CM-695 remained significantly longer times in the target quadrant during the probe tests on days 4th, 7th and 9th (Figure 28B). These results were in the same line as the one obtained in the FC test, suggesting that CM-695 chronic treatment reversed memory deficits in Tg2576 mice.

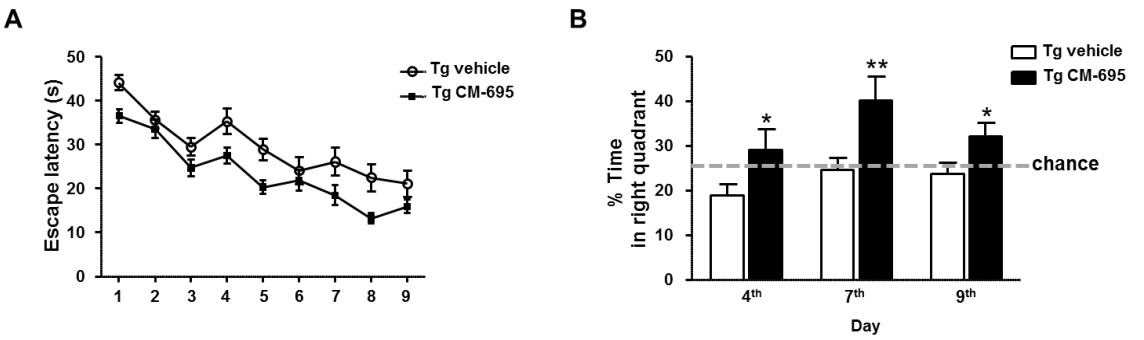

Figure 28. A) Escape latency of the hidden platform in the MWM test for the Tg2576 mice treated with vehicle or CM-695. B) Percentage of time spent in correct quadrant during the probe trials on days 4th, 7th, and 9th (unpaired two-tailed Student's t-test, n=10-12, *p≤0.05, **p≤0.01).

To determine whether the effect of CM-695 persisted when the mice no longer received the compound, mice were re-trained in a reversal phase of the MWM test after 4 weeks of wash-out. The hidden platform training was carried out over 5 days (4 trials per day) and it was followed by a memory retention test on day 6th. As shown in figure, non-significant differences were found between the mice receiving CM-695 or mice receiving vehicle in the hidden platform phase (Figure 29A) or in the probe trial (Figure 29B), indicating that none of the mice learned the platform location. Thus, it appears that the effect of CM-695 did not persist after the 4-week wash-out period.

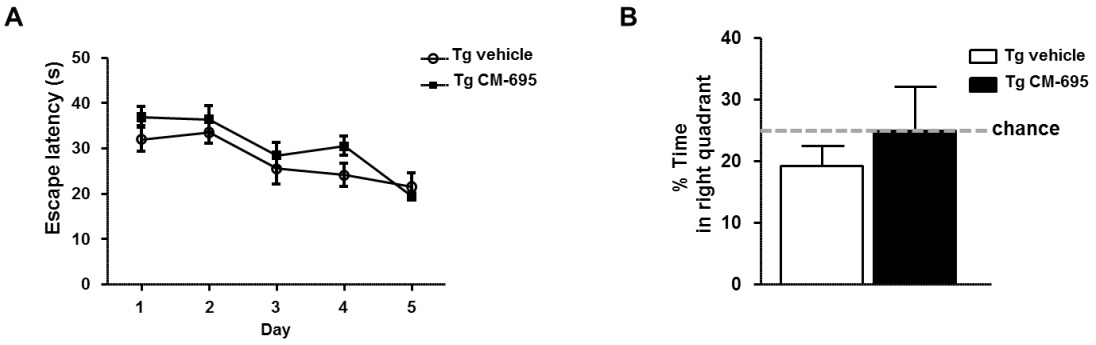

Figure 29. A) Escape latency of the hidden platform in the reversal MWM test for the Tg2576 mice treated with vehicle or CM-695. B) Percentage of time spent in correct quadrant during the probe trial on day 6th (n=10-11).

Altogether, it can be inferred that a chronic treatment with CM-695 ameliorated memory impairment in aged-Tg2576 mice although its effect was lost after a wash-out period of 4 weeks.

2.2. Effect on Alzheimer's disease neuropathology

Mice sacrificed 24 h after the last probe trial of the MWM test (n=4) or of the reversal MWM test (n=6-7) were used to study the effect of CM-695 on AD neuropathology and to determine whether the effect was maintained after a wash-out period of 4 weeks respectively.

2.2.1. Amyloid pathology

To assess the effects of CM-695 on amyloid pathology, an ELISA was used to assess soluble $A\beta_{42}$ in hippocampal SDS 2% extracts. As mentioned above, $A\beta_{42}$ levels were measured in two different groups of animals: one sacrificed at the end of the first MWM (4 weeks after treatment) and the other one sacrificed at the end of the reversal-MWM (after a 4-week wash-out period in which mice were not treated).

As depicted in figure 30, there was a significant decrease in $A\beta_{42}$ in the Tg2576 mice treated with CM-695 and sacrificed at both time points (Figure 30), although the differences with vehicle-treated animals in the group sacrificed after the wash out period (45% reduction) were not as strong as those observed prior to the wash-out period (56% reduction).

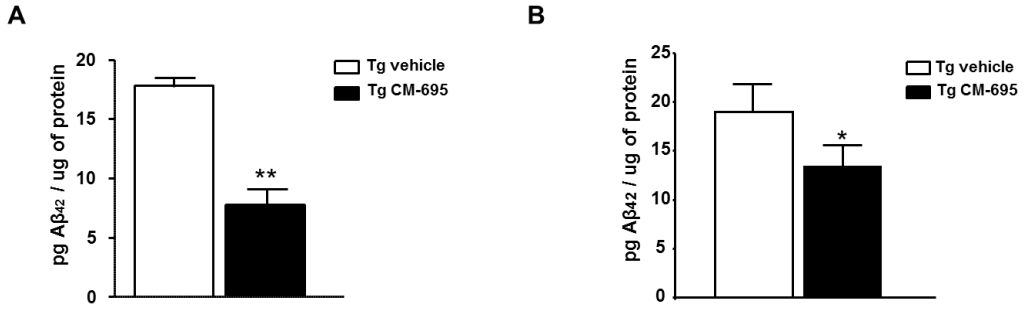

Figure 30. $A\beta_{42}$ levels determined by ELISA in SDS hippocampal tissue extracts of Tg2576 (Tg) mice treated with vehicle or CM-695 after A) four weeks of treatment (n=4) or after B) a washout period of four weeks (n=6-7) (unpaired two-tailed Student's t-test, *p≤0.05, **p≤0.01).

These results suggest that a chronic treatment with CM-695 decreased amyloid pathology in elderly Tg2576 mice.

2.2.2. Synaptic pathology

Given that Tg2576 mice display synaptic loss from 4.5 months (Lanz *et al.*, 2003), a Golgi-Cox staining was performed to explore if the behavioral recovery induced by CM-695 was reflected by structural changes in dendritic spine density. Note that this analysis was exclusively assed in the group of animals sacrificed after the washout period.

Consistent with previous data, there was a significantly lower density of apical dendrites on CA1 pyramidal neurons in Tg2576 mice than in WT mice (Figure 31A). However, when Tg2576 mice were analyzed after the wash-out period, those that received CM-695 did not show any significant change in the density of spines on these neurons. It should be noted that there was a tendency to increase the density of spines that might account for the memory improvement observed after 4 weeks of treatment (Figure 31B). Nevertheless, after the wash-out period neither the effect on memory function nor the potential changes in dendritic spine density persisted.

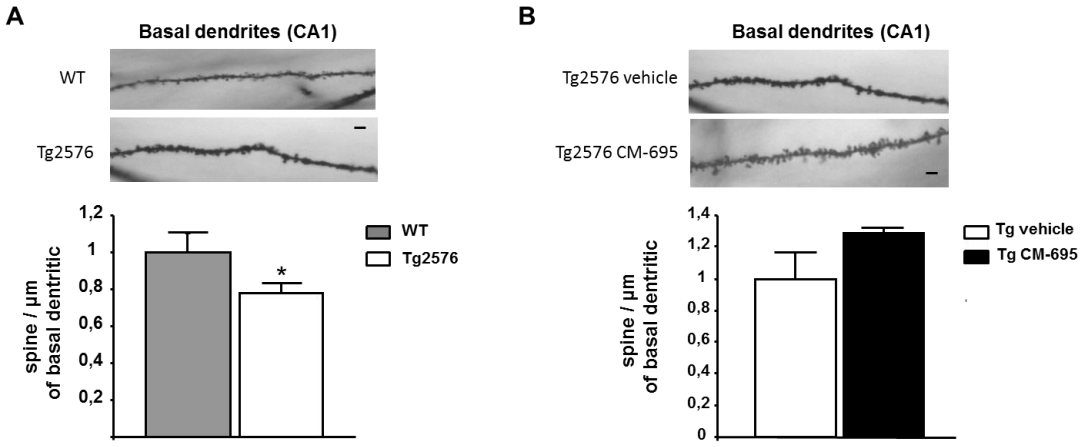

Figure 31. Spine density of basal dendrites of hippocampal CA1 pyramidal neurons from A) 14-16 months-old WT and Tg2576 mice and from B) Tg2576 mice (Tg) treated with vehicle or CM-695 after a 4-week wash-out period (unpaired two-tailed Student's t-test, n=34–36 neurons from 3 animals per group, *p≤0.05). Scale bar=10µm.

2.3. Identification of the mechanisms involved in CM-695 effect on memory function and Alzheimer's disease neuropathology

To explore the mechanisms underlying the effect of CM-695 on amyloid pathology and memory function, the effect of CM-695 on gene expression was analyzed in the hippocampus of the 4-weeks Tg2576 treated-mice (CM-695 and vehicle) using an Affymetrix microarray assay. A LIMMA analysis was then applied to find out the probe sets that showed significant differential expression between experimental conditions (Smyth, 2004) and genes were selected as significant using $p<0.01$ as threshold.

In order to gain information about the mechanistic approach of CM-695 therapeutic effect, differentially expressed genes were analyzed by using the Ingenuity Pathways Analysis. Importantly, the Protein Ubiquitination Pathway (p-value=6.76 E-05) and the Unfolded Protein Response (UPR, p-value=3.1E-05) were included among the top-ranked canonical pathways (Figure 32).

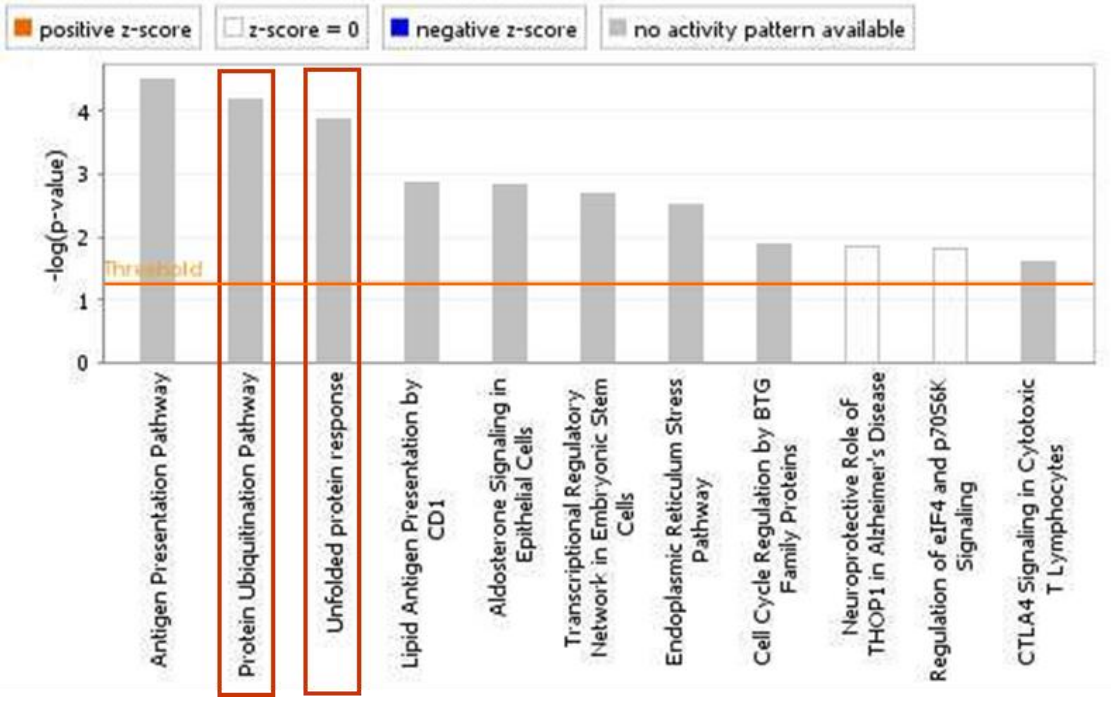

Figure 32. Ingenuity pathway analysis showing the most highly scoring canonical pathways according to p-value. The horizontal orange line running through the bars is the p-value threshold for these pathways. Color coding for positive and negative z-score and for pathways with no activity pattern available are shown in the figure. "Protein Ubiquitination Pathway" and the "Unfolded protein response" (remarked with a red box) were included among the top-ranked canonical pathways.

Specifically, BIP (GRP78) and HSPA1A/B (which encodes Hsp70) were among the genes overexpressed in the hippocampus of mice administered with CM-695 respect to the mice receiving vehicle (Figure 33).

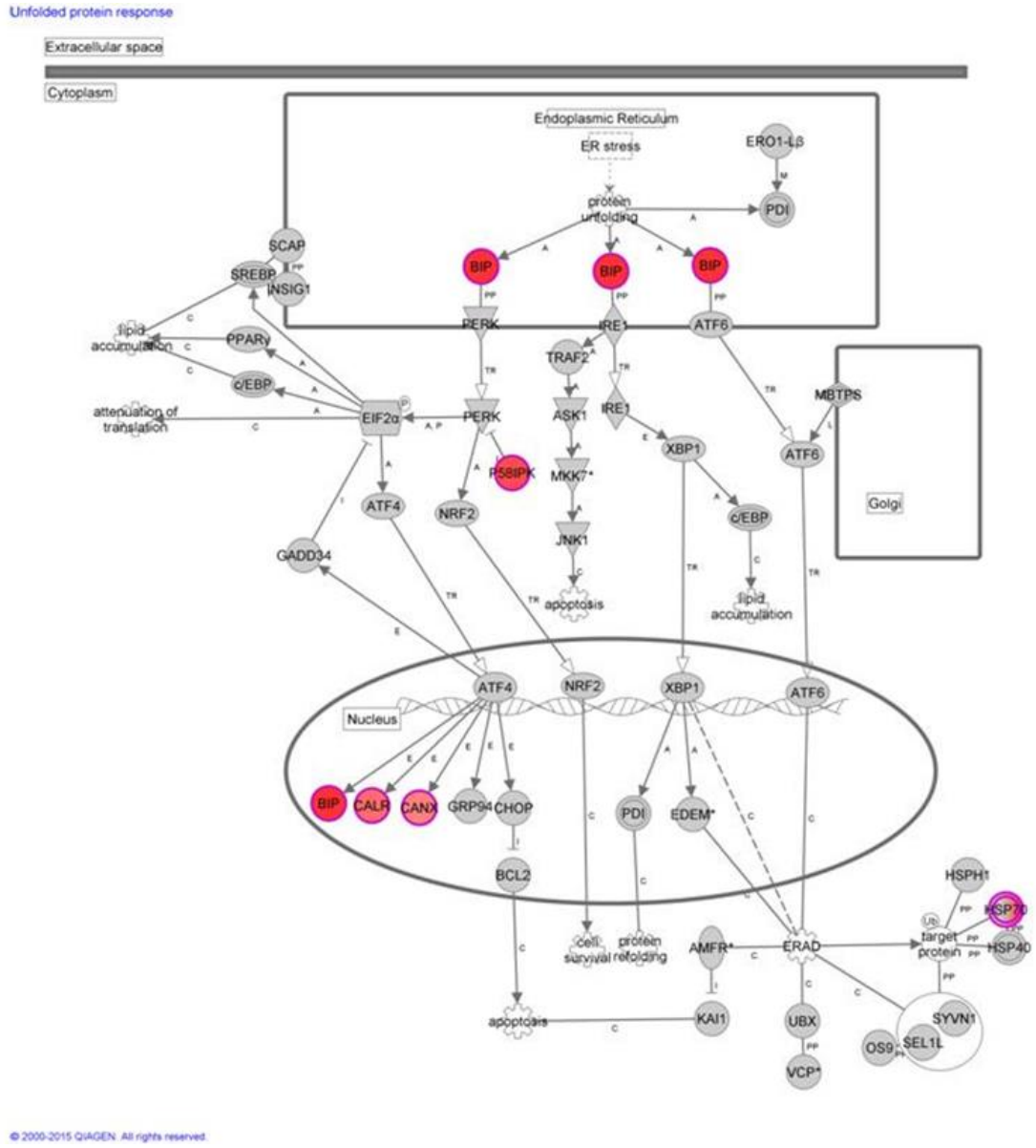

Figure 33. Ingenuity schematic draw showing all regulated potential molecular players of the unfolded protein response. The red-filled symbols represent the entries that are significantly up-regulated by CM-695.

In accordance with the previous analysis, when differentially expressed genes were also categorized to diseases and biological functions, "folding protein" (p-value and molecules) was significantly regulated (Figure 34).

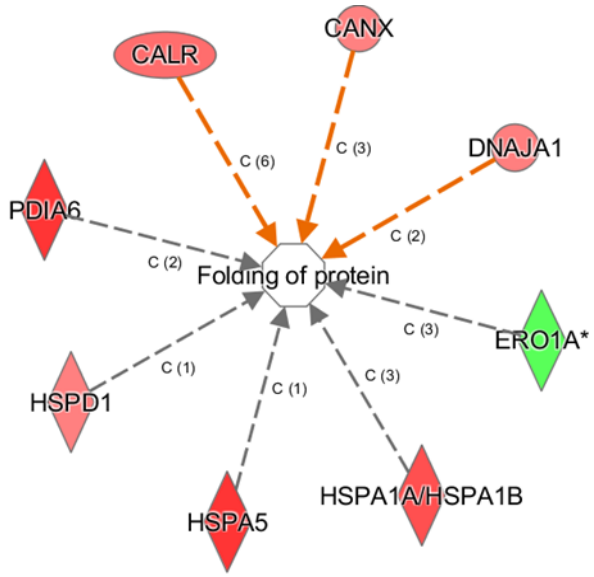

Figure 34. Network of differentially expressed genes categorized in Ingenuity by Disease and biological functions.

Since chaperone activity plays a crucial role to proper protein folding activity, the expression of GRP78 and HSPA1A/B was analyzed by quantitative real-time PCR to study the effect of CM-695. They were analyzed in mice sacrificed 24 h after the last probe trial of the MWM test and also in mice sacrificed 24 h after the last probe of the reversal MWM test.

Accordingly to the results obtained in the array, a significant increase was observed in both GRP78 and HSPA1A/B mRNA levels in the hippocampus of CM-695 treated mice compared to mice receiving vehicle (Figure 35A). However, this effect in gene expression was not maintained after the wash-out period (Figure 35B).

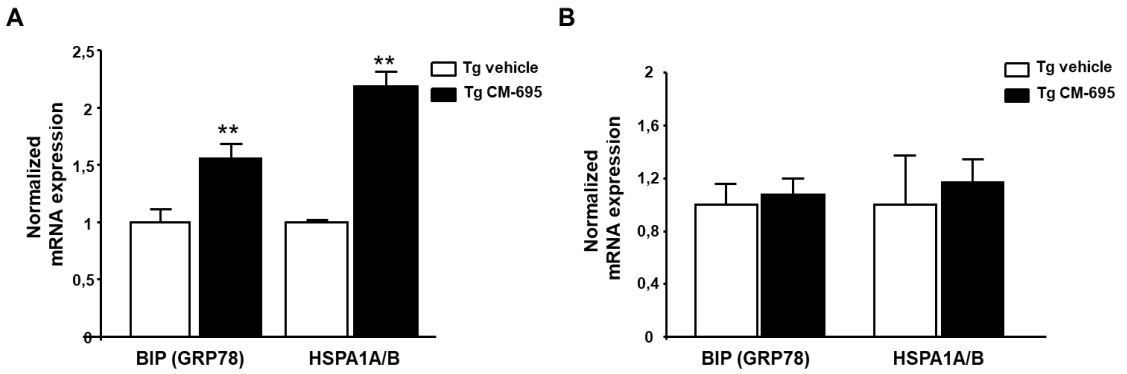

Figure 35. Quantitative RT-PCR analysis of BIP (GRP78) and HSPA1A/B mRNA in the hippocampus of CM-695 treated mice vs vehicle A) 4 weeks after treatment and B) after the washout period (Unpaired two-tailed Student's t-test, **p≤0.01).

These results suggest that the increase in the levels of chaperones GRP78 and Hsp70, which are involved in protein folding, may underlie the improvement in AD symptoms observed after daily administration of the compound.

IDENTIFICATION OF NEW THERAPEUTIC TARGETS FOR ALZHEIMER'S DISEASE BY THE STUDY OF COGNITIVE RESILIENT SUBJETS

Several longitudinal studies have recently shown that there is discordance between the appearance of the main AD hallmarks (amyloid plaques and NFTs) and the symptoms of dementia. As occurs in other diseases, the study of these cognitive resilient subjects, that present amyloid and tau pathology but do not develop cognitive impairment, could facilitate the identification of novel targets for AD.

3. Identification of aged-Tg2576 cognitive resilient mice

Spatial memory was evaluated in a cohort of 14-16 months old Tg2576 mice (n=26) and their negative littermates (n=30) using the MWM test.

During the visible-platform phase of the MWM test, animals should learn how to find an easily identifiable platform to escape from water. This phase is normally used to discard those rodents unable to perform the task. Thus, animals that in the last block of the visible platform phase presented escape latencies higher than 15 s were excluded. Animals that did not reach this criterion comprised a 31% of Tg2576 and a 20% of WT mice, which resulted in the generation of a cohort of n=18 Tg2576 and n=24 WT with no differences in escape latencies neither in the last day of visible-platform (Figure 36A) nor in the first day of the hidden-platform (Figure 36B).

Spatial memory was evaluated in the hidden-platform phase of the test. As depicted in figure 36B, from the 2nd day, Tg2576 mice presented significantly higher escape latencies than their negative littermates, confirming the spatial memory deficit present in this AD *murine* model which is initiated from 12 months of age (Hsiao *et al.*, 1996).

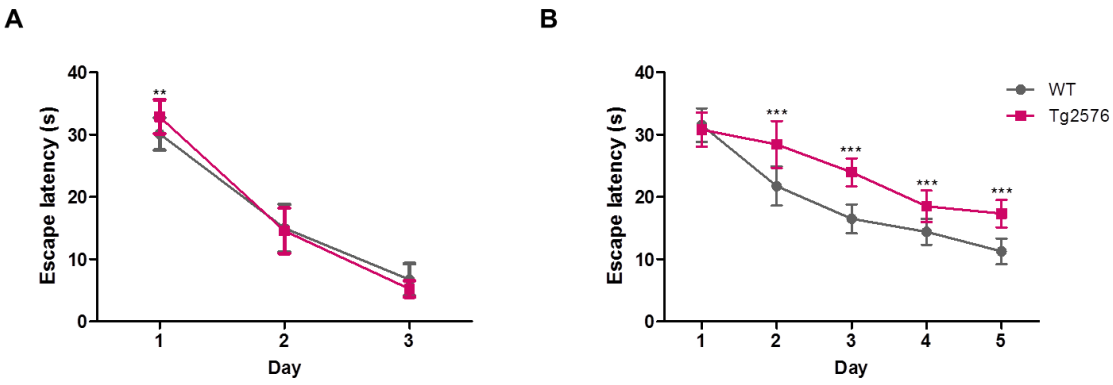

Figure 36. MWM test for aged- WT and Tg2576 mice. A) Escape latency of the visible-platform phase (two-way ANOVA test followed by Bonferroni's *post hoc* test, n=18-24, $^{**}p\leq0.01$) and B) of the hidden-platform phase (two-way ANOVA test followed by Bonferroni's *post hoc* test, n=18-24, $^{***}p\leq0.001$).

Interestingly, when individual escape latencies were taken into account, it was found that 4 out of 18 Tg2576 mice behaved similar to WT mice, representing a 22% of all Tg2576 mice tested in the hidden-platform phase.

In order to confirm this abnormal behavior, a reversal MWM test was performed two months later with these 4 Tg2576 cognitive resilient mice, called from now "good-learners" (GL), another 4 Tg2576 mice with spatial memory impairment called "poor-learners" (PL), and 5 WT mice as controls. Similar to the previous result, GL mice showed similar escape latencies than WT mice and significantly lower than PL mice in the hidden-platform phase of the reversal MWM test (Figure 37A).

Memory retention was also tested in a probe trial carried out on day 5th of the reversal MWM test, where GL mice spent more time in the quadrant where the platform was previously located than PL mice (Figure 37B), thus supporting their better cognitive performance.

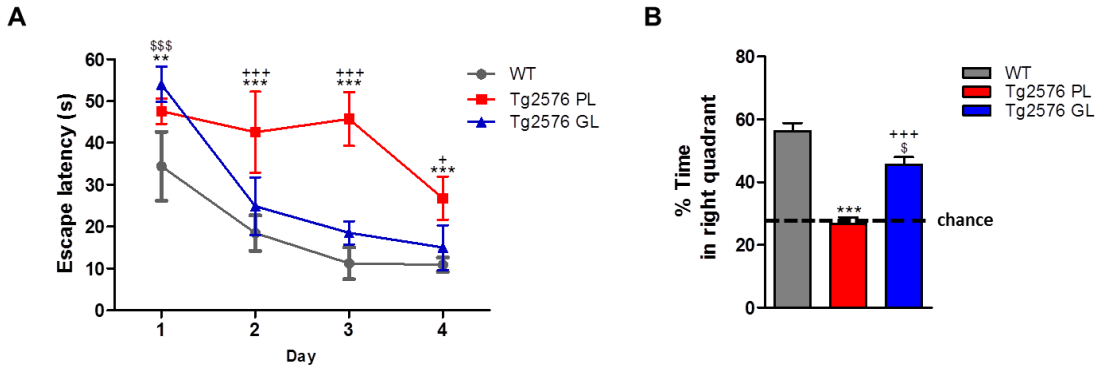

Figure 37. Reversal MWM test for WT, Tg2576 PL and GL mice. A) Escape latency to the hidden-platform (two-way ANOVA test followed by Bonferroni's *post hoc* test, n=4-5, **p≤0.01 WT versus Tg2576 PL, ***p≤0.001 WT versus Tg2576 PL, $^{\$\$\$}$p≤0.001 WT versus Tg2576 GL, $^{+}$p≤0.05 Tg2576 PL versus Tg2576 GL, $^{+++}$p≤0.001 Tg2576 PL versus Tg2576 GL). B) Percentage of time spent in the correct quadrant during the probe trial on day 5th of the reversal MWM test (one-way ANOVA test followed by Newman-Kewls post hoc test, n=4-5, ***p≤0.001 WT versus Tg2576 PL, $^{\$}$p≤0.05 WT versus Tg2576 GL, $^{+++}$p≤0.001 Tg2576 PL versus Tg2576 GL).

Altogether, it can be concluded that about a twenty percent of aged-Tg2576 mice were resilient, thus, behaved similar to WT mice and did not exhibit spatial memory impairment in the MWM test.

4. Neuropathological characterization of aged-Tg2576 cognitive resilient mice

The presence of amyloid and tau pathology together with synaptic dysfunction and increased neuroinflammation constitute the main pathological markers of AD (Serrano-Pozo *et al.*, 2011). In consequence, these factors were studied in the selected animals that were sacrificed by cervical dislocation 2 h after the probe trial of the reversal MWM.

4.1. Amyloid pathology

To check if differences in amyloid pathology could be responsible of the cognitive resilience presented by the Tg2576 GL mice, different intermediaries of this pathway were compared between GL and PL mice: C99/APP, Aβ_{42} and senile plaques.

APP processing was analyzed in SDS parieto-temporal cortex extracts (extracted as describe in section 10.1.1) by immunoblotting and, as depicted in figure 38A, non-significant differences were found in C99/APP levels between Tg2576 PL and GL mice.

Soluble Aβ$_{42}$ levels were assayed in the same extracts by ELISA and, once again, there were no differences between these two groups (Figure 38B).

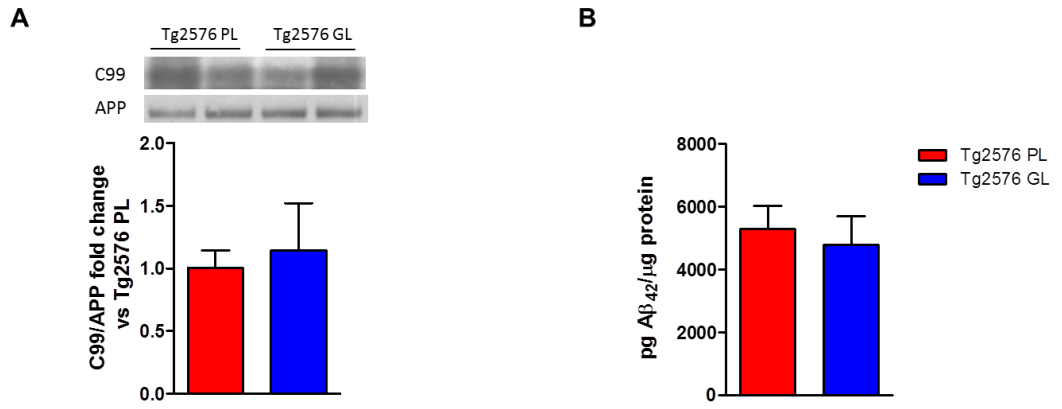

Figure 38. Amyloid pathology in Tg2576 PL and GL mice. A) C99/APP levels measured by immunoblotting in SDS parieto-temporal cortex extracts (n=4). B) Soluble Aβ$_{42}$ levels in SDS parieto-temporal cortex samples measured by ELISA (n=4).

Amyloid plaque accumulation was also detected by immunofluorescence using the 4G8 antibody. As it is shown in figure 39A, both groups presented similar levels of amyloid deposition in two brain regions highly affected by amyloid pathology in AD: hippocampus and cortex.

As it has been described that in humans, one of the differences between AD patients and those cases with intact cognition is the number of compact senile plaques, that are often associated with dystrophic neurites (Perez-Nievas *et al.*, 2013), mature senile plaques were also analyzed by thioflavin T staining in mouse brain slices. As it is shown in figure 39B, Tg2576 PL and GL mice had similar amounts of compact amyloid plaques in the cortex.

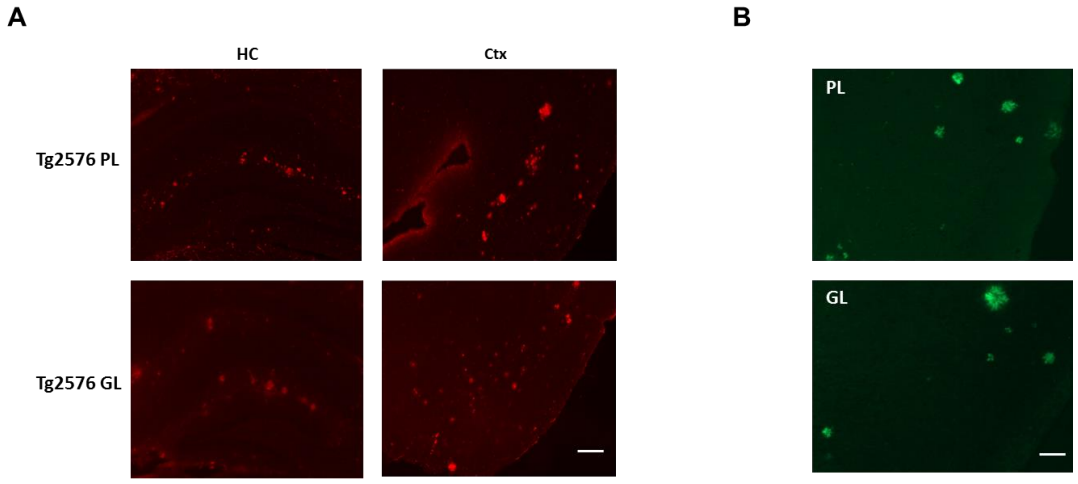

Figure 39. Representative brain sections of Tg2576 PL and GL mice showing A) multiple amyloid extracellular deposits detected with 4G8 antiserum by immunofluorescence or B) compact senile plaques detected by thioflavin T staining. Scale bar= 100 µm.

All of these results pointed out that Tg2576 PL and GL mice presented similar standards of amyloid pathology, discarding the hypothesis that lower levels of amyloidosis could be the responsible of cognitive resilience in GL mice.

4.2. Tau pathology

Although the Tg2576 is a model of amyloidosis, it also presents tau hiperphosphorylation from 12 months-old (Hsiao *et al.*, 1996). In consequence, to discard the hypothesis that differences in tau pathology could be responsible of cognitive resilience in GL mice, levels of ptau (Ser-202:Thr-205) and pGSK3β (the inactive form of the main enzyme responsible of its phosphorylation) were analyzed in SDS pre-frontal cortex extracts by immunoblotting. As depicted in figure 40, no differences were found in any of these markers between PL and GL mice, suggesting that both mice had similar levels of tau pathology.

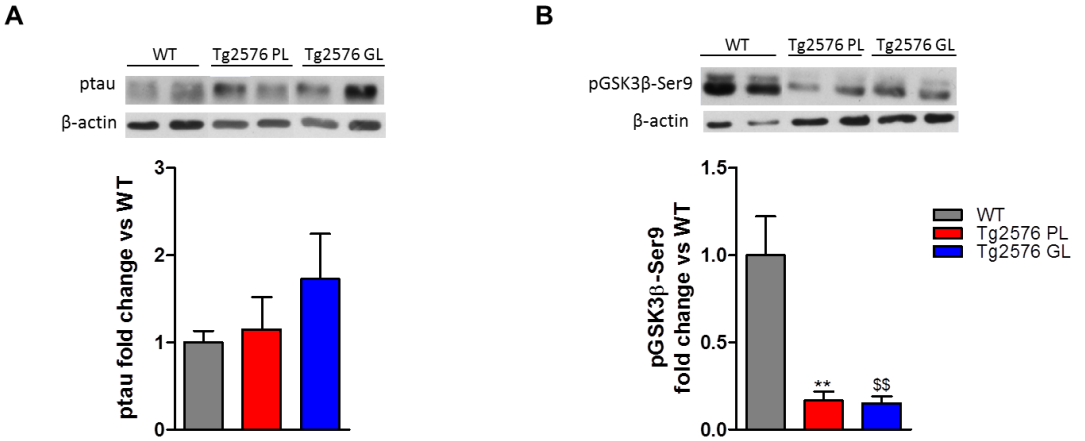

Figure 40. A) ptau levels analyzed by immunoblotting in pre-frontal cortex SDS extracts and normalized vs β-actin. B) Levels of pGSK3β-Ser9 in SDS pre-frontal cortex extracts detected by immunoblotting and

normalized with β-actin (one-way ANOVA test followed by Newman-Kewls *post hoc* test, n=4-5, $^{**}p\leq0.01$ WT versus Tg2576 PL, $^{\$\$}p\leq0.01$ WT versus Tg2576 GL).

4.3. Neuroinflammation

Some studies have suggested that AD and asymptomatic or cognitive resilient AD patients present different levels of astrocytosis and/or microgliosis (Arnold *et al.*, 2013; O'Brien *et al.*, 2009; Perez-Nievas *et al.*, 2013). Therefore, some neuroinflammatory markers had been also studied in PL and GL mice.

Astrogliosis and microgliosis were analyzed by measuring glial fibrillary acidic protein (GFAP) and the cluster of differentiation 11b (CD11b) mRNA respectively through RT-PCR. As depicted in figure 41A, although, as it was expected, AD mice presented higher levels of GFAP mRNA than WT mice, no significant differences were found between PL and GL mice indicating that they presented similar levels of astrocytosis. Moreover, non-differences were found between Tg2576 PL and GL mice in CD11b mRNA levels, thus confirming that they had similar levels of microglia (Figure 41B).

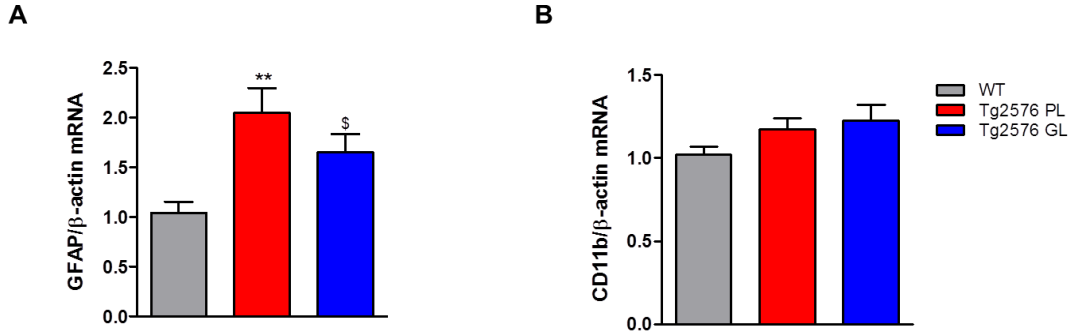

Figure 41. A) Relative hippocampal GFAP and B) CD11b mRNA expression analyzed by RT-PCR and normalized with β-actin (one-way ANOVA test followed by Newman-Kewls *post hoc* test, n=4-5, $^{**}p\leq0.01$ WT versus Tg2576 PL, $^{\$}p\leq0.05$ WT versus Tg2576 GL).

To perform a more exhaustive analysis, the mRNA levels of several pro-inflammatory cytokines (interleukine 1β (IL-1β), tumor necrosis factor α (TNF-α) and interleukine 6 (IL-6) or anti-inflammatory markers (interleukines 4 and 10 (IL-4, IL-10), mannose receptor C-type 1 (MRC1) and arginase 1 (Arg1)) were measured by RT-PCR. In none of the measurements (Figure 42) significant differences were found between demented and resilient Tg2576 mice confirming the absence of differences in neuroinflammation between the two groups. In the case of IL-4 and IL-10, levels were undetectable.

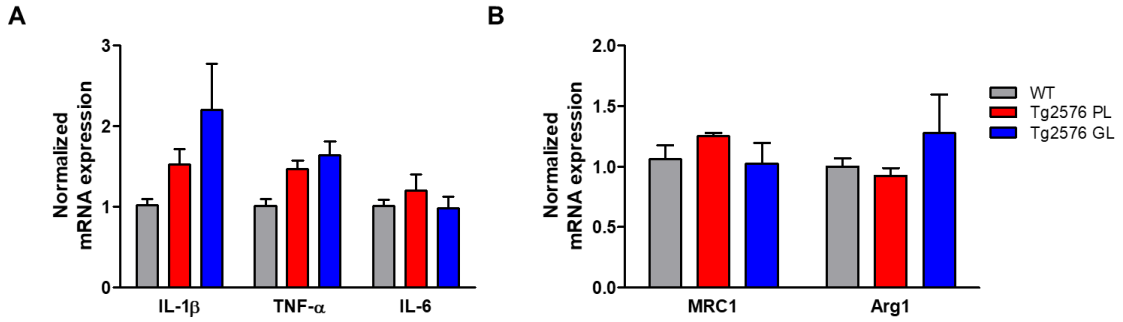

Figure 42. Hippocampal A) pro-inflammatory and B) anti-inflammatory profile of WT (n=5), Tg2576 PL (n=4) and Tg2576 GL (n=4) measured by RT-PCR.

Under normal conditions, the formation of reactive oxygen and nitrogen species, and the consequent oxidative activity encounter a "healthy" balance with immunological responses to maintain cell functions in the brain. However, under different pathological conditions, inflammatory responses recruit pro-oxidant signals and *vice versa* (Aguilera *et al.*, 2018). In consequence, oxidation state was also determined in the present study. Specifically, mRNA levels of cyclooxygenase 2 (COX-2) and inducible nitric oxide synthase (iNOS) were analyzed by RT-PCR. Again, no-differences were found between PL and GL mice (Figure 43).

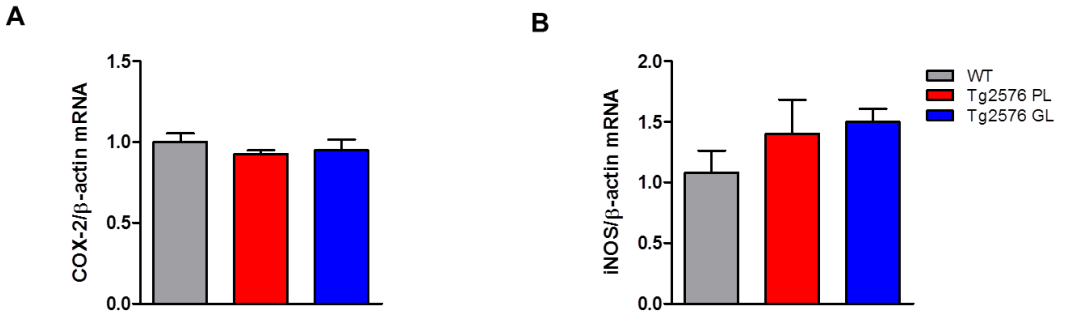

Figure 43. Oxidative state was analyzed by measuring relative hippocampal A) COX-2/ β-actin and B) iNOS/ β-actin mRNA expression through RT-PCR (n=4-5).

Taking all these results into account, differences in neuroinflammation and/or oxidation state can be discarded as causes of cognitive resilience in GL mice.

4.4. Synaptic plasticity

As Tg2576 GL mice performed better than PL and similar to WT in the MWM test, some synaptic plasticity markers (pCREB, synapsin I, postsynaptic density 95 (PSD95), synaptophysin, pCAMKII/CAMKII, phosphorylated extracellular signal-regulated kinase (pERK), NMDA receptor 2B (GluN2B), phosphorylated AMPA receptor subunit GluR1 (p-GluA1) and AMPA receptor subunits GluR2/3 (GluA2-3)) were analyzed in SDS 2% pre-frontal cortex extracts by immunoblotting.

Among all of them (Figure 44), significant differences between PL and GL mice were only observed in the cases of the transcriptional factor pCREB and the presynaptic marker synapsin I. In both cases a significant increase was found in Tg2576 GL mice compared to PL, supporting their better spatial memory performance in the MWM test. It should be noted that, in some synaptic markers, there were not differences between WT and Tg2576 PL mice as expected, maybe due to age-associated changes in synaptic function in WT mice (Weber *et al.*, 2015).

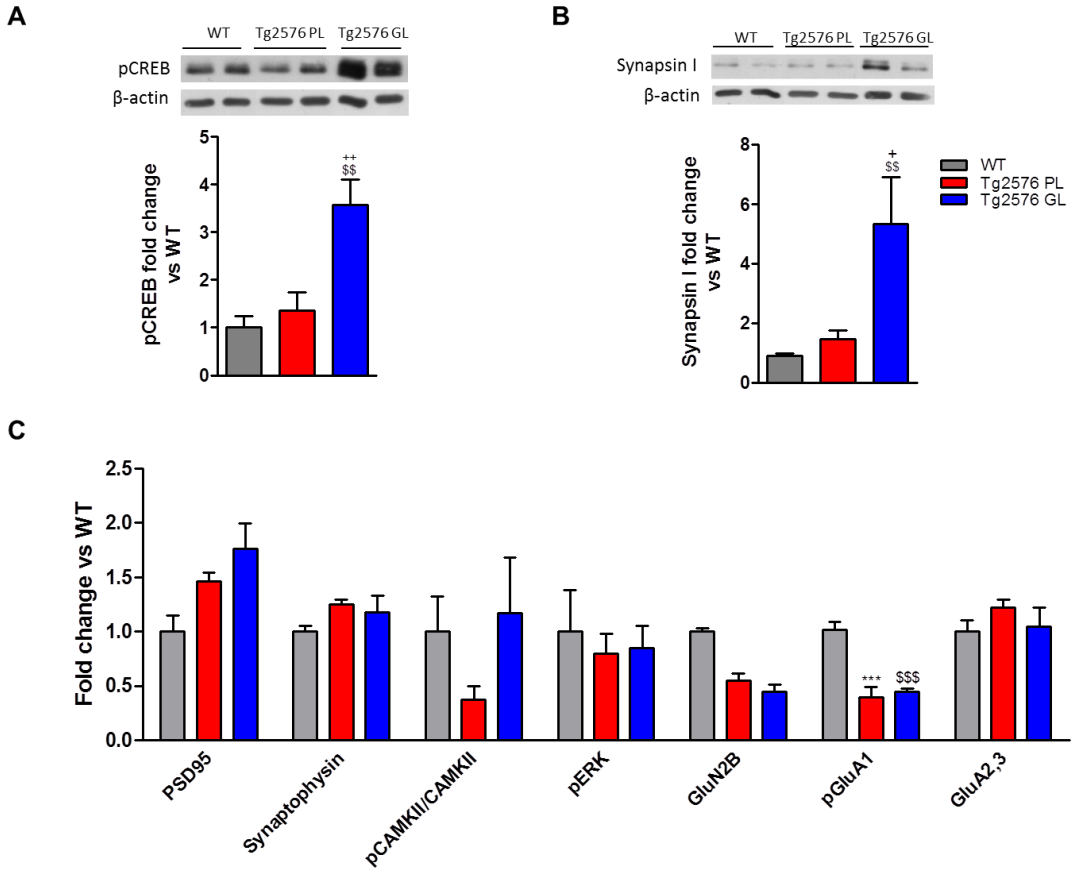

Figure 44. Synaptic plasticity markers. A) Pre-frontal cortex pCREB levels measured by immunoblotting in SDS extracts and normalized vs β-actin (one-way ANOVA test followed by Newman-Kewls *post hoc* test, n=4-5, $^{\$\$}p\leq0.01$ WT versus Tg2576 GL, $^{++}p\leq0.01$ Tg2576 PL versus Tg2576 GL). B) Synapsin I pre-frontal cortex levels assayed by immunoblotting in SDS protein extracts and normalized with β-actin (one-way ANOVA test followed by Newman-Kewls *post hoc* test, n=4-5, $^{\$\$}p\leq0.01$ WT versus Tg2576 GL, $^{+}p\leq0.05$ Tg2576 PL versus Tg2576 GL). C) More synaptic markers analyzed by immunoblotting in SDS pre-frontal cortex extracts (one-way ANOVA test followed by Newman-Kewls *post hoc* test, n=4-5, $^{***}p\leq0.001$ WT versus Tg2576 PL, $^{\$\$\$}p\leq0.001$ WT versus Tg2576 GL).

5. Identification of gen(es) involved in cognitive resilience

As it has been mentioned above, cognitive resilient mice presented higher levels of the transcriptional factor pCREB and the synaptic marker synapsin I than non-resilient mice, thus, supporting their better cognitive performance in the MWM test. However, the mechanism by which they had an increased synaptic plasticity and better spatial memory needs to be elucidated yet.

In order to identify the causal factors of cognitive resilience, transcriptome was analyzed in PL and GL mice. Specifically, an Affymetrix Microarray Hybridization assay followed by a LIMMA analysis was performed to analyze differential hippocampal gene expression between Tg2576 PL and GL. Among all the genes differentially expressed PLA2G4E presented the highest fold change (FC) (log FC=0.97), being its expression significantly higher ($p<0.01$) in the GL group (Table 9).

Table 9. Identification of the most differentially expressed genes in the hippocampus of Tg2576 PL and GL mice using an Affymetrix Microarray Hybridization assay followed by a LIMMA analysis.

probeset_id	GeneID	GeneName	GeneDescription	logFC	AveExpr	t	P.Value	adj.P.Val	B
TC1800000606.mm.2	NM_001033767	Gm4951	predicted gene 4951	-0,78286315	4,2487749	-6,05168685	0,00011775	0,37581169	-1,60884067
TC0600003093.mm.2	NM_001104641	Vmn2r25	vomeronasal 2, receptor 25	-0,77619048	4,12081654	-5,94299077	0,00013629	0,37581169	-1,64630203
TC0X00000277.mm.2	ENSMUST00000178747	Gm21645	predicted gene, 21645 [Source:MGI Symbol;Acc:MGI:5435000]	-0,76982921	4,46334092	-5,8635213	0,00015183	0,37581169	-1,67445277
...	...	...	...	...	...	...	...	...	...
TC1300001526.mm.2	NM_181754	Gpr141	G protein-coupled receptor 141	0,83621369	4,42432997	4,1184396	0,00203375	0,87626368	-2,48685018
TC1400000004.mm.2	ENSMUST00000112797	D830030K20 Rik	RIKEN cDNA D830030K20 gene	0,96176832	5,305224	4,29979578	0,00152238	0,83739155	-2,38283319
TC0200004455.mm.2	NM_177845	Pla2g4e	phospholipase A2, group IVE	0,96862853	7,527345	4,1001912	0,0020944	0,87626368	-2,49759337

As depicted in Figure 45A, the increase in PLA2G4E mRNA levels in the GL group compared to PL was validated by RT-PCR. PLA2G4E protein levels were also analyzed by immunoblotting in both, SDS parieto-temporal (Figure 45B) and pre-frontal (Figure 45C) cortex extracts. Similar to mRNA expression, in both areas enzyme levels were higher in Tg2576 GL than in PL. Moreover, Tg2576 PL mice presented lower protein levels than WT mice, suggesting that this enzyme could be down regulated in AD.

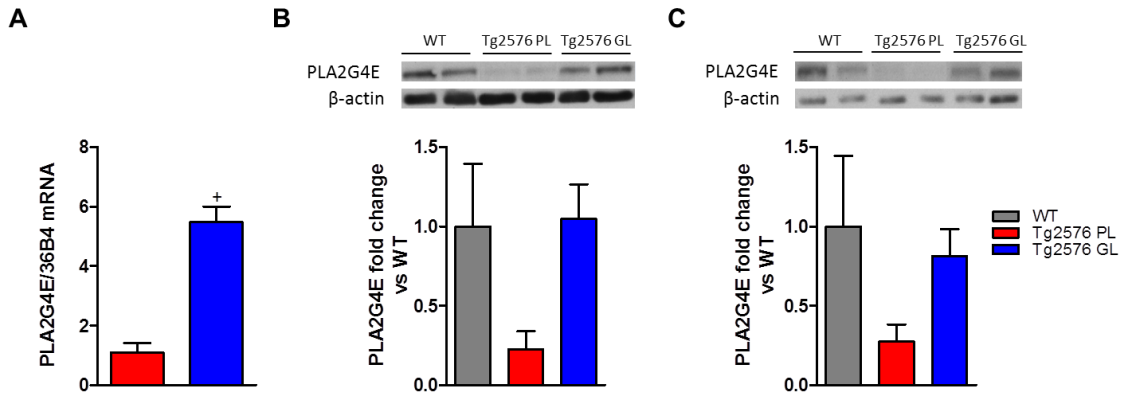

Figure 45. Regulation of PLA2G4E expression levels in AD conditions. A) Relative hippocampal PLA2G4E mRNA expression analyzed by RT-PCR and normalized with 36B4 (unpaired two-tailed Student's t-test, n=4, $^{+}P\leq0.05$ Tg2576 PL versus Tg2576 GL). B) Parieto-temporal and C) pre-frontal cortex PLA2G4E levels assayed by immunoblotting in SDS protein extracts and normalized with β-actin (n=4-5).

6. PLA2G4E in Alzheimer's disease

To test if PLA2G4E is down-regulated in AD patients, and to evaluate if this enzyme is also up-regulated in human cognitive resilient or asymptomatic individuals, its expression was analyzed in the brain of human controls, AD and AAD patients.

Specifically, protein expression levels of PLA2G4E were analyzed by immunoblotting in the temporal cortex of a cohort of AD patients with severe cognitive impairment (n=9), AAD patients with AD-patology but without memory impairment (n=10) and in age-matched controls (n=8). As depicted in figure 46, AD patients showed lower levels of PLA2G4E than controls thus supporting the fact that PLA2G4E is down regulated in AD. Interestingly, as in mice, asymptomatic individuals presented significantly higher levels of enzyme than AD patients, pointing out to a plausible implication of PLA2G4E in cognitive resilience.

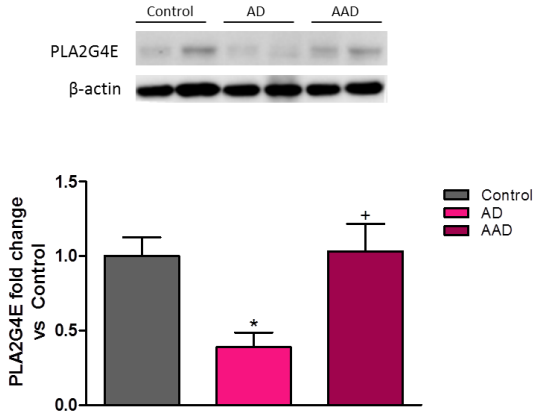

Figure 46. PLA2G4E levels from controls (n=8), AD (n=9) and asymptomatic (AAD) patients (n=10) measured by immunoblotting in cytosolic extracts and normalized vs β-actin (one-way ANOVA test followed by Newman-Keuls *post hoc* test, n=8-10, $^{*}p\leq0.05$ control versus AD, $^{+}p\leq0.05$ AD vs AAD).

As mini mental scores were not available for all subjects, the synaptic marker synapsin I was also analyze by immunoblotting in synaptosome-enriched extracts. As expected, this marker was reduced in AD patients compared to both controls and AAD subjects (Figure 47), supporting their better cognitive status.

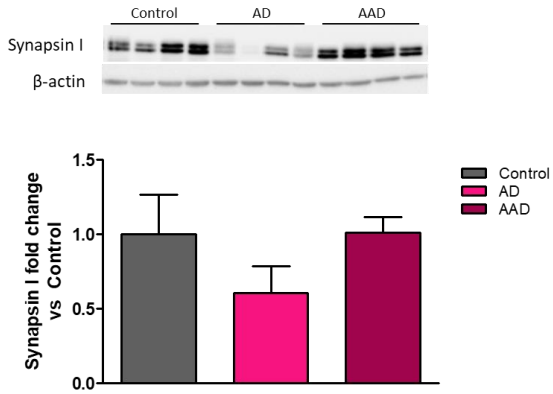

Figure 47. Synapsin I levels from controls (n=8), AD (n=9) and asymptomatic (AAD) patients (n=10) measured by immunoblotting in synaptosome-enriched extracts and normalized vs β-actin.

Cruchaga *et al.* has shown that the rs12232304 SNP located in an intron of PLA2G4E gene, that respond to a guanosine to an adenine change, correlates with CSF APOE protein levels (Cruchaga *et al.*, 2012). Consequently, this SNP was analyzed in controls, AD and AAD patients.

The rs12232304 SNP was not present in control individuals and it was found in heterozygosis in a 22% of AD patients and a 50% of AAD ones (Table 10). APOE genotype was also analyzed in the same samples showing no-correlation between the presence of the mentioned SNP and a specific APOE genotype (Table 10).

Table 10. Table showing data obtained from rs12232304 SNP and APOE genotyping in control, AD and AAD individuals.

	Case	rs12232304 SNP (G>A)	APOE genotype
Control	BCN251	No	ApoE 3,3
Control	BCN256	No	ApoE 2,4
Control	BCN283	No	ApoE 2,3
Control	BCN362	No	ApoE 3,3
Control	BCN382	No	ApoE 3,3
Control	BCN473	No	ApoE 3,3
Control	BCN600	No	ApoE 3,4
Control	BCN618	No	ApoE 3,3
AD	BCN62	No	ApoE 3,3
AD	BCN112	No	ApoE 3,3
AD	BCN267	Heterozygosis	ApoE 3,3
AD	BCN277	No	ApoE 3,3
AD	BCN288	No	ApoE 3,4
AD	BCN291	No	ApoE 3,3
AD	BCN341	No	ApoE 3,3
AD	BCN369	Heterozygosis	ApoE 3,4
AD	BCN549	No	ApoE 3,4
AAD	BCN66	No	ApoE 3,3
AAD	BCN162	No	ApoE 3,4
AAD	BCN181	Heterozygosis	ApoE 3,3
AAD	BCN207	Heterozygosis	ApoE 3,4
AAD	BCN238	No	ApoE 3,3

	Case	rs12232304 SNP (G>A)	APOE genotype
AAD	BCN241	Heterozygosis	ApoE 2,4
AAD	BCN302	Heterozygosis	ApoE 3,4
AAD	BCN438	Heterozygosis	ApoE 3,3
AAD	BCN442	No	ApoE 3,3
AAD	BCN446	No	ApoE 3,3

In the same line, soluble levels of $A\beta_{42}$ were analyzed by ELISA in SDS 2% extracts of control, AD and AAD patients to discard a possible correlation of the SNP with $A\beta_{42}$ levels. As expected, AD and AAD individuals showed higher amounts of soluble $A\beta_{42}$ than controls. Moreover, it was confirmed that both AD and AAD individuals presented similar $A\beta_{42}$ levels, independently on the presence of the SNP (Figure 48).

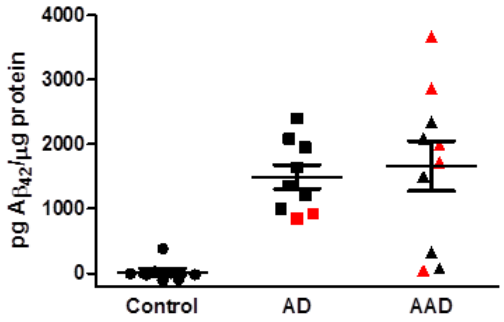

Figure 48. Soluble $A\beta_{42}$ levels in temporal cortical SDS 2% extracts from control, AD and AAD subjects (n=8-10). Note that individual cases in red indicate the presence of rs12232304 SNP in PLA2G4E gene in heterozygosis.

7. PLA2G4E characterization

PLA2G4E is a poorly characterized member of the PLA2G4 clan of cytosolic phospholipases. It is known that this enzyme is highly expressed in several tissues including brain, heart, skeletal muscle, and testis. In the brain, it has been reported that it is expressed in neurons, but not in astrocytes or microglia and that its expression is higher in neonates than in adults (Ogura *et al.*, 2016).

7.1. Neural location

In order to confirm that PLA2G4E has a cytosolic location within the neurons, an immunohistochemistry was performed in formalin-fixed paraffin-embedded hippocampal sections from human subjects. Tissue was also counterstained with hematoxylin–eosin. As shown in figure 49, PLA2G4E was expressed in the neurons where it mainly had a cytosolic location. However, as indicated in figure 49B (red arrow), it also seemed to be expressed in the apical dendrites in some neurons.

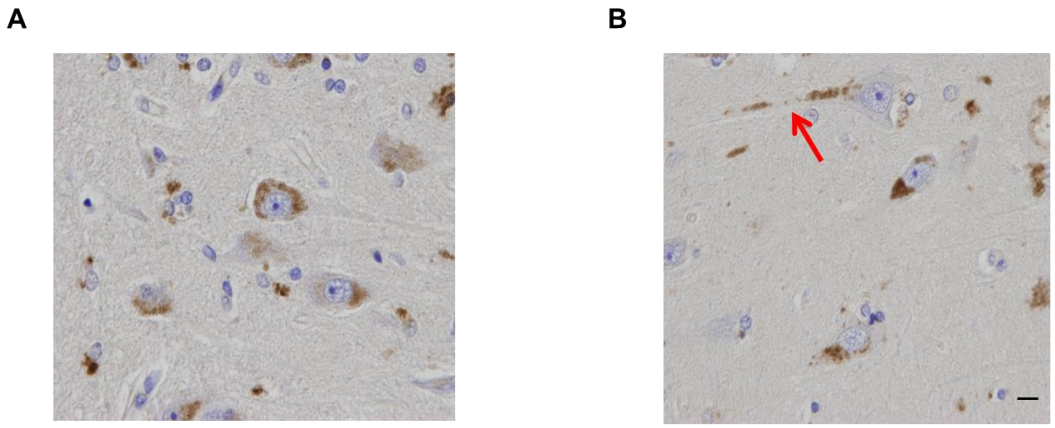

Figure 49. Hippocampal paraffin-embedded human sections immunostained with PLA2G4E anti-serum and counterstained with hematoxylin–eosin showing A) an abundant cytosolic PLA2G4E location and B) a less abundant location at the apical dendrites (red arrow) within the neurons. Scale bar=20μm.

As PLA2G4E seemed to be in the apical dendrites, its subcellular and subsynaptic distribution was also studied in the CA1 region of mice hippocampi using the pre-embedding immunogold technique. As depicted in figure 50, PLA2G4E immuno particles were mostly found at the dendrite (Den) of pyramidal cells (arrows, Figure 50A), and on the extrasynaptic plasma membrane (arrows, Figure 50B) of dendritic spines (s) that establish excitatory synapses with axon terminals (at). Few immunoparticles were observed at intracellular sites (crossed arrows) in dendritic spines (s) (Scale bars = 500 nm).

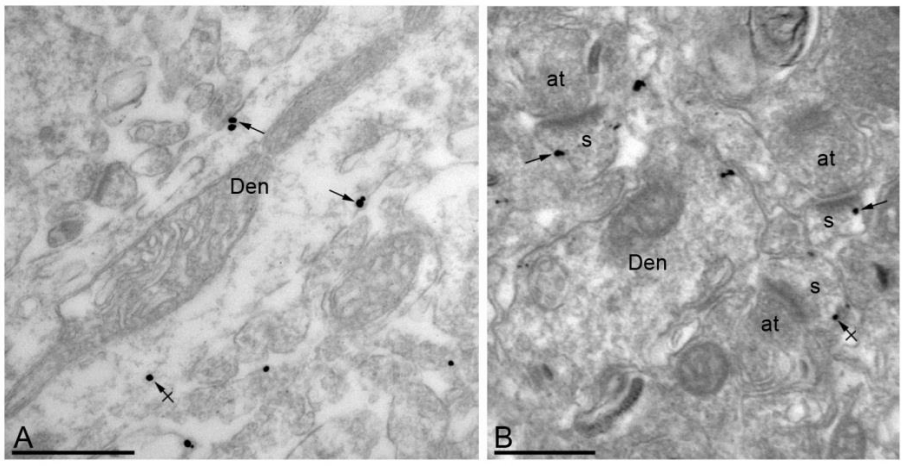

Figure 50. Subsynaptic distribution of PLA2G4E in the CA1 region of mice hippocampi using the pre-embedding immunogold technique. Den: dendrite (Den); s:dendritic spines; at: axon terminals. Arrows indicates extrasynaptic plasma membrane location and crossed arrows intracellular sites in dendritic spines. Scale bar = 500 nm.

7.2. Expression during postnatal brain development

As it has been mentioned before, previous studies have reported that PLA2G4E expression is higher in neonates than in adult mice (Ogura *et al.*, 2016).

To specifically analyze its expression pattern during postnatal brain development, immunoblotting assays were done using half-brain SDS 2% extracts of an embryo at day 17 (E17) and mice from the same litter sacrificed at different days after birth until adulthood (P0-P60). PLA2G4E expression was compared to that of the pre-synaptic marker synapsin I and the neuronal marker NeuN. As observed in figure 51A, PLA2G4E increased during the first days of postnatal development reaching its maximum point of expression at about post-natal day 10 (P10) and then, decreased again, presenting lower expression values during adulthood (P30, P60). On the other hand, synapsin I expression was low during the first days of postnatal development and reached a maximum and plateau expression from about P15-P30 (Figure 51B). NeuN expression increased during the initial days of postnatal brain development, reaching its maximum expression at about P15, point from which expression seemed to stabilize (Figure 51C). Note that this experiment was repeated with 4 different mice litters to confirm the results shown in figure 51.

When comparing both PLA2G4E and synapsin I expression, it can be observed that synapsin I reached its highest expression when PLA2G4E started to decrease. On the contrary, PLA2G4E seemed to present the same expression pattern than NeuN during the first days of postnatal brain development and then, when PLA2G4E expression decreased, NeuN stabilized (Figure 51).

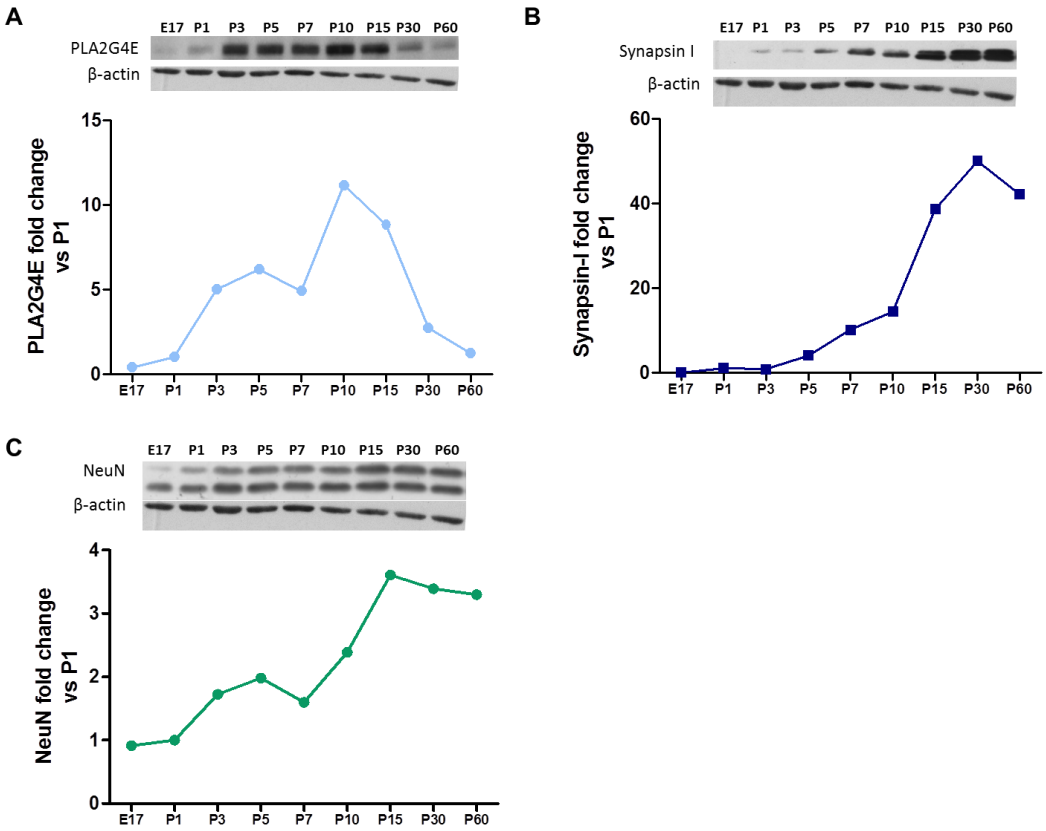

Figure 51. A) PLA2G4E, B) synapsin I and C) NeuN expression during post-natal brain development measured by immunoblotting and normalized *vs* β-actin. E: embryo; P: postnatal. (n=1; confirmation of these results in 4 different mice litters).

These results suggest a role of PLA2G4E in modulating synaptogenesis and/or synaptic plasticity and neuronal maturation during postnatal brain development.

8. Role of PLA2G4E in memory

PLA2G4E up-regulation in aged-Tg2576 that show intact cognition together with its neural location and expression pattern during neural development pointed out to a possible role of this enzyme in synaptic plasticity and, in consequence, in memory function.

In order to elucidate its possible role in memory, PLA2G4E expression was analyzed by immunoblotting after fear-memory consolidation in 2 months-old C57BL/6J WT mice sacrificed one hour after the fear conditioning test (TT group; n=8) and compared to that of mice sacrificed 24 h after the training (T24 group; n=7) and to that of a group of mice that were not subjected to any step of the FC test (naïve group; n=8). Scheme of the FC experiment is shown in figure 52A. PLA2G4E expression was analyzed by immunoblotting in the hippocampus and pre-frontal cortex. As depicted in figures 52B and 52C, PLA2G4E was augmented in the TT group compared to T24 and naïve groups in both areas.

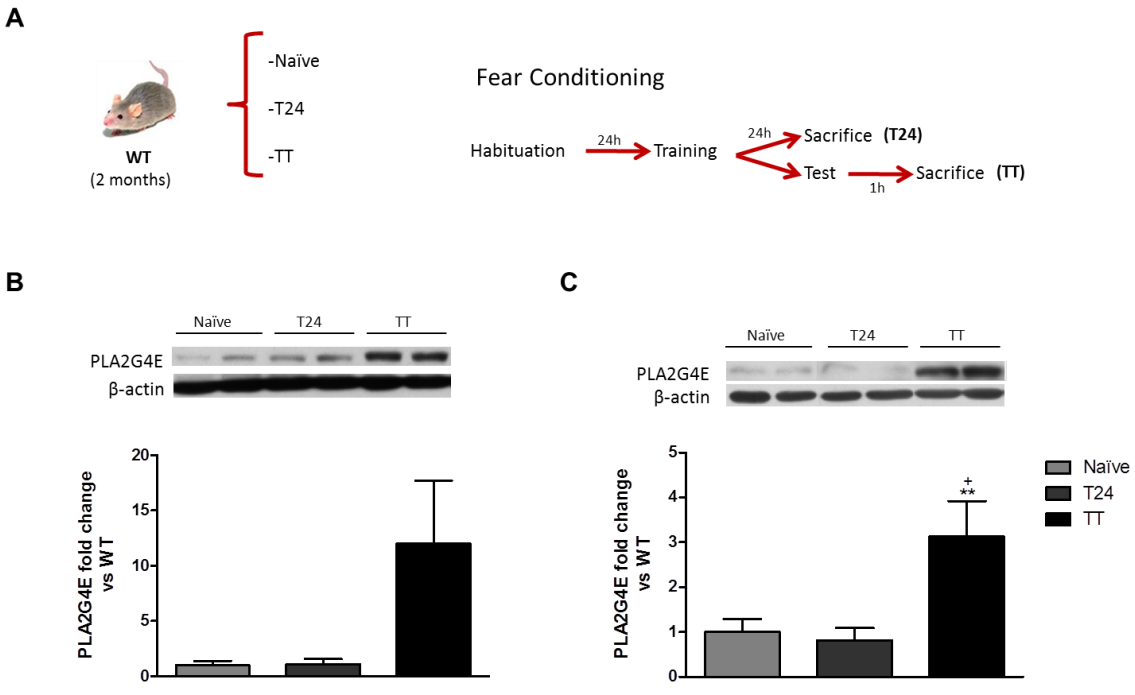

Figure 52. A) Diagram showing the experimental design of the Fear Conditioning paradigm used to elucidate the role of PLA2G4E in memory function. B) PLA2G4E hippocampal levels measured by immunoblotting in SDS 2% extracts. C) PLA2G4E levels measured by immunoblotting in SDS 2% extracts from the pre-frontal cortex (one-way ANOVA test followed by Newman-Kewls *post hoc* test, n=7-8, $^{**}p\leq0.01$ Naïve *vs* TT, $^{+}p\leq0.05$ T24 *vs* TT).

As PLA2G4E was only increased in the group that performed the test (TT group), it could be inferred that this enzyme might be playing a role in memory retrieval.

9. Validation of PLA2G4E overexpression as a possible therapeutic target for AD

9.1. In vitro PLA2G4E overexpression

Before producing the AAV2/9-PLA2G4E virus, its effectiveness overexpressing murine PLA2G4E was tested *in vitro*.

SH-SY5Y cells were transfected with the pRK5-PLA2G4E plasmid (Ogura *et al.*, 2016) using Lipofectamine. At the same time, other cells were co-transfected with the pRK5-PLA2G4E plasmid and with a specific siRNA for murine PLA2G4E to check the specificity of PLA2G4E overexpression with the mentioned plasmid. PLA2G4E protein levels were analyzed by immunoblotting in SDS 2% extracts of these cells and compared to those of control SH-SY5Y cells (non-transfected). As shown in figure 53, PLA2G4E levels were increased in SH-SY5Y cells transfected with the pRK5-PLA2G4E and this increase was specifically reduced in the cells co-transfected with the siRNA-PLA2G4E confirming that pRK5-PLA2G4E plasmid is able to specifically induce PLA2G4E overexpression.

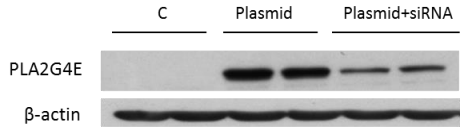

Figure 53. Immunoblot showing PLA2G4E and β-actin levels in SDS 2% extracts of SH-SY5Y cells non-transfected (C), transfected with pRK5-PLA2G4E (Plasmid) and co-transfected with pRK5-PLA2G4E and a specific siRNA for murine PLA2G4E (Plasmid+siRNA) (n=4).

9.2. AAV-mediated hippocampal PLA2G4E overexpression in elderly APP/PS1 mice

To confirm the effect of PLA2G4E overexpression on memory function and to analyze its potentiality as a novel therapy for AD, this enzyme was overexpressed in the hippocampus of elderly APP/PS1 mice (16-19 months), a more aggressive model of amyloidosis, using an AAV9-PLA2G4E adeno-associated virus. The mentioned virus, that overexpressed the murine form of PLA2G4E, was injected specifically in the CA1 region of the hippocampus by stereotactic surgery.

9.2.1. Effect on spatial memory

Two months after injection, memory capacity was assessed using the MWM test in APP/PS1 AAV9-PLA2G4E injected mice (n=10) and compared with that of sham-injected APP/PS1 (n=9) and their negative littermates (n=9). Note that along the study, APP/PS1 sham-injected mice presented a mortality rate of 33% while APP/PS1 mice injected with the AAV9-PLA2G4E and WT mice only presented a mortality rate of 10% and 0% respectively.

During the visible-platform phase, both groups of APP/PS1 mice showed higher escape latencies than WT animals on days 1 and 2 which demonstrates significant main effect of

genotype, however, no significant differences were observed among groups in the last trial of the visible-platform phase (Figure 54A), indicating that at the end of this phase all animals were able to perform the task in the same conditions.

In the hidden-platform phase, as it was expected, sham APP/PS1 mice behaved significantly worse than WT mice (Figure 54B) confirming the spatial memory impairment associated with this AD mouse model (Serneels *et al.*, 2009). Interestingly, PLA2G4E overexpression significantly rescued spatial working-memory impairment in the APP/PS1 model (Figure 54B).

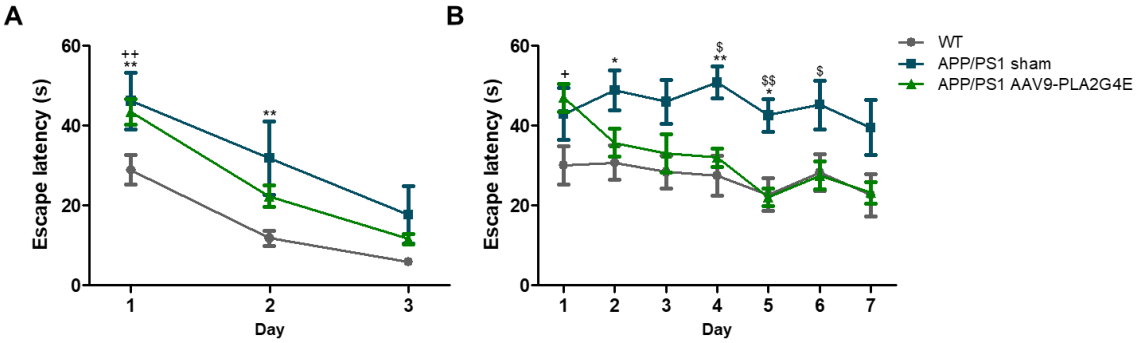

Figure 54. MWM for elderly WT, APP/PS1 sham and APP/PS1 AAV9-PLA2G4E performed two months after stereotactic surgery. A) Escape latency of the visible-platform phase (two-way ANOVA test followed by Bonferroni's *post hoc* test, n=6-9, $^{**}p\leq0.01$ WT vs APP/PS1 sham, $^{++}p\leq0.01$ WT vs APP/PS1 AAV9-PLA2G4E). B) Escape latency to the hidden-platform (two-way ANOVA test followed by Bonferroni's *post hoc* test, n=6-9, $^{*}p\leq0.05$ WT vs APP/PS1 sham, $^{**}p\leq0.01$ WT vs APP/PS1 sham, $^{+}p\leq0.05$ WT vs APP/PS1 AAV9-PLA2G4E, $^{\$}p\leq0.05$ APP/PS1 sham versus APP/PS1 AAV9-PLA2G4E, $^{\$\$}p\leq0.01$ APP/PS1 sham versus APP/PS1 AAV2/9-PLA2G4E).

Moreover, as depicted in figure 55, mice treated with the AAV9-PLA2G4E virus spent more time in the right quadrant than sham-injected mice during the probe trials on days 6th and 8th. This indicates that PLA2G4E overexpression also reversed the memory retention deficits presented by APP/PS1 elderly mice.

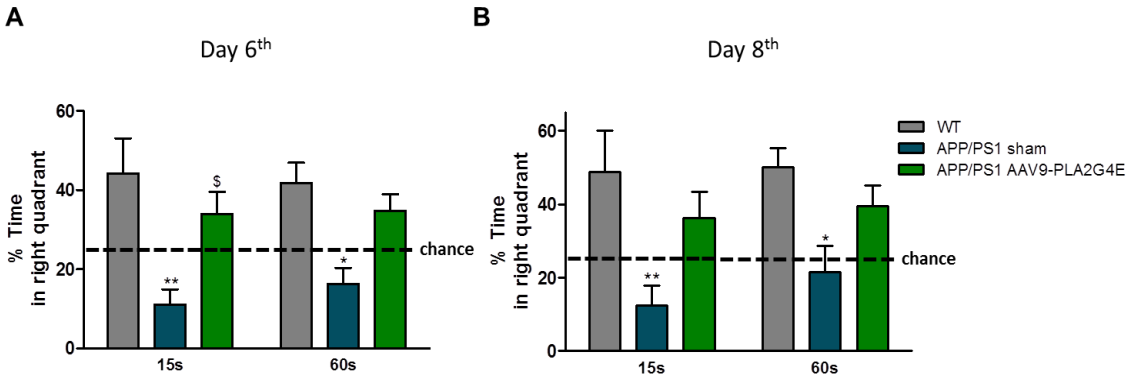

Figure 55. Percentage of time spent in the correct quadrant during the probe trials on day A) 6th and B) 8th of the MWM test performed two months after injection for elderly WT, APP/PS1 sham and APP/PS1 AAV9-PLA2G4E (two-way ANOVA test followed by Bonferroni's *post hoc* test, n=6-9, $^{*}P\leq0.05$ WT vs APP/PS1 sham, $^{**}P\leq0.01$ WT vs APP/PS1 sham, $^{\$}P\leq0.05$ APP/PS1 sham versus APP/PS1 AAV9-PLA2G4E).

In conclusion, hippocampal AAV9-mediated PLA2G4E overexpression in elderly APP/PS1 mice significantly rescued spatial memory impairment two months after stereotactic injection.

9.2.2. Confirmation of hippocampal PLA2G4E overexpression

The effectiveness of the viral vector employed on overexpressing murine PLA2G4E *in vivo* was assessed in the hippocampus of APP/PS1 AAV9-PLA2G4E compared to that of sham-injected mice both by RT-PCR and immunoblotting.

As shown in figure 56, APP/PS1 AAV9-PLA2G4E mice presented higher levels of PLA2G4E mRNA and protein levels than sham-injected mice, thus confirming an effective AAV-mediated PLA2G4E hippocampal overexpression.

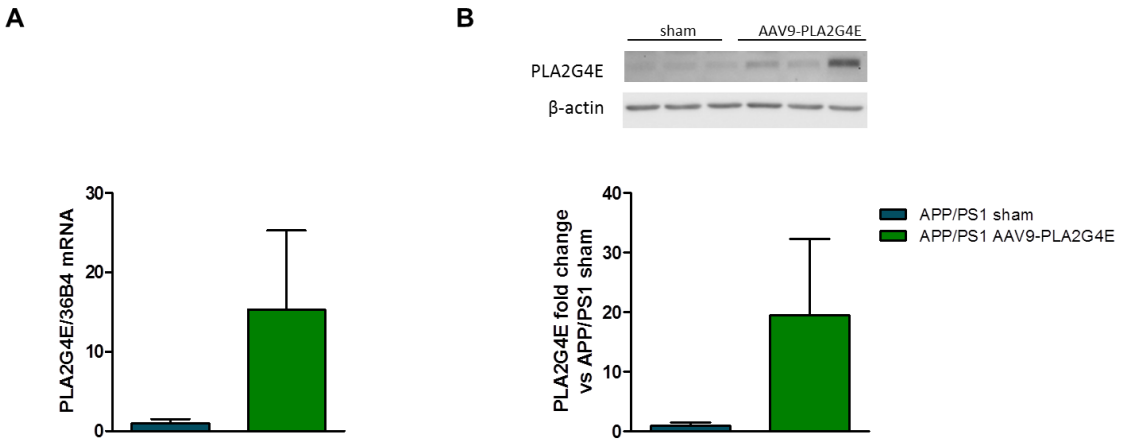

Figure 56. A) Relative hippocampal PLA2G4E mRNA expression analyzed by RT-PCR and normalized with 36B4. B) Hippocampal PLA2G4E levels assayed by immunoblotting in SDS protein extracts and normalized with β-actin (n=3).

9.2.3. Effect on synaptic plasticity

The Golgi-Cox method was used to analyze whether the behavioral recovery induced by PLA2G4E overexpression was reflected by structural changes in dendritic spine density. Specifically, apical dendrites from pyramidal neurons of the CA1 region of the hippocampus were studied.

As depicted in figure 57, treatment with AAV9-PLA2G4E virus was able to significantly increase dendritic spine density respect to both WT, and APP/PS1 sham mice. Non-differences were found between WT and APP/PS1 sham mice.

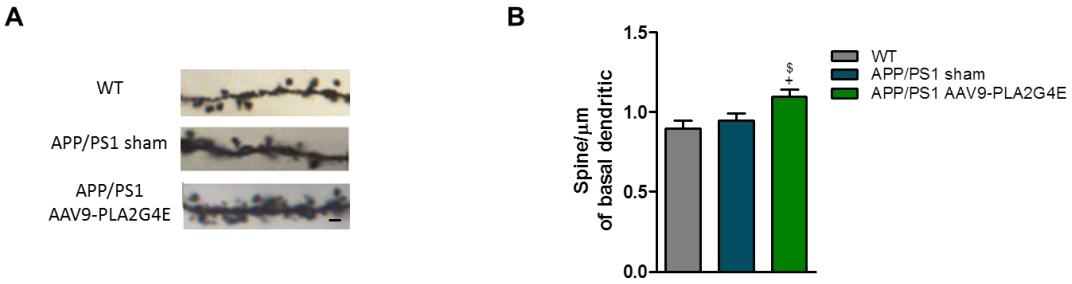

Figure 57. Effect of PLA2G4E overexpression on dendritic spine density in pyramidal neurons of the hippocampus of elderly APP/PS1 mice. A) Representative Golgi staining images of apical dendrites on CA1 hippocampal pyramidal neurons. Scale bar=10 µm. B) Histoblot showing spine density quantification of those neurons in WT, APP/PS1 sham and AAV9-PLA2G4E treated mice (one-way ANOVA test followed by Newman-Kewls *post hoc* test, n=4, $^{+}p \leq 0.05$ WT vs APP/PS1 AAV9-PLA2G4E, $^{\$}p \leq 0.05$ APP/PS1 sham versus APP/PS1 AAV9-PLA2G4E).

These results suggest that changes in spine density might account for the memory recovery observed in the group of APP/PS1 mice overexpressing PLA2G4E.

9.2.4. Effect on amyloid pathology

Soluble $A\beta_{42}$ levels in APP/PS1 sham and AAV9-PLA2G4E injected mice were assayed in hippocampal extracts by ELISA to confirm whether PLA2G4E overexpression had an effect on amyloid pathology.

As shown in figure 58, non-differences were found between groups, indicating that PLA2G4E overexpression did not affect amyloid pathology in elderly APP/PS1 mice.

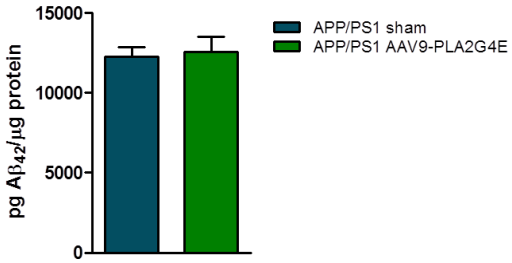

Figure 58. Soluble $A\beta_{42}$ levels in SDS 2% hippocampal samples from elderly APP/PS1 sham or AAV9-PLA2G4E injected mice measured by ELISA (n=6-9).

9.2.5. Effect on tau pathology

To check whether PLA2G4E overexpression had an effect in tau pathology, levels of tau phosphorylation were detected by immunoblotting using PHF1 antibody.

As expected, ptau (Ser-366:Ser-404) levels tend to decrease in WT mice compared to APP/PS1. However, there were not differences between sham and AAV9-PLA2G4E injected APP/PS1 mice (Figure 59), which suggest that PLA2G4E overexpression do not affect tau pathology.

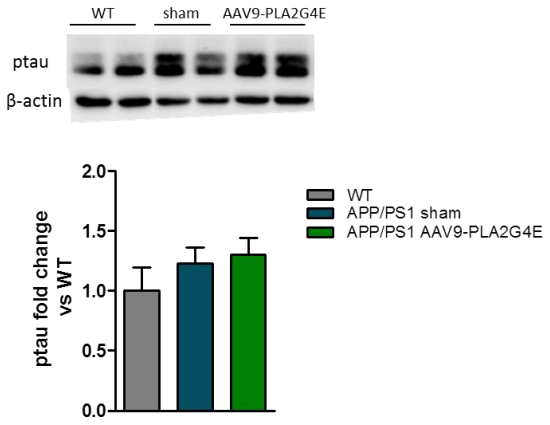

Figure 59. ptau levels analyzed by immunoblotting in hippocampal SDS extracts and normalized vs β-actin.

10. Validation of PLA2G4E overexpression as a possible therapeutic target for age-related cognitive impairment

As PLA2G4E overexpression seemed to rescue memory impairment in elderly-APP/PS1 mice, its effect was also test in elderly WT mice to confirm if it was able to reverse age-related memory impairment in this mice.

10.1. AAV-mediated hippocampal PLA2G4E overexpression in elderly C57BL/6/SJL WT mice

A pilot study was performed to check the effect of PLA2G4E overexpression on memory function in 17 months old C57BL/6/SJL WT mice injected with the adeno-associated virus AAV9-PLA2G4E in the CA1 region of the hippocampus.

10.1.1. Effect on spatial memory

Three months after stereotactic surgery procedure, spatial memory was tested in elderly WT mice injected with AAV9-PLA2G4E (n=5) and compare with that of WT sham-injected (n=4) mice using the MWM test.

In the visible-platform phase (Figure 60A), non-significant differences were found between groups indicating that all animals were able to perform the task similarly. In the same line, as shown in figure 60B, there were non-significant differences between both groups during the hidden-platform phase.

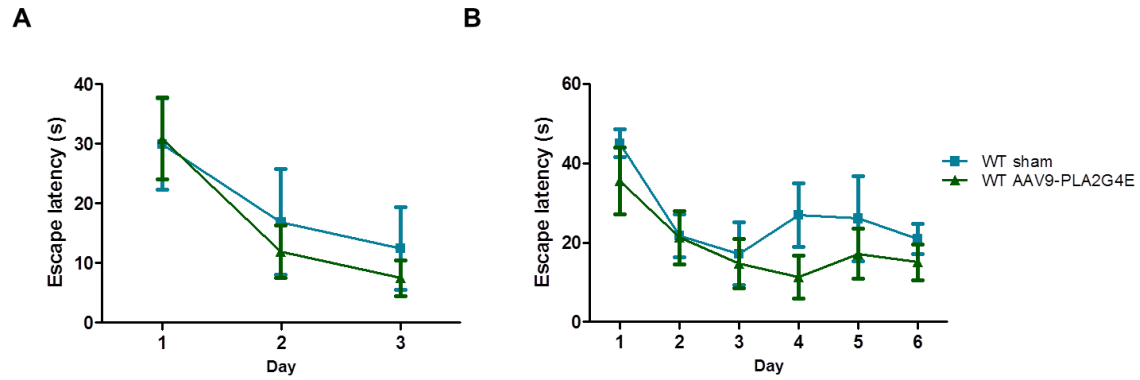

Figure 60. MWM test performed three months after stereotactic surgery for elderly WT sham and AAV9-PLA2G4E (n=4-5). A) Escape latency of the visible-platform phase and B) escape latency to the hidden-platform.

However, mice treated with AAV9-PLA2G4E spent more time in the right quadrant during the probe trials performed on day 5th (Figure 61A) and 7th (Figure 61B) than sham-injected mice, indicating that AAV-mediated PLA2G4E hippocampal overexpression improves memory retention rates in elderly WT mice.

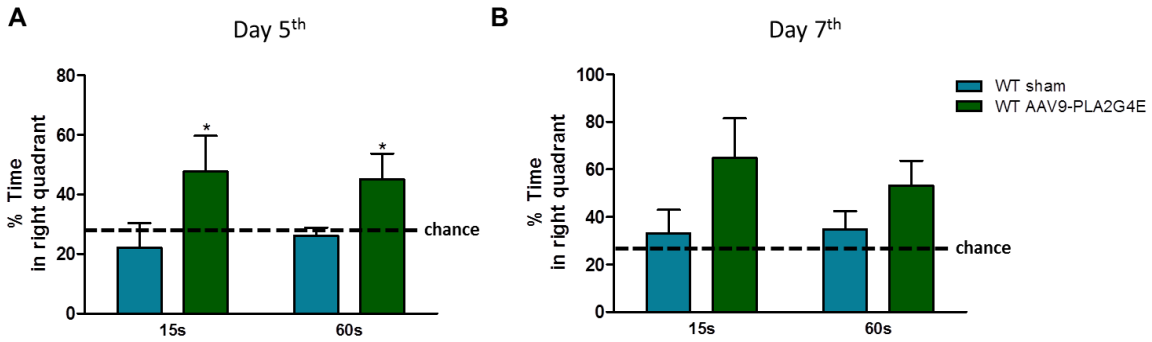

Figure 61. Percentage of time spent in the correct quadrant during the 15s and 60s probe trials carried out on days A) 5th and B) 7th for elderly WT sham and WT AAV9-PLA2G4E mice 3 months after stereotactic surgery (one-way ANOVA test followed by Newman-Kewls post hoc test, n=4-5, *P≤0.05 WT sham vs WT AAV9-PLA2G4E).

10.1.2. Effect on synaptic plasticity

To check if PLA2G4E overexpression was also able to increase synaptic spine density in elderly WT mice, Golgi-Cox method was used to analyze it in apical dendrites from pyramidal neurons of the CA1 region of the hippocampus.

As depicted in figure 62, non-differences were found between WT sham and AAV9-PLA2G4E treated mice, so treatment with AAV9-PLA2G4E virus was unable to increase dendritic spine density in these mice.

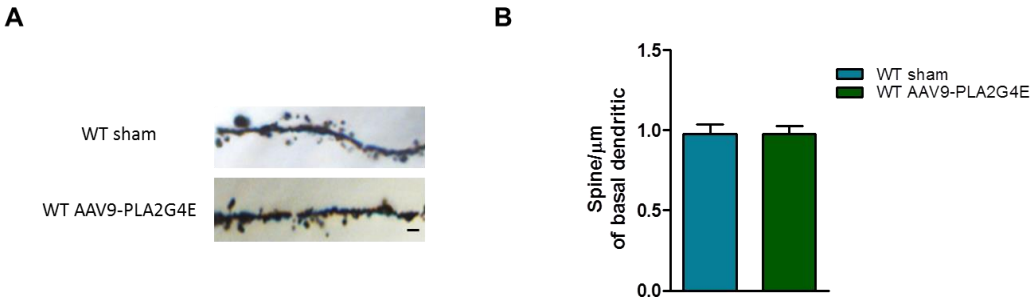

Figure 62. Effect of PLA2G4E overexpression on dendritic spine density in pyramidal neurons of the hippocampus of 17-months old C57BL/6/SJL WT mice. A) Representative Golgi staining images of apical dendrites on CA1 hippocampal pyramidal neurons. Scale bar=10 µm. B) Graph showing spine density quantification of those neurons in WT sham and AAV9-PLA2G4E treated mice.

DISCUSSION

The current increase in life expectancy and consequent population aging is significantly rising the incidence of neurodegenerative disorders, including AD (Martin Prince *et al.*, 2014). This fact, together with the lack of effective therapies for this progressive and irreversible neurodegenerative disease, makes essential to promote AD research to find efficient treatments. However, despite years of efforts trying to achieve it, the failure rate in AD drug development is almost 100% (Mullane & Williams, 2019), indicating that is clearly necessary to change the way of approaching the search for new AD targets.

In line with this idea, the use of multi-therapies, targeting different aspects of AD pathogenesis at the same time, has been proposed as a promising strategy to obtain an effective treatment (Mangialasche *et al.*, 2010; Cummings *et al.*, 2018). Nevertheless, it is possible that a more drastic change in the way of studying AD would be needed.

Accordingly, on the one hand, a novel multitarget approach based on dual HDAC6 and PDE9 inhibition for AD was tested in the present thesis and, on the other hand, a newfangled strategy: the study of cognitive resilient subjects was employed to identify new therapeutic targets for AD.

NOVEL MULTITARGET APPROACH FOR ALZHEIMER'S DISEASE TREATMENT: DUAL HDAC6 AND PDE9 INHIBITION

In the present thesis, a NCE, called CM-695 (Rabal *et al.*, submitted), is proposed as a promising therapy for AD as it presented potential therapeutic effects in a well-established mouse model of AD. In aged-Tg2576 mice, cognitive impairment and amyloid pathology were ameliorated after chronic administration of the compound. The improvement observed seems to be mediated by an increase in the expression of the chaperones GRP78 and Hsp70, which are involved in protein folding. Thus, CM-695 appears to be a safe and efficient disease-modifying agent for AD treatment, confirming that multi-target therapies may represent a good option for the treatment of complex diseases.

HDAC inhibitors have been proposed as potential therapies for AD by several authors (Peixoto & Abel, 2012; Sharma *et al.*, 2019). It is extensively believed that HDAC class I inhibition facilitates gene transcription and the formation of new synapses (Rumbaugh *et al.*, 2015) while HDAC class IIb (HDAC6) inhibition, by targeting cytoplasmic proteins, is involved in the clearance of misfolded proteins (Sung *et al.*, 2013). In consequence, the inhibition of both isoforms exerts a promising and cooperative action to counteract AD, which effectiveness has been demonstrated by using pan-HDAC inhibitors. However, since these compounds may present unfavorable side effects when administered chronologically and at a dose sufficient to reach the brain at appropriate concentrations (Subramanian *et al.*, 2010), its combination with other molecules with different activities such as PDEi or glycogen synthase kinase 3β inhibitors could be an effective strategy to reduce toxicity while maintaining effectiveness (De Simone & Milelli, 2019).

Accordingly, and taking into account the multifactorial origin of AD, acting on different pathways could be the best strategy to achieve a substantial improvement of AD phenotype (Mangialasche *et al.*, 2010; Cummings *et al.*, 2018). Thus, during the last few years, in the laboratory, the concomitant inhibition of HDAC and PDE has been postulated as a novel multitarget therapeutic approach to treat AD (Cuadrado-Tejedor *et al.*, 2015; and 2017). Firstly, by using the reference compounds vorinostat (pan-HDACi) and tadalafil (PDE5i), a synergistic effect on amelioration of the AD phenotype in Tg2576 mice was demonstrated, confirming the efficacy of this new multitarget therapeutic approach (Cuadrado-Tejedor *et al.*, 2015). Next, the lead compound CM-414, a moderate class I HDACi with potent inhibition of HDAC6 and PDE5 was also successfully tested in aged-Tg2576 (Cuadrado-Tejedor *et al.*, 2017; Rabal *et al.*, 2016).

In order to reduce the toxicity associated with class I inhibition, which may complicate the further therapeutic development, a new series of compounds targeting specifically HDAC6 over class I HDAC isoforms (Rabal *et al.*, submitted) were recently designed. Moreover, since cGMP-specific PDE inhibitors have pro-cognitive and neuroprotective effects, the inhibition of PDE9 was selected rather than PDE5 as its brain expression and affinity for cGMP is higher (Figure 22)(Andreeva *et al.*, 2001; Singh & Patra, 2014). Among the new compounds designed, CM-695 was tested in the Tg2576 AD model following the same guidelines used with CM-414 (Cuadrado-Tejedor *et al.*, 2017) in order to compare the efficacy between the two compounds.

The therapeutic effects obtained in memory function after chronic treatment with CM-695 were similar to those obtained with CM-414, except that the effect did not persist when the drug was no longer administered (long-lasting changes on memory were observed after a wash out period of 4-weeks in the case of the combination of vorinostat and tadalafil (Cuadrado-Tejedor *et al.*, 2015) or CM-414 administration (Cuadrado-Tejedor *et al.*, 2017). Taking into account the different inhibition profile of CM-695, it can be confirmed that class I HDACs inhibition, and more specifically HDAC2 inhibition (more selectively inhibited by CM-414 and/or vorinostat than by CM-695), seems to play an important a role in maintaining memory function.

Interestingly, the effect of CM-695 on Aβ clearance, which may be mediated by the inhibition of HDAC6 (Boyault *et al.*, 2007), was maintained after the wash-out period. Heat-shock protein 90 (Hsp90) is one of the targets of HDAC6. The inhibition of HDAC6 increases Hsp90 acetylation, releasing its client proteins like heat shock transcription factor 1 (HSF1), which in turn translocates to the nucleus and mediates the transcription of HSPA1A/B genes, and ultimately, Hsp70 (Wang *et al.*, 2014). HSPA1A/B was among the genes overexpressed in the Affymetrix microarray analysis, and validated by RT-PCR, in the hippocampus of mice administered with CM-695 compared to vehicle. Significantly, a similar induction of Hsp70 was observed in a mice model of thrombosis after CM-695 administration (Allende *et al.*, 2017). It has been demonstrated that Hsp70 fulfils a neuroprotective role in AD by decreasing the oligomerization and production of toxic Aβ isoforms, and by increasing its degradation (Magrané *et al.*, 2004; Muchowski & Wacker, 2005; Kumar *et al.*, 2007). Interestingly, Hsp70 upregulation by inhibiting

Hsp90 was also proposed as a mechanism to normalize synaptic transmission in a transgenic model of tau aggregation (Thirstrup *et al.*, 2016). These results suggest that the increase in HSPA1A/B expression detected in the brain at the end of treatment is at least partially responsible for the marked decrease in hippocampal Aβ levels observed in CM-695 treated mice.

As demonstrated by Affymetrix microarray analysis and qRT-PCR, the chaperone GRP78 was also up-regulated in the hippocampus of mice administered with CM-695 compared to vehicle. It is extensively believed that, under physiological conditions, the bulk of immature APP associates with GRP78 in the endoplasmic reticulum (ER), where this enzyme plays important roles facilitating APP correct folding and modulating its maturation and processing (Yang *et al.*, 1998)(Kudo *et al.*, 2006). However, under ER stress, overexpression of GRP78 retains APP in the early secretory compartments causing a reduction of Aβ production (Kudo *et al.*, 2006). Regarding AD, it has been shown that GRP78 levels are two-fold higher in the temporal cortex and hippocampus of AD patients than in non-demented control cases. More interestingly, it seems that this increase was specifically found in neurons that were still healthy, thus, indicating that GRP78 overexpression may slow down neurodegeneration (Hoozemans *et al.*, 2009). A similar increase was found in the AD mice model 3xFAD, correlating with the presence of accumulated toxic Aβ species (Soejima *et al.*, 2013). So, the increase in GRP78 expression observed with the treatment suggests that this chaperone may also be participating in the reduction of hippocampal Aβ levels observed in CM-695 treated mice.

These results pointed out that, together with PDE9 inhibition, the increase of Hsp70 and GRP78 may be playing a role in memory restoration as these two proteins were no longer up-regulated after the 4-week washout period, when the effect on memory function was not anymore maintained.

In conjunction, it seems that CM-695 is a safe and efficient disease-modifying agent to treat AD, confirming that multitarget therapies may provide good options to combat AD, as seen in other multifactorial diseases like cancer or AIDS. Accordingly, and taking into account its safe profile, a chronic treatment, without wash-out periods, could be an option to considerer for this NCE.

IDENTIFICATION OF NEW THERAPEUTIC TARGETS FOR ALZHEIMER'S DISEASE BY THE STUDY OF COGNITIVE RESILIENT SUBJETS

Along this thesis, a new therapeutic target for AD, the phospholipase A2 group IVE (PLA2G4E), was identified using a novel strategy based on the study of cognitive resilient AD mice.

Several longitudinal studies have clearly demonstrated that amyloid plaques and NFTs, the main hallmarks of AD, are not limited to individuals with dementia (Crystal *et al.*, 1988; Dickson *et al.*, 1992; Hulette *et al.*, 1998; Katzman *et al.*, 1988; Knopman *et al.*, 2003; Price *et al.*, 1991; Schmitt *et al.*, 2000; Tomlinson *et al.*, 1968). In general, it can be inferred that a 25-50% of elderly individuals with normal cognition present AD

pathology in their brains (Riley *et al.*, 2005; Price *et al.*, 2009; O'Brien *et al.*, 2009; Balasubramanian *et al.*, 2012). Although some authors have suggested that the presence of these markers is indicative of AD preclinical stages (Hyman, 1997; Morris, 2005; Morris *et al.*, 1996; Reiman *et al.*, 1996; Tagliavini *et al.*, 1988), others consider it as part of the normal aging process (Delaère *et al.*, 1990, 1993; Mrak *et al.*, 1997). In any case, understanding the mechanism by which these individuals are able to cope with AD pathology without developing dementia would be of great interest to find novel biochemical targets that may be associated with cognitive brain aging in the setting of pathological AD (Arnold *et al.*, 2013).

Factors such as "brain reserve", "cognitive reserve", education, physical performance and specific diets have emerged as possible contributors of cognitive resilience in these asymptomatic AD patients (Arnold *et al.*, 2013; Bullain *et al.*, 2013; Negash *et al.*, 2013; Shlisky *et al.*, 2017; Stern, 2012). Taking all of them into account, it can be inferred that an increased synaptic plasticity, either in an innate way or promoted by external agents, allows these subjects to deal better with AD pathology. These findings suggest that therapies that increase synaptic plasticity would be really valuable for AD treatment. In fact, it has been shown that cognitive training, by enhancing synaptic plasticity, improves cognition, activities of daily living and decision making in AD patients at early-stages (Yu *et al.*, 2009).

In the present thesis, to minimize the intrinsic limitations of using postmortem brain samples (Ferrer *et al.*, 2008) and its variability (Caspers *et al.*, 2014), it has been proposed to study the mechanisms underlying cognitive resilience in an AD mouse model.

Using the MWM test, it was observed that a 22% of elderly Tg2576 mice, with an established AD-neuropathological phenotype, did not present spatial cognitive deficits. This result is in accordance with a previous study performed in the AD mouse model 5xFAD, where a 30% of 8 months-old mice showed intact memory in the FC test (Neuner *et al.*, 2017), thus confirming that, similarly to humans, cognitive resilience also occurs in AD mice. These results pointed out to the worth of these models for studying AD, because although they do not reproduce well all the processes involved in AD pathogenesis, they are able to mimic more uncommon effects such as the existence of cognitive resilient subjects.

The better cognitive performance of the mice identified as "cognitive resilient" correlated with the increased synaptic plasticity observed in their brains, which was manifested as higher levels of the transcriptional factor pCREB and the presynaptic marker synapsin I. It is believed that synapsin I, which is involved in synaptic vesicle release and in the establishment of the reserve pool of synaptic vesicles (Llinás *et al.*, 1991; Melloni *et al.*, 1994; Li *et al.*, 1995; Jovanovic *et al.*, 2000), is among the memory-related genes regulated by the transcriptional factor CREB (Guibinga *et al.*, 2013), thus, explaining the simultaneous increase of both markers. However, differences between WT and Tg2576 mice (PL) were not as marked as expected and, even, inexistent in some cases. This fact may be explained by age-associated changes in synaptic function (Weber *et al.*, 2015).

As lower amounts of mature senile plaques, associated to dystrophic neurites, have been linked with cognitive resilience in elderly human subjects (Perez-Nievas *et al.*, 2013), amyloid pathology was analyzed in cognitive resilient mice. No differences in the levels of $A\beta_{42}$, C99/APP or diffuse and mature senile plaques were observed between cognitive resilient and demented mice, thus discarding the implication of amyloid pathology in the observed cognitive resilience.

In the same line, due to the good correlation between NFTs distribution and AD clinical symptoms in AD patients (Arriagada *et al.*, 1992), tau pathology was also analyzed in these mice. As Tg2576 mice do not present NFTs, ptau and pGSK3β (the main kinase responsible of tau phosphorylation) levels were analyzed. Again, no differences were found between groups in any of these proteins, suggesting that tau pathology does not seem to be implicated in cognitive resilience in elderly-Tg2576 mice.

Taken together, these results support the idea that the presence of amyloid and/or tau pathology does not necessary lead to cognitive impairment, which experimentally supports those mismatched human cases that presenting AD neuropathological features do not develop any signs of dementia (Tomlinson *et al.*, 1968; Katzman *et al.*, 1988; Crystal *et al.*, 1988; Price *et al.*, 1991; Dickson *et al.*, 1992; Hulette *et al.*, 1998; Schmitt *et al.*, 2000; Knopman *et al.*, 2003).

Some studies performed in asymptomatic or cognitive resilient individuals have come up with the idea that differences in neuroinflammation, specifically astrogliosis and/or microgliosis, could be playing a role in AD cognitive resilience. Nevertheless, there is some controversy about whether an increase (Arnold *et al.*, 2013) or a decrease (Perez-Nievas *et al.*, 2013) in GFAP, an astrogliosis marker, is protective against AD-related dementia. Therefore, several neuroinflammatory and other related markers were also analyzed, although non-significant differences were found between resilient and demented Tg2576 mice. Thus, it seems that, at least in this case, neuroinflammatory response may not be responsible of the cognitive resilience observed.

Next, to get insight the mechanisms underlying the resistance against dementia in aged-Tg2576 mice, an Affymetrix Microarray Hibridization assay was performed to identify possible genes implicated in this protective mechanism. PLA2G4E, a poorly characterized member of the PLA2G4 clan of cytosolic phospholipases (Ogura *et al.*, 2016), was the gene most differentially expressed between demented and cognitive resilient AD mice. This phospholipase showed to be up-regulated in cognitive resilient mice compared to memory impaired ones.

Phospholipases A2 (PLA2s) are enzymes involved in the metabolism of membrane phospholipids. Specifically, they catalyze the hydrolysis of membrane glycerophospholipids at the sn-2 position to generate lysophospholipids and free fatty acids, frequently arachidonic acid (AA), which is a precursor of eicosanoids, signaling molecules in which are included prostaglandins and leukotrienes. PLA2s include several unrelated protein families with common enzymatic activity and can be divided into

secreted, cytosolic, calcium-independent and lipoprotein-associated PLA2s (Dennis, 1994).

In the CNS, these enzymes are thought to be involved in important processes such as neuroinflammation, exocytosis, maintenance of membrane fluidity, generation of acetylcholine, memory and protection against oxidative damage (Sun *et al.*, 2004). However, their specific implication in neurodegenerative disorders such as AD is still controversial as some studies have suggested a beneficial role of PLA2 activation (Schaeffer *et al.*, 2009; Mury *et al.*, 2016; Gama *et al.*, 2015) while others pointed out to a detrimental one (Doody *et al.*, 2015; Cakir *et al.*, 2017; Yun *et al.*, 2013).

The obtaining of these controversial results might be explained by the differential functions of each single PLA2 isozyme. For example, it has been demonstrated that the isozymes PLA2G4A and PLA2G6 play important roles in Wallerian degeneration, process which includes axonal degeneration and myelin clearance, as well as in axon regeneration after sciatic nerve crush injury (López-Vales *et al.*, 2008). In the same line, mutations in PLA2G6 gene have been linked with neurodegenerative disorders characterized by high iron accumulation in the brain and neuroaxonal dystrophy, including Parkinson disease (Morgan *et al.*, 2006; Lv *et al.*, 2012; Malaguti *et al.*, 2015).

Thus, one of the aims of this project was to specifically elucidate the possible implication of PLA2G4E, also named cytosolic phospholipase A2 epsilon (PLA2Ɛ), in AD pathogenesis and/or memory function.

In the present thesis, it was demonstrated for the first time that PLA2G4E seems to be down-regulated in AD. It was shown that elderly Tg2576 mice tend to have lower levels of this enzyme than their negative littermates. In the same line, the enzyme was also decreased in AD patients compared to controls. The down-regulation observed in AD could be in accordance with previous studies reporting reduced PLA2-activity in blood samples, postmortem neuronal tissue and CSF of AD patients (Ross *et al.*, 1998; Gattaz *et al.*, 1996, 2004; Talbot *et al.*, 2000; Smesny *et al.*, 2008). Summarising, in these studies, it is suggested that decreased PLA2 activity may cause a reduction of acetylcholine, as this enzyma regulates its synthesis, and also that it may contribute to the production of amyloidogenic peptides by decreasing APP secretion. However, taking into account that PLA2G4E seems to exhibit very low phospholipase activity (Ohto *et al.*, 2005; Ghomashchi *et al.*, 2010), its contribution to total PLA2 activity would be minimum.

Surprisingly and in accordance to data of resilient-Tg2576 mice, it was found that PLA2G4E was up-regulated in the temporal cortex of asymptomatic AD patients (AAD) and that such increase correlated with high levels of the synaptic marker synapsin I. To understand PLA2G4E implication in AD phenotype it should be very interesting to analyze why these “cognitive resilient” patients (AADs) show a different expression pattern of PLA2G4E compared to AD cases. Accordingly, and as a previous study has shown a specific SNP, rs12232304, in an intron of PLA2G4E gene correlating with CSF APOE protein levels (Cruchaga *et al.*, 2012), being APOE4 genotype the major genetic

risk factor for AD (Kim *et al.*, 2009), it was analyzed here if variants in this SNP and/or APOE genotype could be related with cognitive resilience.

The results obtained demonstrated that rs12232304 SNP was not present in control individuals but was in heterozygosis in a 22% of AD patients and a 50% of AAD ones, however, the SNP did not correlate with APOE genotype or soluble $A\beta_{42}$ levels. Its higher frequency in AAD cases could be account for the cognitive resilience observed although this should be confirmed in a higher cohort of patients. Moreover, it would be convenient to analyze also if the presence of the SNP affects PLA2G4E protein expression levels. Likewise, as other variants in PLA2G4E gene has been recently associated with CSF TREM2 soluble levels, which are higher in AD than controls individuals (Piccio *et al.*, 2016), as well as with panic disorder (Morimoto *et al.*, 2018), it should be also interesting to analyze other SNPs in this gene in human control, AD and AAD samples and correlate them with PLA2G4E brain levels.

Before studying the possible implication of PLA2G4E in AD-related pathology, its cellular and subcellular distribution was characterized. Its neural and cytosolic location (Ogura *et al.*, 2016) was confirmed by immunohistochemistry in human brain slices. Nevertheless, as shown by pre-embedding immunogold, PLA2G4E seems to be also present in the dendrites of pyramidal cells and in the extrasynaptic plasma membrane in mice.

NMDA receptors (NMDARs) and other glutamate receptor subtypes are clustered in dendritic spines (Craig *et al.*, 1994; Kornau *et al.*, 1995; Rao & Craig, 1997; O'Brien, Lau & Huganir, 1998), which act as integrative units in synaptic circuitry thus participating in synaptic plasticity (Harris & Kater, 1994; Yuste & Denk, 1995). It is believed that NMDARs location to synaptic sites depends on interactions between their intracellular domains with cytoskeletal elements (Wyszynski *et al.*, 1997; Allison *et al.*, 1998; Ehlers *et al.*, 1998) and with cytoplasmic submembrane proteins in the postsynaptic density (Gomperts, 1996)(Ponting *et al.*, 1997). In the same line, its endocytosis and removal from the plasma membrane is thought to occur during different paradigms of synaptic plasticity (Roche *et al.*, 2001; Snyder *et al.*, 2001) Consequently, as it has been recently shown that PLA2G4E regulates trafficking processes within the clathrin-independent endocytic and recycling route through tubule formation in transfected HeLa cell line (Capestrano *et al.*, 2014), it could be hypothesized that due to its location in neurons, this enzyme may be participating in the traffic of receptors or other cargoes at the synapses, although this hypothesis should be experimentally confirmed.

To continue with PLA2G4E characterization and considering that Ogura *et al.* have postulated that, in mice, PLA2G4E expression is higher in neonatal than in adults (Ogura *et al.*, 2016), its expression was analyzed at different stages of brain development and compared to that of neuronal (NeuN) and synaptic (synapsin I) markers, to understand its role during postnatal brain development.

The neuronal maturation that occurs during postnatal brain development (Radic *et al.*, 2017) was reflected, as expected, in a constant increased in NeuN expression from birth

and was stabilized at about P30. In the same line, it is believed that, in mammals, neurons existent at birth undergo a period of overproduction of their arborization and synaptic contacts to increase synaptic density, followed by an elimination or pruning phase of refinement important for synaptic plasticity (Semple *et al.*, 2013), which is in accordance with the synapsin I pattern of expression observed in the postnatal mice studied here. Surprisingly, when comparing PLA2G4E expression, which increased from birth until P10-15 and then decreased, with that of NeuN and synapsin I, it can be observed that the decrease in PLA2G4E coincides with NeuN stabilization and with a dramatic increase of synapsin I. Although it should be confirmed with more experiments, these results suggest a possible role of PLA2G4E in neural development, allowing neuronal maturation by modulating synaptogenesis/synaptic plasticity.

Considering these results, its possible implication in memory function was tested analyzing its expression upon a simple FC paradigm. An overexpression of PLA2G4E was observed, both in the hippocampus and pre-frontal cortex, one hour after mice were re-introduced in the FC chamber one day after the training phase, which suggest that this enzyme may be playing a role in memory retrieval. Using a dual cPLA2 and iPLA2 inhibitor, a previous study have reported that hippocampal PLA2 activity is required for long-term memory retrieval in rats (Schaeffer & Gattaz, 2007) so, despite the low phospholipase activity of PLA2G4E (Ogura *et al.*, 2016), it seems to be participating in that process, although the mechanism of action could be independent of its phospholipase activity.

Finally, in order to analyze the potentiality of PLA2G4E overexpression as a novel therapy for AD and/or dementia, the enzyme was overexpressed by AAV9 in hippocampal neurons of elderly APP/PS1 mice and WT mice using a specific neuronal promoter.

Viral vectors based on AAV are widely used for CNS delivery due to its high efficacy to transduce both dividing and non-dividing cells (Bourdenx *et al.*, 2014; Bartlett *et al.*, 1998). Specifically, AAV9 has become a preferred vector for this purpose because of its increased ability to cross the BBB compared to other AAV serotypes, which make it an attractive choice to achieve future clinical use; although complications associated with its systemic delivery such as expression in non-CNS tissues are still important barriers to their success (Lukashchuk *et al.*, 2016). Nevertheless, here they were intrahipocampally administered to direct the expression specifically to CA1 neurons.

In elderly individuals of the AD mice model APP/PS1, with an established phenotype, PLA2G4E overexpression in hippocampal neurons was able to completely reverse cognitive deficits and to increase dendritic spine density without affecting amyloid or tau pathology. Likewise, in a pilot probe performed in elderly WT mice, PLA2G4E overexpression improved spatial memory retention although it did not affect dendritic spine density. In the case of WT, it seems that, as PLA2G4E overexpression only had an effect on memory retention, not on working memory, the improvement observed was not enough to increase synaptic density, as happened in APP/PS1 mice, where both working

and retention memory were augmented by AAV-mediated PLA2G4E overexpression. The lack of effect on dendritic spine density in WT mice could be explained if it is taken into account that animals of both groups were able to learn properly the platform location during the hidden platform phase. Consequently, the number of spines would be a reflection of this behavior. In any case, considering the significant increase in memory retention observed in the probe test for the group of AAV-PLA2G4E injected mice, this enzyme seems to participate in memory consolidation although its mechanism has not been yet elucidated.

These results suggest a potential therapeutic role of PLA2G4E overexpression for cognitive impairment both in AD and other diseases that course with memory deficits thus, supporting the idea that therapies which increase synaptic plasticity may be of special interest for AD.

PLA2G4E has been recently described as the calcium-dependent N-acyltransferase that produces N-acyl phosphatidylethanolamines (NAPEs), which are precursors for N-acyl ethanolamine (NAE) lipid transmitters, such as the endocannabinoid anandamide (Ogura *et al.*, 2016). Maroof *et al.* have postulated that levels of the endocannabinoids anandamide and 2-arachidonoyl glycerol, which interact with the G protein-coupled type-1 and type-2 cannabinoid receptors, are reduced in the striatum of 8 mo APP/PS1 mice and that this reduction seems to enhance the coupling of cannabinoid receptors/effectors contributing to cognitive impairments in these mice (Maroof *et al.*, 2014). According to these studies, the restoration of memory deficits observed in AAV9-PLA2G4E treated mice could be caused by an augmentation of the levels of those endocannabinoids, although to confirm this hypothesis further studies would be required.

Moreover, it was shown that PLA2G4E activity *in vitro* was remarkably activated by phosphatidylserine (PS) (Binte *et al.*, 2019). In the same line, it has been demonstrated that memory deficits were improved in both AD rats and patients after treatment with PS (Zhang *et al.*, 2015). Thus, the improvement observed in that study may be caused by a PS-mediated activation of PLA2G4E, thus increasing endocannabinoid levels.

However, although PLA2G4E overexpression seems to be an attractive treatment for AD, its mode of action needs to be yet elucidated. In order to achieve it, several experiments trying to silence its expression in neonatal and adult mice, as well as in neuronal cultures, are being carried out in our laboratory at this moment.

Anyway, the results obtained along the present thesis have allowed the identification of a novel target for AD with a high therapeutic potential. Its overexpression, either by AAV or other methodologies, seems to be a promising therapeutic strategy not only for AD but also for other diseases that course with cognitive impairment. Moreover, in line with the use of combined therapies for AD, using the mentioned strategy to improve memory function in combination with another one that allows amyloid and tau amelioration could even increase its effectiveness. As a consequence, it would be really interesting to continue with the study of this poorly characterize phospholipase to allow a future safe and efficient clinical use.

CONCLUSSIONS

The following conclusions can be drawn from the study of the effect of CM-695, a dual HDAC6 and PDE9 inhibitor, in the AD mouse model Tg2576 mice:

1. A chronic treatment with CM-695 reversed cognitive deficits and significantly reduced amyloid pathology in the brain of aged-Tg2576. These effects were not maintained after a wash-out period of 4-weeks.

2. Considering that CM-695 is a less potent HDAC2 inhibitor that the lead compound CM-414, it seems that HDAC2, is the HDAC isoform responsible of the long-lasting changes on memory function although it is also more related to toxic effects.

3. CM-695 induced a significant increase of the chaperones GRP78 and Hsp70 in the hippocampus of treated-mice that may account for the amelioration of amyloid pathology and the improvement of memory function.

The following conclusions can be drawn from the study of cognitive resilient AD individuals:

4. As occurs in humans, there is an important percentage (22%) of the AD transgenic mice model Tg2576 that are able to cope with AD neuropathology without developing dementia, thus presenting cognitive resilience.

5. The enzyme PLA2G4E seems to be down-regulated in the brain of AD patients and elderly Tg2576 mice with cognitive impairment, suggesting a role of this phospholipase in AD pathology.

6. PLA2G4E is increased in the brain of asymptomatic AD patients as well as in cognitive resilient elderly Tg2576 mice and correlates with the expression of the synaptic marker synapsin I, pointing out to a possible involvement of this enzyme in cognitive resilience.

7. The presence of the rs12232304 SNP in PLA2G4E gene in 50% of AAD cases suggests that this SNP could be involved in cognitive resilience although its expression does not correlate with APOE genotype or $A\beta_{42}$ levels.

8. In the brain, PLA2G4E is a neuronal protein mainly located in the cytosol but also present in dendrites and dendritic spines. PLA2G4E expression pattern during post-natal brain development suggests a possible involvement of this phospholipase in regulating neuronal maturation. However, during adulthood, this enzyme seems to be implicated in memory function, although its mode of action needs to be yet elucidated.

9. AAV9-mediated PLA2G4E overexpression in hippocampal neurons of elderly APP/PS1 mice reversed cognitive impairment and increased synaptic spine

density without affecting amyloid or tau pathology, thus representing a promising strategy to treat dementia in AD.

10. Spatial memory retention was improved in elderly WT mice by AAV9-PLA2G4E mediated overexpression in hippocampal neurons, but did not affect dendritic spines density. It suggests that the overexpression of this enzyme may be a hopeful treatment for age-related cognitive impairment, although it should be confirmed with further studies.

11. The study of cognitive resilient AD subjects, both in humans and animal models, represents a newfangled effective methodology to identify novel therapies for AD and another related disorders that course with cognitive impairment.

BIBLIOGRAPHY

Abel, T., Nguyen, P., Barad, M., Deuel, T., *et al.* (1997). Genetic demonstration of a role for PKA in the late phase of LTP and in hippocampus-based long-term memory. *Cell* 88 (5), 615–625.

Abel, T. & Zukin, R.S. (2008). Epigenetic targets of HDAC inhibition in neurodegenerative and psychiatric disorders. *Current opinion in pharmacology* 8 (1), 57–64.

Adwan Lina, Z.N.H. (2013). Epigenetics: A novel therapeutic approach for the treatment of Alzheimer's disease. *Pharmacol Ther* 139 (1), 41–50.

Aggarwal, N.T., Bienias, J.L., Bennett, D.A., Wilson, R.S., *et al.* (2006). The relation of cigarette smoking to incident Alzheimer's disease in a biracial urban community population. *Neuroepidemiology* 26 (3), 140–146.

Aguilera, G., Colín-González, A.L., Rangel-López, E., Chavarría, A., *et al.* (2018). Redox Signaling, Neuroinflammation, and Neurodegeneration. *Antioxidants & Redox Signaling* 28 (18), 1626–1651.

Ahmad, F., Murata, T., Shimizu, K., Degerman, E., *et al.* (2015). Cyclic Nucleotide Phosphodiesterases: important signaling modulators and therapeutic targets. *Oral Diseases*. 21 (1), e25–e50.

Akamine, R., Yamamoto, T., Watanabe, M., Yamazaki, N., *et al.* (2007). Usefulness of the 5′ region of the cDNA encoding acidic ribosomal phosphoprotein P0 conserved among rats, mice, and humans as a standard probe for gene expression analysis in different tissues and animal species. *Journal of Biochemical and Biophysical Methods* 70 (3), 481–486.

Allende, M., Molina, E., Lecumberri, R., Sanchez-Arias, J.A., *et al.* (2017). Inducing heat shock protein 70 expression provides a robust antithrombotic effect with minimal bleeding risk. *Thrombosis and haemostasis* 117 (9), 1722–1729.

Allison, D.W., Gelfand, V.I., Spector, I. & Craig, A.M. (1998). Role of actin in anchoring postsynaptic receptors in cultured hippocampal neurons: differential attachment of NMDA versus AMPA receptors. *The Journal of neuroscience* 18 (7), 2423–2436.

Almeida, C.G., Tampellini, D., Takahashi, R.H., Greengard, P., *et al.* (2005). Beta-amyloid accumulation in APP mutant neurons reduces PSD-95 and GluR1 in synapses. *Neurobiology of Disease* 20 (2), 187–198.

Altuna-Azkargorta, M. & Mendioroz-Iriarte, M. (2018). Biomarcadores sanguíneos en la enfermedad de Alzheimer. *Neurología*.

Alzheimer's association (2018). *2018 ALZHEIMER'S DISEASE FACTS AND FIGURES*. Available from: https://www.alz.org/media/HomeOffice/Facts and Figures/facts-and-figures.pdf.

Andreeva, S.G., Dikkes, P., Epstein, P.M. & Rosenberg, P.A. (2001). Expression of cGMP-specific phosphodiesterase 9A mRNA in the rat brain. *The Journal of neuroscience* 21 (22), 9068–9076.

Anon (n.d.). *Confederación Española de Familiares de personas con Alzheimer y otras demencias (CEAFA)*.

Anttila, T., Helkala, E.-L., Viitanen, M., Kåreholt, I., *et al.* (2004). Alcohol drinking in middle age and subsequent risk of mild cognitive impairment and dementia in old age: a prospective population based study. *BMJ* 329 (7465), 539.

Arnold, S.E., Louneva, N., Cao, K., Wang, L.-S., *et al.* (2013). Cellular, synaptic, and biochemical features of resilient cognition in Alzheimer's disease. *Neurobiology of aging* 34 (1), 157–168.

Arriagada, P. V, Growdon, J.H., Hedley-Whyte, E.T. & Hyman, B.T. (1992). Neurofibrillary tangles but not senile plaques parallel duration and severity of Alzheimer's disease. *Neurology* 42 (3), 631–639.

Avila, J. & Hernández, F. (2007). GSK-3 inhibitors for Alzheimer's disease. *Expert Review of Neurotherapeutics* 7 (11), 1527–1533.

Baki, L., Shioi, J., Wen, P., Shao, Z., *et al.* (2004). PS1 activates PI3K thus inhibiting GSK-3 activity and tau overphosphorylation: effects of FAD mutations. *The EMBO journal* 23 (13), 2586–2596.

Balasubramanian, A.B., Kawas, C.H., Peltz, C.B., Brookmeyer, R., *et al.* (2012). Alzheimer disease pathology and longitudinal cognitive performance in the oldest-old with no dementia. *Neurology* 79 (9), 915–921.

Ballard, C., Gauthier, S., Corbett, A., Brayne, C., *et al.* (2011a). Alzheimer's disease. *The Lancet* 377 (9770), 1019–1031.

Ballard, C., Khan, Z., Clack, H. & Corbett, A. (2011b). Nonpharmacological Treatment of Alzheimer Disease. *The Canadian Journal of Psychiatry* 56 (10), 589–595.

Bannerman, D.M., Deacon, R.M.J., Brady, S., Bruce, A., *et al.* (2004). A comparison of GluR-A-deficient and wild-type mice on a test battery assessing sensorimotor, affective, and cognitive behaviors. *Behavioral neuroscience* 118 (3), 643–647.

Bannister, A.J. & Kouzarides, T. (2011). Regulation of chromatin by histone modifications. *Cell research* 21 (3), 381–395.

Bard, J.B.L. (2008). Waddington's Legacy to Developmental and Theoretical Biology. *Biological Theory*. 3 (3), 188–197.

Bartlett, J.S., Samulski, R.J. & McCown, T.J. (1998). Selective and Rapid Uptake of Adeno-Associated Virus Type 2 in Brain. *Human Gene Therapy* 9 (8), 1181–1186.

Beavo, A. (1995). Cyclic Nucleotide Phosphodiesterases : Functional Implications of Multiple Isoforms. *Physiological Reviews*. 75 (4), 725–748.

Belyaev, N.D., Nalivaeva, N.N., Makova, N.Z. & Turner, A.J. (2009). Neprilysin gene expression requires binding of the amyloid precursor protein intracellular domain to its promoter: implications for Alzheimer disease. *EMBO reports* 10 (1), 94–100.

Benito, E., Urbanke, H., Ramachandran, B., Barth, J., *et al.* (2015). HDAC inhibitor-dependent transcriptome and memory reinstatement in cognitive decline models. *The Journal of clinical investigation* 125 (9), 3572–3584.

Bernabeu, R., Schroder, N., Quevedo, J., Cammarota, M., *et al.* (1997). Further evidence

for the involvement of a hippocampal cGMP/cGMP-dependent protein kinase cascade in memory consolidation. *Neuroreport* 8 (9–10), 2221–2224.

Binte M.S.S., Uyama, T., Hussain, Z., Kawai, K., *et al.* (2019). The role of intracellular anionic phospholipids in the production of *N* -acyl-phosphatidylethanolamines by cytosolic phospholipase A2ε. *The Journal of Biochemistry* 165 (4), 343–352.

Bird, T.D. (2008). Genetic aspects of Alzheimer disease. *Genetics in medicine* 10 (4), 231–239.

Birks, J.S. (2006). Cholinesterase inhibitors for Alzheimer's disease. *Cochrane Database of Systematic Reviews*.

Blanpied, T.A. & Ehlers, M.D. (2004). Microanatomy of dendritic spines: emerging principles of synaptic pathology in psychiatric and neurological disease. *Biological psychiatry* 55 (12), 1121–1127.

Boehringer Ingelheim (2018). Boehringer Ingelheim Bails on Candidate Alzheimer's Drug. Available from: https://www.alzforum.org/news/research-news/boehringer-ingelheim-bails-candidate-alzheimers-drug.

Bourdenx, M., Dutheil, N., Bezard, E. & Dehay, B. (2014). Systemic gene delivery to the central nervous system using Adeno-associated virus. *Frontiers in Molecular Neuroscience* 7, 50.

Boyault, C., Zhang, Y., Fritah, S., Caron, C., *et al.* (2007). HDAC6 controls major cell response pathways to cytotoxic accumulation of protein aggregates. *Genes and Development* 21 (17), 2172–2181.

Braak, E., Braak, H. & Mandelkow, E.M. (1994). A sequence of cytoskeleton changes related to the formation of neurofibrillary tangles and neuropil threads. *Acta neuropathologica* 87 (6), 554–567.

Braak, H., Alafuzoff, I., Arzberger, T., Kretzschmar, H., *et al.* (2006). Staging of Alzheimer disease-associated neurofibrillary pathology using paraffin sections and immunocytochemistry. *Acta neuropathologica* 112 (4), 389–404.

Braak, H. & Braak, E. (1991). Neuropathological stageing of Alzheimer-related changes. *Acta neuropathologica* 82 (4), 239–259.

Braak, H. & Braak, E. (1995). Staging of Alzheimer's disease-related neurofibrillary changes. *Neurobiology of aging* 16 (3), 271-8; discussion 278-84.

Brinkmalm, G., Hong, W., Wang, Z., Liu, W., *et al.* (2019). Identification of neurotoxic cross-linked amyloid-β dimers in the Alzheimer's brain. *Brain* 142 (5), 1441–1457.

Bullain, S.S., Corrada, M.M., Shah, B.A., Mozaffar, F.H., *et al.* (2013). Poor Physical Performance and Dementia in the Oldest Old. *JAMA Neurology* 70 (1), 107.

Cakir, M., Duzova, H., Tekin, S., Taslıdere, E., *et al.* (2017). ACA, an inhibitor phospholipases A2 and transient receptor potential melastatin-2 channels, attenuates okadaic acid induced neurodegeneration in rats. *Life sciences* 176, 10–20.

Callahan, M.J., Lipinski, W.J., Bian, F., Durham, R.A., *et al.* (2001). Augmented senile

plaque load in aged female beta-amyloid precursor protein-transgenic mice. *The American journal of pathology* 158 (3), 1173–1177.

Campion, D., Dumanchin, C., Hannequin, D., Dubois, B., *et al.* (1999). Early-Onset Autosomal Dominant Alzheimer Disease: Prevalence, Genetic Heterogeneity, and Mutation Spectrum. *The American Journal of Human Genetics* 65 (3), 664–670.

Capestrano, M., Mariggio, S., Perinetti, G., Egorova, A. V., *et al.* (2014). Cytosolic phospholipase A2 drives recycling through the clathrin-independent endocytic route. *Journal of Cell Science* 127 (5), 977–993.

Caspers, S., Moebus, S., Lux, S., Pundt, N., *et al.* (2014). Studying variability in human brain aging in a population-based German cohort-rationale and design of 1000BRAINS. *Frontiers in aging neuroscience* 6, 149.

Di Cerbo, V., Mohn, F., Ryan, D.P., Montellier, E., *et al.* (2014). Acetylation of histone H3 at lysine 64 regulates nucleosome dynamics and facilitates transcription. *eLife* 3.

Chapman, P.F., White, G.L., Jones, M.W., Cooper-Blacketer, D., *et al.* (1999). Impaired synaptic plasticity and learning in aged amyloid precursor protein transgenic mice. *nature neuroscience* 2, 271–276.

Chun, W. & Johnson, G.V.W. (2007). The role of tau phosphorylation and cleavage in neuronal cell death. *Frontiers in bioscience* 12, 733–756.

Cook, C., Gendron, T.F., Scheffel, K., Carlomagno, Y., *et al.* (2012). Loss of HDAC6, a novel CHIP substrate, alleviates abnormal tau accumulation. *Human molecular genetics* 21 (13), 2936–2945.

Cotter, V.T. (2007). The burden of dementia. *The American Journal of Managed Care*. 13, S193-7.

Craig, A.M., Blackstone, C.D., Huganir, R.L. & Banker, G. (1994). Selective clustering of glutamate and gamma-aminobutyric acid receptors opposite terminals releasing the corresponding neurotransmitters. *Proceedings of the National Academy of Sciences of the United States of America* 91 (26), 12373–12377.

Cruchaga, C., Kauwe, J.S.K., Nowotny, P., Bales, K., *et al.* (2012). Cerebrospinal fluid APOE levels: an endophenotype for genetic studies for Alzheimer's disease. *Human molecular genetics* 21 (20), 4558–4571.

Crystal, H., Dickson, D., Fuld, P., Masur, D., *et al.* (1988). Clinico-pathologic studies in dementia: Nondemented subjects with pathologically confirmed Alzheimer's disease. *Neurology* 38 (11), 1682–1682.

Cuadrado-Tejedor, M., Garcia-Barroso, C., Sánchez-Arias, J.A., Rabal, O., *et al.* (2017). A First-in-Class Small-Molecule that Acts as a Dual Inhibitor of HDAC and PDE5 and that Rescues Hippocampal Synaptic Impairment in Alzheimer's Disease Mice. *Neuropsychopharmacology* 42 (2), 524–539.

Cuadrado-Tejedor, M., Garcia-Barroso, C., Sanzhez-Arias, J., Mederos, S., *et al.* (2015). Concomitant histone deacetylase and phosphodiesterase 5 inhibition synergistically prevents the disruption in synaptic plasticity and it reverses cognitive impairment in a mouse model of Alzheimer's disease. *Clinical Epigenetics* 7 (1), 108.

Cuadrado-Tejedor, M., Hervias, I., Ricobaraza, a., Puerta, E., *et al.* (2011). Sildenafil restores cognitive function without affecting β-amyloid burden in a mouse model of Alzheimer's disease. *British Journal of Pharmacology* 164 (8), 2029–2041.

Cuadrado-Tejedor, M., Pérez-González, M., García-Muñoz, C., Muruzabal, D., *et al.* (2019). Taking Advantage of the Selectivity of Histone Deacetylases and Phosphodiesterase Inhibitors to Design Better Therapeutic Strategies to Treat Alzheimer's Disease. *Frontiers in Aging Neuroscience* 11, 149.

Cuadrado-Tejedor, M., Ricobaraza, A.L., Torrijo, R., Franco, R., *et al.* (2013). Phenylbutyrate is a multifaceted drug that exerts neuroprotective effects and reverses the Alzheimer´s disease-like phenotype of a commonly used mouse model. *Current pharmaceutical design* 19 (28), 5076–5084.

Cummings, J. (2018). Lessons Learned from Alzheimer Disease: Clinical Trials with Negative Outcomes. *Clinical and Translational Science* 11 (2), 147–152.

Cummings, J., Lee, G., Ritter, A. & Zhong, K. (2018). Alzheimer's disease drug development pipeline: 2018. *Alzheimer's & dementia* 4, 195–214.

Cummings, J.L. (2004). Alzheimer's disease. *The New England Journal of Medicine*. 351 (1), 56–67.

Cummings, J.L. & Cole, G. (2002). Alzheimer disease. *JAMA* 287 (18), 2335–2338.

D'Hooge, R. & Deyn, P.P. De (2001). Applications of the Morris water maze in the study of learning and memory. *Brain research reviews* 36 (1), 60-90.

Delaère, P., Duyckaerts, C., Masters, C., Beyreuther, K., *et al.* (1990). Large amounts of neocortical beta A4 deposits without neuritic plaques nor tangles in a psychometrically assessed, non-demented person. *Neuroscience letters* 116 (1–2), 87–93.

Delaère, P., He, Y., Fayet, G., Duyckaerts, C., *et al.* (1993). Beta A4 deposits are constant in the brain of the oldest old: an immunocytochemical study of 20 French centenarians. *Neurobiology of aging* 14 (2), 191–194.

Dennis, E.A. (1994). Diversity of group types, regulation, and function of phospholipase A2. *The Journal of biological chemistry* 269 (18), 13057–13060.

Dickson, D.W. (1997). The pathogenesis of senile plaques. *Journal of neuropathology and experimental neurology* 56 (4), 321–339.

Dickson, D.W., Crystal, H.A., Mattiace, L.A., Masur, D.M., *et al.* (1992). Identification of normal and pathological aging in prospectively studied nondemented elderly humans. *Neurobiology of aging* 13 (1), 179–189.

Ding, H., Dolan, P.J. & Johnson, G.V.W. (2008). Histone deacetylase 6 interacts with the microtubule-associated protein tau. *Journal of neurochemistry* 106 (5), 2119–2130.

Domek-Łopacińska, K.U. & Strosznajder, J.B. (2010). Cyclic GMP and Nitric Oxide Synthase in Aging and Alzheimer's Disease. *Molecular Neurobiology* 41 (2–3), 129–137.

Doody, R.S., Demirovic, J., Ballantyne, C.M., Chan, W., *et al.* (2015). Lipoprotein-associated phospholipase A2, homocysteine, and Alzheimer's disease. *Alzheimer's & dementia* 1 (4), 464–471.

Drubin, D. & Kirschner, M. (1986). Tau protein function in living cells. *The Journal of Cell Biology* 103 (6), 2739.

Duce, J.A., Tsatsanis, A., Cater, M.A., James, S.A., *et al.* (2010). Iron-export ferroxidase activity of β-amyloid precursor protein is inhibited by zinc in Alzheimer's disease. *Cell* 142 (6), 857–867.

Durocher, Y., Perret, S. & Kamen, A. (2002). High-level and high-throughput recombinant protein production by transient transfection of suspension-growing human 293-EBNA1 cells. *Nucleic Acids Research* 30 (2), 9e–9.

van Dyck, C.H. (2018). Anti-Amyloid-β Monoclonal Antibodies for Alzheimer's Disease: Pitfalls and Promise. *Biological Psychiatry* 83 (4), 311–319.

Ehlers, M.D., Fung, E.T., O'Brien, R.J. & Huganir, R.L. (1998). Splice variant-specific interaction of the NMDA receptor subunit NR1 with neuronal intermediate filaments. *The Journal of neuroscience* 18 (2), 720–730.

Evin, G., Sernee, M.F. & Masters, C.L. (2006). Inhibition of gamma-secretase as a therapeutic intervention for Alzheimer's disease: prospects, limitations and strategies. *CNS drugs* 20 (5), 351–372.

Farlow, M.R. & Cummings, J.L. (2007). Effective Pharmacologic Management of Alzheimer's Disease. *The American Journal of Medicine* 120 (5), 388–397.

FDA U.S. Food and Drug Administration (2014). Namzaric (memantine hydrochloride extended-release/donepezil hydrochloride) Capsules. Available from: https://www.accessdata.fda.gov/drugsatfda_docs/nda/2014/206439Orig1s000TOC.cfm

De Felice, F.G., Wasilewska-Sampaio, A.P., Barbosa, A.C.A.P., Gomes, F.C.A., *et al.* (2007). Cyclic AMP enhancers and Abeta oligomerization blockers as potential therapeutic agents in Alzheimer's disease. *Current Alzheimer research* 4 (3), 263–271.

Ferrer, I., Martinez, A., Boluda, S., Parchi, P., *et al.* (2008). Brain banks: benefits, limitations and cautions concerning the use of post-mortem brain tissue for molecular studies. *Cell and Tissue Banking* 9 (3), 181–194.

Ferri, C.P., Prince, M., Brayne, C., Brodaty, H., *et al.* (2005). Global prevalence of dementia: a Delphi consensus study\n. *The Lancet 366, 2112 - 2117* .

Fischer, A., Sananbenesi, F., Wang, X., Dobbin, M., *et al.* (2007). Recovery of learning and memory is associated with chromatin remodelling. *Nature* 447 (7141), 178–182.

Floudas, C.S., Um, N., Kamboh, M.I., Barmada, M.M., *et al.* (2014). Identifying genetic interactions associated with late-onset Alzheimer's disease. *BioData Mining* 7 (1), 35.

Gama, M.A.S., Raposo, N.R.B., Mury, F.B., Lopes, F.C.F., *et al.* (2015). Conjugated

linoleic acid-enriched butter improved memory and up-regulated phospholipase A2 encoding-genes in rat brain tissue. *Journal of neural transmission* 122 (10), 1371–1380.

García-Barroso, C., Ricobaraza, A., Pascual-Lucas, M., Unceta, N., *et al.* (2013). Tadalafil crosses the blood–brain barrier and reverses cognitive dysfunction in a mouse model of AD. *Neuropharmacology* 64, 114–123.

García-Osta, A., Cuadrado-tejedor, M., García-Barroso, C., Oyarzábal, J., *et al.* (2012). Phosphodiesterases as Therapeutic Targets for Alzheimer ' s Disease. *ACS Chemical Neuroscience*. 3, 832–844.

Gattaz, W., Levy, R., Cairns, N., Förstl, H., *et al.* (1996). Relevance of metabolism of membrane phospholipids for Alzheimer dementia. *Progress in Neurology and Psychiatry* 64 (01), 8–12.

Gattaz, W.F., Forlenza, O. V., Talib, L.L., Barbosa, N.R., *et al.* (2004). Platelet phospholipase A(2) activity in Alzheimer's disease and mild cognitive impairment. *Journal of Neural Transmission* 111 (5), 591–601.

Gauthier, S., Loft, H. & Cummings, J. (2008). Improvement in behavioural symptoms in patients with moderate to severe Alzheimer's disease by memantine: a pooled data analysis. *International journal of geriatric psychiatry* 23 (5), 537–545.

Gerlai, R. (2001). Behavioral tests of hippocampal function: Simple paradigms complex problems. *Behavioural Brain Research* 125 (1–2), 269–277.

Ghomashchi, F., Naika, G.S., Bollinger, J.G., Aloulou, A., *et al.* (2010). Interfacial kinetic and binding properties of mammalian group IVB phospholipase A2 (cPLA2beta) and comparison with the other cPLA2 isoforms. *The Journal of biological chemistry* 285 (46), 36100–36111.

Glaser, E.M. & Van der Loos, H. (1981). Analysis of thick brain sections by obverse—Reverse computer microscopy: Application of a new, high clarity Golgi—Nissl stain. *Journal of Neuroscience Methods* 4 (2), 117–125.

Goedert, M., Spillantini, M.G., Potier, M.C., Ulrich, J., *et al.* (1989). Cloning and sequencing of the cDNA encoding an isoform of microtubule-associated protein tau containing four tandem repeats: differential expression of tau protein mRNAs in human brain. *The EMBO journal* 8 (2), 393–399.

Golde, T.E., DeKosky, S.T. & Galasko, D. (2018). Alzheimer's disease: The right drug, the right time. *Science* 362 (6420), 1250–1251.

Gomperts, S.N. (1996). Clustering membrane proteins: It's all coming together with the PSD-95/SAP90 protein family. *Cell* 84 (5), 659–662.

Gong, C.-X., Liu, F., Grundke-Iqbal, I. & Iqbal, K. (2005). Post-translational modifications of tau protein in Alzheimer's disease. *Journal of Neural Transmission* 112 (6), 813–838.

Govindarajan, N., Rao, P., Burkhardt, S., Sananbenesi, F., *et al.* (2013). Reducing HDAC6 ameliorates cognitive deficits in a mouse model for Alzheimer's disease. *EMBO Molecular Medicine* 5 (1), 52–63.

Gräff, J., Rei, D., Guan, J.-S., Wang, W.-Y., *et al.* (2012). An epigenetic blockade of cognitive functions in the neurodegenerating brain. *Nature* 483 (7388), 222–226.

Gräff, J. & Tsai, L.-H. (2013). Histone acetylation: molecular mnemonics on the chromatin. *Nature reviews. Neuroscience* 14 (2), 97–111.

Guan, J.-S., Haggarty, S.J., Giacometti, E., Dannenberg, J.-H., *et al.* (2009). HDAC2 negatively regulates memory formation and synaptic plasticity. *Nature* 459 (7243), 55–60.

Guibinga, G.-H., Murray, F. & Barron, N. (2013). HPRT-Deficiency Dysregulates cAMP-PKA Signaling and Phosphodiesterase 10A Expression: Mechanistic Insight and Potential Target for Lesch-Nyhan Disease? *PLoS ONE* 8 (5), e63333.

Guo, W., Naujock, M., Fumagalli, L., Vandoorne, T., *et al.* (2017). HDAC6 inhibition reverses axonal transport defects in motor neurons derived from FUS-ALS patients. *Nature Communications* 8 (1), 861.

Gustafson, D. (2006). Adiposity indices and dementia. *The Lancet Neurology* 5 (8), 713–720.

Hama, E. & Saido, T.C. (2005). Etiology of sporadic Alzheimer's disease: Somatostatin, neprilysin, and amyloid β peptide. *Medical Hypotheses* 65 (3), 498–500.

Hanger, D.P., Hughes, K., Woodgett, J.R., Brion, J.P., *et al.* (1992). Glycogen synthase kinase-3 induces Alzheimer's disease-like phosphorylation of tau: generation of paired helical filament epitopes and neuronal localisation of the kinase. *Neuroscience letters* 147 (1), 58–62.

Hardy, J. (2006). A Hundred Years of Alzheimer's Disease Research. *Neuron* 52 (1), 3–13.

Hardy, J. & Selkoe, D.J. (2002). Amyloid and Hypothesis of Problems Alzheimer ' s Road to Disease : the Therapeutics. *Science Compass Review* 297 (5580), 353–356.

Hardy, J.A. & Higgins, G.A. (1992). Alzheimer's disease: the amyloid cascade hypothesis. *Science* 256 (5054), 184–185.

Harris, K.M. & Kater, S.B. (1994). Dendritic spines: cellular specializations imparting both stability and flexibility to synaptic function. *Annual review of neuroscience*. 17 (1), 341–371.

Hernández, F., Borrell, J., Guaza, C., Avila, J., *et al.* (2002). Spatial learning deficit in transgenic mice that conditionally over-express GSK-3beta in the brain but do not form tau filaments. *Journal of neurochemistry* 83 (6), 1529–1533.

Hippius, H. & Neundörfer, G. (2003). The discovery of Alzheimer's disease. *Dialogues in clinical neuroscience* 5 (1), 101–108.

Holland, P.M., Abramson, R.D., Watson, R. & Gelfand, D.H. (1991). Detection of specific polymerase chain reaction product by utilizing the 5'----3' exonuclease activity of Thermus aquaticus DNA polymerase. *Proc Natl Acad Sci U S A* 88(16):7276-7280.

Honig, L.S. & Boyd, C.D. (2013). Treatment of Alzheimer's Disease: Current Management and Experimental Therapeutics. *Current Translational Geriatrics and Experimental Gerontology Reports* 2 (3), 174–181.

Hooper, C., Markevich, V., Plattner, F., Killick, R., *et al.* (2007). Glycogen synthase kinase-3 inhibition is integral to long-term potentiation. *The European journal of neuroscience* 25 (1), 81–86.

Hoozemans, J.J.M., van Haastert, E.S., Nijholt, D.A.T., Rozemuller, A.J.M., *et al.* (2009). The Unfolded Protein Response Is Activated in Pretangle Neurons in Alzheimer's Disease Hippocampus. *The American Journal of Pathology* 174 (4), 1241–1251.

Houslay, M.D., Schafer, P. & Zhang, K.Y.J. (2005). Keynote review: Phosphodiesterase-4 as a therapeutic target. *Drug Discovery Today* 10 (22), 1503–1519.

Hsiao, K., Chapman, P., Nilsen, S., Eckman, C., *et al.* (1996). Correlative Memory Deficits, Aβ Elevation, and Amyloid Plaques in Transgenic Mice. *Science*. 274 (5284), 99–103.

Hubbert, C., Guardiola, A., Shao, R., Kawaguchi, Y., *et al.* (2002) HDAC6 is a microtubule-associated deacetylase. *Nature* 417 (6887), 455–458.

Hulette, C.M., Welsh-Bohmer, K.A., Murray, M.G., Saunders, A.M., *et al.* (1998). Neuropathological and neuropsychological changes in normal aging: evidence for preclinical Alzheimer disease in cognitively normal individuals. *Journal of neuropathology and experimental neurology* 57 (12), 1168–1174.

Hyman, B.T. (1997). The neuropathological diagnosis of Alzheimer's disease: clinical-pathological studies. *Neurobiology of aging* 18 (4 Suppl), S27-32.

Iacono, D., Markesbery, W.R., Gross, M., Pletnikova, O., *et al.* (2009). The Nun Study: Clinically silent AD, neuronal hypertrophy, and linguistic skills in early life. *Neurology* 73 (9), 665–673.

Impey, S., Mark, M., Villacres, E.C., Poser, S., *et al.* (1996). Induction of CRE-mediated gene expression by stimuli that generate long-lasting LTP in area CA1 of the hippocampus. *Neuron* 16 (5), 973–982.

Iqbal, K., Liu, F., Gong, C.-X., Alonso, A.D.C., *et al.* (2009). Mechanisms of tau-induced neurodegeneration. *Acta neuropathologica* 118 (1), 53–69.

Iqbal, K., Liu, F., Gong, C.-X. & Grundke-Iqbal, I. (2010). Tau in Alzheimer disease and related tauopathies. *Current Alzheimer research* 7 (8), 656–664.

Irizarry, R.A., Bolstad, B.M., Collin, F., Cope, L.M., *et al.* (2003). Summaries of Affymetrix GeneChip probe level data. *Nucleic acids research* 31 (4), e15.

Iwatsubo, T., Odaka, A., Suzuki, N., Mizusawa, H., *et al.* (1994). Visualization of A beta 42(43) and A beta 40 in senile plaques with end-specific A beta monoclonals: evidence that an initially deposited species is A beta 42(43). *Neuron* 13 (1), 45–53.

Janczura, K.J., Volmar, C.-H., Sartor, G.C., Rao, S.J., *et al.* (2018). Inhibition of HDAC3 reverses Alzheimer's disease-related pathologies in vitro and in the 3xTg-AD mouse model. *Proceedings of the National Academy of Sciences* 115 (47), E11148–E11157.

Janus, C. & Westaway, D. (2001). Transgenic mouse models of Alzheimer's disease. *Physiology & behavior* 73 (5), 873–886.

Jarrett, J.T., Berger, E.P. & Lansbury, P.T. (1993). The carboxy terminus of the beta amyloid protein is critical for the seeding of amyloid formation: implications for the pathogenesis of Alzheimer's disease. *Biochemistry* 32 (18), 4693–4697.

Jin, L.W., Ninomiya, H., Roch, J.M., Schubert, D., et al. (1994). Peptides containing the RERMS sequence of amyloid beta/A4 protein precursor bind cell surface and promote neurite extension. *The Journal of neuroscience* 14 (9), 5461–5470.

Jin, M., Shepardson, N., Yang, T., Chen, G., *et al.* (2011). Soluble amyloid -protein dimers isolated from Alzheimer cortex directly induce Tau hyperphosphorylation and neuritic degeneration. *Proceedings of the National Academy of Sciences*. 108 (14), 5819–5824.

Jovanovic, J.N., Czernik, A.J., Fienberg, A.A., Greengard, P., *et al.* (2000). Synapsins as mediators of BDNF-enhanced neurotransmitter release. *Nature neuroscience*. 3 (4), 323–329.

Karp, A., Paillard-Borg, S., Wang, H.-X., Silverstein, M., *et al.* (2006). Mental, physical and social components in leisure activities equally contribute to decrease dementia risk. *Dementia and geriatric cognitive disorders* 21 (2), 65–73.

Katzman, R., Terry, R., DeTeresa, R., Brown, T., *et al.* (1988). Clinical, pathological, and neurochemical changes in dementia: a subgroup with preserved mental status and numerous neocortical plaques. *Annals of neurology* 23 (2), 138–144.

Kim, C., Choi, H., Jung, E.S., Lee, W., *et al.* (2012). HDAC6 inhibitor blocks amyloid beta-induced impairment of mitochondrial transport in hippocampal neurons. *PLoS ONE* 7 (8), 2–8.

Kim, J., Basak, J.M. & Holtzman, D.M. (2009). The Role of Apolipoprotein E in Alzheimer's Disease. *Neuron* 63 (3), 287–303.

Knobloch, M. & Mansuy, I.M. (2008). Dendritic spine loss and synaptic alterations in Alzheimer's disease. *Molecular neurobiology* 37 (1), 73–82.

Knopman, D.S., Parisi, J.E., Salviati, A., Floriach-Robert, M., *et al.* (2003). Neuropathology of cognitively normal elderly. *Journal of neuropathology and experimental neurology* 62 (11), 1087–1095.

Kornau, H., Schenker, L., Kennedy, M. & Seeburg, P. (1995). Domain interaction between NMDA receptor subunits and the postsynaptic density protein PSD-95. *Science* 269 (5231), 1737–1740.

Kosik, K.S., Joachim, C.L. & Selkoe, D.J. (1986). Microtubule-associated protein tau (tau) is a major antigenic component of paired helical filaments in Alzheimer disease. *Proceedings of the National Academy of Sciences* 83 (11), 4044–4048.

Kroker, K.S., Mathis, C., Marti, A., Cassel, J.-C., *et al.* (2014). PDE9A inhibition rescues amyloid beta-induced deficits in synaptic plasticity and cognition. *Neurobiology of aging* 35 (9), 2072–2078.

Kudo, T., Okumura, M., Imaizumi, K., Araki, W., *et al.* (2006). Altered localization of amyloid precursor protein under endoplasmic reticulum stress. *Biochemical and Biophysical Research Communications* 344 (2), 525–530.

Kumar, P., Ambasta, R.K., Veereshwarayya, V., Rosen, K.M., *et al.* (2007). CHIP and HSPs interact with β-APP in a proteasome-dependent manner and influence Aβ metabolism. *Human Molecular Genetics* 16 (7), 848–864.

Lagman, D., Franzén, I.E., Eggert, J., Larhammar, D., *et al.* (2016). Evolution and expression of the phosphodiesterase 6 genes unveils vertebrate novelty to control photosensitivity. *BMC Evolutionary Biology* 16 (1), 124.

Lammich, S., Kojro, E., Postina, R., Gilbert, S., *et al.* (1999). Constitutive and regulated -secretase cleavage of Alzheimer's amyloid precursor protein by a disintegrin metalloprotease. *Proceedings of the National Academy of Sciences* 96 (7), 3922–3927.

Lanz, T.A., Carter, D.B. & Merchant, K.M. (2003). Dendritic spine loss in the hippocampus of young PDAPP and Tg2576 mice and its prevention by the ApoE2 genotype. *Neurobiology of disease* 13 (3), 246–253.

Legdeur, N., Badissi, M., Carter, S.F., de Crom, S., *et al.* (2018). Resilience to cognitive impairment in the oldest-old: design of the EMIF-AD 90+ study. *BMC geriatrics*. 18 (1), 289.

Lehár, J., Krueger, A.S., Avery, W., Heilbut, A.M., *et al.* (2009). Synergistic drug combinations tend to improve therapeutically relevant selectivity. *Nature biotechnology* 27 (7), 659–666.

Levenson, J.M., O'Riordan, K.J., Brown, K.D., Trinh, M.A., *et al.* (2004). Regulation of Histone Acetylation during Memory Formation in the Hippocampus. *Journal of Biological Chemistry* 279 (39), 40545–40559.

Levy-Lahad, E., Wasco, W., Poorkaj, P., Romano, D.M., *et al.* (1995). Candidate gene for the chromosome 1 familial Alzheimer's disease locus. *Science* 269 (5226), 973–977.

Lewis, J., Dickson, D.W., Lin, W.L., Chisholm, L., *et al.* (2001). Enhanced Neurofibrillary Degeneration in Transgenic Mice Expressing Mutant Tau and APP. *Science* 293 (5534), 1487–1491.

Li, L., Chin, L.S., Shupliakov, O., Brodin, L., *et al.* (1995). Impairment of synaptic vesicle clustering and of synaptic transmission, and increased seizure propensity, in synapsin I-deficient mice. *Proceedings of the National Academy of Sciences* 92 (20), 9235–9239.

Liu, T., Lipnicki, D.M., Zhu, W., Tao, D., *et al.* (2012). Cortical gyrification and sulcal spans in early stage Alzheimer's disease. *PloS one* 7 (2), e31083.

Livak, K.J. & Schmittgen, T.D. (2001). Analysis of relative gene expression data using real-time quantitative PCR and the 2(-Delta Delta C(T)) Method. *Methods* 25 (4), 402–408.

Llinás, R., Gruner, J.A., Sugimori, M., McGuinness, T.L., *et al.* (1991). Regulation by

synapsin I and Ca(2+)-calmodulin-dependent protein kinase II of the transmitter release in squid giant synapse. *The Journal of Physiology* 436 (1), 257–282.

López-Vales, R., Navarro, X., Shimizu, T., Baskakis, C., *et al.* (2008). Intracellular phospholipase A(2) group IVA and group VIA play important roles in Wallerian degeneration and axon regeneration after peripheral nerve injury. *Brain* 131 (10), 2620–2631.

Lovestone, S., Reynolds, C.H., Latimer, D., Davis, D.R., *et al.* (1994). Alzheimer's disease-like phosphorylation of the microtubule-associated protein tau by glycogen synthase kinase-3 in transfected mammalian cells. *Current biology* 4 (12), 1077–1086.

Lu, Y.F., Kandel, E.R. & Hawkins, R.D. (1999). Nitric oxide signaling contributes to late-phase LTP and CREB phosphorylation in the hippocampus. *The Journal of neuroscience* 19 (23), 10250–10261.

Lukashchuk, V., Lewis, K.E., Coldicott, I., Grierson, A.J., *et al.* (2016). AAV9-mediated central nervous system–targeted gene delivery via cisterna magna route in mice. *Molecular Therapy - Methods & Clinical Development* 3, 15055.

Lv, Z., Guo, J., Sun, Q., Li, K., *et al.* (2012). Association between PLA2G6 gene polymorphisms and Parkinson's disease in the Chinese Han population. *Parkinsonism & Related Disorders* 18 (5), 641–644.

Ma, Q.-L., Lim, G.P., Harris-White, M.E., Yang, F., *et al.* (2006). Antibodies against beta-amyloid reduce Abeta oligomers, glycogen synthase kinase-3beta activation and tau phosphorylation in vivo and in vitro. *Journal of neuroscience research* 83 (3), 374–384.

Magrané, J., Smith, R.C., Walsh, K. & Querfurth, H.W. (2004). Heat shock protein 70 participates in the neuroprotective response to intracellularly expressed beta-amyloid in neurons. *The Journal of neuroscience* 24 (7), 1700–1706.

Mahady, L., Nadeem, M., Malek-Ahmadi, M., Chen, K., *et al.* (2018). Frontal Cortex Epigenetic Dysregulation During the Progression of Alzheimer's Disease. *Journal of Alzheimer's disease* 62 (1), 115–131.

Mahady, L., Nadeem, M., Malek-Ahmadi, M., Chen, K., *et al.* (2019). HDAC2 dysregulation in the nucleus basalis of Meynert during the progression of Alzheimer's disease. *Neuropathology and applied neurobiology* 45 (4), 380–397.

Maia LF, Kaeser SA, Reichwald J, Hruscha M, Martus P, Staufenbiel M, J.M. (2013). Changes in amyloid-β and tau in the cerebrospinal fluid of transgenic mice overexpressing amyloid precursor protein. *Science translational medicine* 5 (194), 94re2-194re2.

Malaguti, M.C., Melzi, V., Di Giacopo, R., Monfrini, E., *et al.* (2015). A novel homozygous PLA2G6 mutation causes dystonia-parkinsonism. *Parkinsonism & Related Disorders* 21 (3), 337–339.

Mangialasche, F., Solomon, A., Winblad, B., Mecocci, P., *et al.* (2010). Alzheimer's disease: clinical trials and drug development. *The Lancet Neurology* 9 (7), 702–716.

Maren, S. (2008). Pavlovian fear conditioning as a behavioral assay for hippocampus and amygdala function: Cautions and caveats. *European Journal of Neuroscience* 28 (8), 1661–1666.

Martin, L., Latypova, X., Wilson, C.M., Magnaudeix, A., *et al.* (2013). Tau protein phosphatases in Alzheimer's disease: The leading role of PP2A. *Ageing Research Reviews* 12 (1), 39–49.

Martin Prince, A., Albanese, E., Guerchet, M., Prina, M., *et al.* (2014). *World Alzheimer Report 2014 Dementia and Risk Reduction an Analysis of Protective and Modifiable Factors Supported*. 102.

Masters, C.L., Simms, G., Weinman, N.A., Multhaup, G., *et al.* (1985). Amyloid plaque core protein in Alzheimer disease and Down syndrome. *Proceedings of the National Academy of Sciences* 82 (12), 4245–4249.

Mattson, M.P. (2004). Pathways towards and away from Alzheimer's disease. *Nature* 430 (7000), 631–639.

McKhann, G.M., Knopman, D.S., Chertkow, H., Hyman, B.T., *et al.* (2011). The diagnosis of dementia due to Alzheimer's disease: recommendations from the National Institute on Aging-Alzheimer's Association workgroups on diagnostic guidelines for Alzheimer's disease. *Alzheimer's & dementia* 7 (3), 263–269.

McQuown, S.C., Barrett, R.M., Matheos, D.P., Post, R.J., *et al.* (2011). HDAC3 Is a Critical Negative Regulator of Long-Term Memory Formation. *Journal of Neuroscience* 31 (2), 764–774.

Megías, M., Emri, Z., Freund, T. & Gulyás, A. (2001). Total number and distribution of inhibitory and excitatory synapses on hippocampal CA1 pyramidal cells. *Neuroscience* 102 (3), 527–540.

Melloni, R.H., Apostolides, P.J., Hamos, J.E. & DeGennaro, L.J. (1994). Dynamics of synapsin I gene expression during the establishment and restoration of functional synapses in the rat hippocampus. *Neuroscience* 58 (4), 683–703.

Meziane, H., Dodart, J.C., Mathis, C., Little, S., *et al.* (1998). Memory-enhancing effects of secreted forms of the beta-amyloid precursor protein in normal and amnestic mice. *Proceedings of the National Academy of Sciences of the United States of America*. 95 (21), 12683–12688.

Mielke, M.M., Vemuri, P. & Rocca, W. A. (2014). Clinical epidemiology of Alzheimer's disease: Assessing sex and gender differences. *Clinical Epidemiology* 6 (1), 37–48.

Moreno-Gonzalo, O., Mayor, F. & Sánchez-Madrid, F. (2018). HDAC6 at Crossroads of Infection and Innate Immunity. *Trends in immunology* 39 (8), 591–595.

Morgan, N. V, Westaway, S.K., Morton, J.E. V, Gregory, A., *et al.* (2006). PLA2G6, encoding a phospholipase A2, is mutated in neurodegenerative disorders with high brain iron. *Nature Genetics* 38 (7), 752–754.

Morimoto, Y., Shimada-Sugimoto, M., Otowa, T., Yoshida, S., *et al.* (2018). Whole-exome sequencing and gene-based rare variant association tests suggest that PLA2G4E might be a risk gene for panic disorder. *Translational psychiatry* 8 (1),

41.

Morishima-Kawashima, M., Hasegawa, M., Takio, K., Suzuki, M., *et al.* (1995). Proline-directed and Non-proline-directed Phosphorylation of PHF-tau. *Journal of Biological Chemistry* 270 (2), 823–829.

Morris, J.C. (2005). Mild cognitive impairment and preclinical Alzheimer's disease. *Geriatrics*. Suppl, 9–14.

Morris, J.C., Storandt, M., McKeel, D.W., Rubin, E.H., *et al.* (1996). Cerebral amyloid deposition and diffuse plaques in ``normal'' aging: Evidence for presymptomatic and very mild Alzheimer's disease. *Neurology* 46 (3), 707–719.

Mrak, R., Griffin, S. & Graham, D. (1997). Aging-associated Changes in Human Brain. *Journal of Neuropathology and Experimental Neurology* 56 (12), 1269–1275.

Muchowski, P.J. & Wacker, J.L. (2005). Modulation of neurodegeneration by molecular chaperones. *Neuroscience* 6 (1), 11–22.

Mucke, L. & Selkoe, D.J. (2012). Neurotoxicity of amyloid β-protein: synaptic and network dysfunction. *Cold Spring Harbor perspectives in medicine* 2 (7), a006338.

Mullan, M., Crawford, F., Axelman, K., Houlden, H., *et al.* (1992). A pathogenic mutation for probable Alzheimer's disease in the APP gene at the N–terminus of β–amyloid. *Nature Genetics* 1 (5), 345–347.

Mullane, K. & Williams, M. (2019). Preclinical Models of Alzheimer's Disease: Relevance and Translational Validity. *Current Protocols in Pharmacology* 84 (1), e57.

Mury, F.B., da Silva, W.C., Barbosa, N.R., Mendes, C.T., *et al.* (2016). Lithium activates brain phospholipase A2 and improves memory in rats: implications for Alzheimer's disease. *European archives of psychiatry and clinical neuroscience* 266 (7), 607–618.

Negash, S., Xie, S., Davatzikos, C., Clark, C.M., *et al.* (2013). Cognitive and functional resilience despite molecular evidence of Alzheimer's disease pathology. *Alzheimer's & dementia* 9 (3), e89-95.

Neuner, S.M., Wilmott, L.A., Hoffmann, B.R., Mozhui, K., *et al.* (2015). Hippocampal proteomics defines pathways associated with memory decline and resilience in 'normal' aging and Alzheimer's disease mouse models. *Analytical Chemistry* 25 (4), 368–379.

O'Brien, R.J., Lau, L.F. & Huganir, R.L. (1998). Molecular mechanisms of glutamate receptor clustering at excitatory synapses. *Current opinion in neurobiology* 8 (3), 364–369.

O'Brien, R.J., Resnick, S.M., Zonderman, A.B., Ferrucci, L., *et al.* (2009). Neuropathologic studies of the Baltimore Longitudinal Study of Aging (BLSA). *Journal of Alzheimer's disease* 18 (3), 665–675.

Octave, J.-N., Pierrot, N., Ferao Santos, S., Nalivaeva, N.N., *et al.* (2013). From synaptic spines to nuclear signaling: nuclear and synaptic actions of the amyloid precursor

protein. *Journal of Neurochemistry* 126 (2), 183–190.

Oddo, S., Caccamo, A., Shepherd, J.D., Murphy, M.P., *et al.* (2003). Triple-transgenic model of Alzheimer's disease with plaques and tangles: intracellular Abeta and synaptic dysfunction. *Neuron* 39 (3), 409–421.

Ogura, Y., Parsons, W.H., Kamat, S.S. & Cravatt, B.F. (2016). A calcium-dependent acyltransferase that produces N-acyl phosphatidylethanolamines. *Nature Chemical Biology* 12 (9), 669–671.

Ohto, T., Uozumi, N., Hirabayashi, T. & Shimizu, T. (2005). Identification of novel cytosolic phospholipase A(2)s, murine cPLA(2){delta}, {epsilon}, and {zeta}, which form a gene cluster with cPLA(2){beta}. *The Journal of biological chemistry* 280 (26), 24576–24583.

Omori, K. & Kotera, J. (2007). Overview of PDEs and Their Regulation. *Circulation Research* 100 (3), 309–327.

Paxinos, G. & Franklin, K. (1997). The mouse brain in stereotaxic coordinates.

Peixoto, L. & Abel, T. (2012). The Role of Histone Acetylation in Memory Formation and Cognitive Impairments. *Neuropsychopharmacology* 38 (1), 62–76.

Perez-Nievas, B.G., Stein, T.D., Tai, H.-C., Dols-Icardo, O., *et al.* (2013). Dissecting phenotypic traits linked to human resilience to Alzheimer's pathology. *Brain* 136 (Pt 8), 2510–2526.

Pérez, M., Ribe, E., Rubio, A., Lim, F., *et al.* (2005). Characterization of a double (amyloid precursor protein-tau) transgenic: tau phosphorylation and aggregation. *Neuroscience* 130 (2), 339–347.

Perez, R.G., Zheng, H., Van der Ploeg, L.H. & Koo, E.H. (1997). The beta-amyloid precursor protein of Alzheimer's disease enhances neuron viability and modulates neuronal polarity. *The Journal of neuroscience* 17 (24), 9407–9414.

Piccio, L., Deming, Y., Del-Águila, J.L., Ghezzi, L., *et al.* (2016). Cerebrospinal fluid soluble TREM2 is higher in Alzheimer disease and associated with mutation status. *Acta neuropathologica* 131 (6), 925–933.

Plassman, B.L., Havlik, R.J., Steffens, D.C., Helms, M.J., *et al.* (2000). Documented head injury in early adulthood and risk of Alzheimer's disease and other dementias. *Neurology* 55 (8), 1158–1166.

Ponting, C.P., Phillips, C., Davies, K.E. & Blake, D.J. (1997). PDZ domains: targeting signalling molecules to sub-membranous sites. *BioEssays* 19 (6), 469–479.

Price, J.L., Davis, P.B., Morris, J.C. & White, D.L. (1991). The distribution of tangles, plaques and related immunohistochemical markers in healthy aging and Alzheimer's disease. *Neurobiology of aging* 12 (4), 295–312.

Price, J.L., McKeel, D.W., Buckles, V.D., Roe, C.M., *et al.* (2009). Neuropathology of nondemented aging: presumptive evidence for preclinical Alzheimer disease. *Neurobiology of aging* 30 (7), 1026–1036.

Priller, C., Bauer, T., Mitteregger, G., Krebs, B., *et al.* (2006). Synapse Formation and Function Is Modulated by the Amyloid Precursor Protein. *Journal of Neuroscience* 26 (27), 7212–7221.

Purandare, N., Burns, A., Daly, K.J., Hardicre, J., *et al.* (2006). Cerebral emboli as a potential cause of Alzheimer's disease and vascular dementia: case-control study. *BMJ* 332 (7550), 1119–1124.

Puzzo, D., Sapienza, S., Arancio, O. & Palmeri, A. (2008). Role of phosphodiesterase 5 in synaptic plasticity and memory. *Neuropsychiatric disease and treatment* 4 (2), 371–387.

Qiu, C., Winblad, B. & Fratiglioni, L. (2005). The age-dependent relation of blood pressure to cognitive function and dementia. *The Lancet Neurology* 4 (8), 487–499.

Rabal, O., Sánchez-Arias, J., Cuadrado-Tejedor, M., De Miguel, I., *et al.* (submitted). Multitarget Approach for the Treatment of Alzheimer`s Disease: Inhibition of Phosphodiesterase 9 (PDE9) and Histone Deacetylases (HDACs) covering diverse selectivity profiles. *Journal of Medicinal Chemistry*.

Rabal, O., Sánchez-Arias, J.A., Cuadrado-Tejedor, M., de Miguel, I., *et al.* (2016). Design, Synthesis, and Biological Evaluation of First-in-Class Dual Acting Histone Deacetylases (HDACs) and Phosphodiesterase 5 (PDE5) Inhibitors for the Treatment of Alzheimer's Disease. *Journal of Medicinal Chemistry* 59 (19), 8967–9004.

Radde, R., Bolmont, T., Kaeser, S. A, Coomaraswamy, J., *et al.* (2006). Abeta42-driven cerebral amyloidosis in transgenic mice reveals early and robust pathology. *EMBO reports* 7 (9), 940–946.

Radic, T., Frieß, L., Vijikumar, A., Jungenitz, T., *et al.* (2017). Differential Postnatal Expression of Neuronal Maturation Markers in the Dentate Gyrus of Mice and Rats. *Frontiers in Neuroanatomy* 11.

Rao, A. & Craig, A.M. (1997). Activity regulates the synaptic localization of the NMDA receptor in hippocampal neurons. *Neuron* 19 (4), 801–812.

Reiman, E.M., Caselli, R.J., Yun, L.S., Chen, K., *et al.* (1996). Preclinical Evidence of Alzheimer's Disease in Persons Homozygous for the ε4 Allele for Apolipoprotein E. *New England Journal of Medicine* 334 (12), 752–758.

Ricobaraza, A., Cuadrado-Tejedor, M., Pérez-Mediavilla, A., Frechilla, D., *et al.* (2009). Phenylbutyrate Ameliorates Cognitive Deficit and Reduces Tau Pathology in an Alzheimer's Disease Mouse Model. *Neuropsychopharmacology* 34 (7), 1721–1732.

Riley, K.P., Snowdon, D.A., Desrosiers, M.F. & Markesbery, W.R. (2005). Early life linguistic ability, late life cognitive function, and neuropathology: Findings from the Nun Study. *Neurobiology of Aging* 26 (3), 341–347.

Roche, K.W., Standley, S., McCallum, J., Dune Ly, C., *et al.* (2001). Molecular determinants of NMDA receptor internalization. *Nature Neuroscience* 4 (8), 794–802.

Rodionova, E., Conzelmann, M., Maraskovsky, E., Hess, M., *et al.* (2007). GSK-3

mediates differentiation and activation of proinflammatory dendritic cells. *Blood* 109 (4), 1584–1592.

Rodriguez-Rodero S., Fernandez-Morera J.L., Fernandez A.F., Menendez-Torre E., *et al.* (2010). Epigenetic regulation of aging. *Discovery Medicine*. 10 (52), 225–233.

Ross, B.M., Moszczynska, A., Erlich, J. & Kish, S.J. (1998). Phospholipid-metabolizing enzymes in Alzheimer's disease: increased lysophospholipid acyltransferase activity and decreased phospholipase A2 activity. *Journal of neurochemistry* 70 (2), 786–793.

von Rotz, R.C., Kohli, B.M., Bosset, J., Meier, M., *et al.* (2004). The APP intracellular domain forms nuclear multiprotein complexes and regulates the transcription of its own precursor. *Journal of cell science* 117 (19), 4435–4448.

Rovelet-Lecrux, A., Hannequin, D., Raux, G., Meur, N. Le, *et al.* (2006). APP locus duplication causes autosomal dominant early-onset Alzheimer disease with cerebral amyloid angiopathy. *Nature Genetics* 38 (1), 24–26.

Rumbaugh, G., Sillivan, S.E., Ozkan, E.D., Rojas, C.S., *et al.* (2015). Pharmacological Selectivity Within Class I Histone Deacetylases Predicts Effects on Synaptic Function and Memory Rescue. *Neuropsychopharmacology* 40 (10), 2307–2316.

Schaeffer, E.L., Forlenza, O. V & Gattaz, W.F. (2009). Phospholipase A2 activation as a therapeutic approach for cognitive enhancement in early-stage Alzheimer disease. *Psychopharmacology* 202 (1–3), 37–51.

Schaeffer, E.L. & Gattaz, W.F. (2007). Requirement of hippocampal phospholipase A2 activity for long-term memory retrieval in rats. *Journal of Neural Transmission* 114 (3), 379–385.

Scheff, S.W., Price, D.A., Schmitt, F.A., DeKosky, S.T., *et al.* (2007). Synaptic alterations in CA1 in mild Alzheimer disease and mild cognitive impairment. *Neurology* 68 (18), 1501–1508.

Schmitt, F.A., Davis, D.G., Wekstein, D.R., Smith, C.D., *et al.* (2000). 'Preclinical' AD revisited: Neuropathology of cognitively normal older adults. *Neurology* 55 (3), 370–376.

Selkoe, D.J. (2002). Alzheimer's Disease Is a Synaptic Failure. *Science* 298 (5594), 789–791.

Selkoe, D.J. (2004). Cell biology of protein misfolding: the examples of Alzheimer's and Parkinson's diseases. *Nature cell biology* 6 (11), 1054–1061.

Selkoe, D.J. & Hardy, J. (2016). The amyloid hypothesis of Alzheimer's disease at 25 years. *EMBO Molecular Medicine* 8 (6), 595–608.

Semple, B.D., Blomgren, K., Gimlin, K., Ferriero, D.M., *et al.* (2013). Brain development in rodents and humans: Identifying benchmarks of maturation and vulnerability to injury across species. *Progress in neurobiology* 106–107, 1–16.

Serneels, L., Van Biervliet J., Craessaerts K., Dejaegere T., *et al.* (2009). γ-Secretase heterogeneity in the Aph1 subunit: relevance for Alzheimer's disease. *Science*. 324

(5927), 639–642.

Serrano-Pozo, A., Frosch, M.P., Masliah, E. & Hyman, B.T. (2011). Neuropathological alterations in Alzheimer disease. *Cold Spring Harbor perspectives in medicine* 1 (1), 1–23.

Setter, S.M., Iltz, J.L., Fincham, J.E., Campbell, R.K., *et al.* (2005). Phosphodiesterase 5 Inhibitors for Erectile Dysfunction. *Annals of Pharmacotherapy* 39 (7–8), 1286–1295.

Shankar, G.M., Li, S., Mehta, T.H., Garcia-Munoz, A., *et al.* (2008). Amyloid-β protein dimers isolated directly from Alzheimer's brains impair synaptic plasticity and memory. *Nature Medicine* 14 (8), 837–842.

Sharma, S., Sarathlal, K.C. & Taliyan, R. (2019). Epigenetics in Neurodegenerative Diseases: The Role of Histone Deacetylases. *CNS & Neurological Disorders - Drug Targets* 18 (1), 11–18.

Sherrington, R., Rogaev, E.I., Liang, Y., Rogaeva, E.A., *et al.* (1995). Cloning of a gene bearing missense mutations in early-onset familial Alzheimer's disease. *Nature* 375 (6534), 754–760.

Shimura, H., Schwartz, D., Gygi, S.P. & Kosik, K.S. (2004). CHIP-Hsc70 complex ubiquitinates phosphorylated tau and enhances cell survival. *The Journal of biological chemistry* 279 (6), 4869–4876.

Shivers, B.D., Hilbich, C., Multhaup, G., Salbaum, M., *et al.* (1988). Alzheimer's disease amyloidogenic glycoprotein: expression pattern in rat brain suggests a role in cell contact. *The EMBO journal*. 7 (5), 1365–1370.

Shlisky, J., Bloom, D.E., Beaudreault, A.R., Tucker, K.L., *et al.* (2017). Nutritional Considerations for Healthy Aging and Reduction in Age-Related Chronic Disease. *Advances in Nutrition* 8 (1), 17.2-26.

De Simone, A. & Milelli, A. (2019). Histone Deacetylase Inhibitors as Multitarget Ligands: New Players in Alzheimer's Disease Drug Discovery? *ChemMedChem* 14 (11), 1067–1073.

Sims, R., van der Lee, S.J., Naj, A.C., Bellenguez, C., *et al.* (2017). Rare coding variants in PLCG2, ABI3, and TREM2 implicate microglial-mediated innate immunity in Alzheimer's disease. *Nature Genetics* 49 (9), 1373–1384.

Singh, N. & Patra, S. (2014). Phosphodiesterase 9: insights from protein structure and role in therapeutics. *Life sciences* 106 (1–2), 1–11.

Small GW, Rabins PV, Barry PP, Buckholtz NS, *et al.* (1997). Diagnosis and treatment of Alzheimer disease and related disorders. *JAMA.* 278 (16), 1363–1371.

Smesny, S., Stein, S., Willhardt, I., Lasch, J., *et al.* (2008). Decreased phospholipase A2 activity in cerebrospinal fluid of patients with dementia. *Journal of neural transmission* 115 (8), 1173–1179.

Smyth, G.K. (2004). Linear models and empirical bayes methods for assessing differential expression in microarray experiments. *Statistical applications in*

genetics and molecular biology 3 (1), Article3.

Snyder, E.M., Philpot, B.D., Huber, K.M., Dong, X., *et al.* (2001). Internalization of ionotropic glutamate receptors in response to mGluR activation. *Nature Neuroscience* 4 (11), 1079–1085.

Soejima, N., Ohyagi, Y., Nakamura, N., Himeno, E., *et al.* (2013). Intracellular accumulation of toxic turn amyloid-β is associated with endoplasmic reticulum stress in Alzheimer's disease. *Current Alzheimer research* 10 (1), 11–20.

van der Staay, F.J., Rutten, K., Bärfacker, L., Devry, J., *et al.* (2008). The novel selective PDE9 inhibitor BAY 73-6691 improves learning and memory in rodents. *Neuropharmacology*. 55 (5), 908–918.

Steinerman, J.R., Irizarry, M., Scarmeas, N., Raju, S., *et al.* (2008). Distinct pools of beta-amyloid in Alzheimer disease-affected brain: a clinicopathologic study. *Archives of neurology* 65 (7), 906–912.

Stern, Y. (2012). Cognitive reserve in ageing and Alzheimer's disease. *The Lancet Neurology* 11 (11), 1006–1012.

Subramanian, S., Bates, S.E., Wright, J.J., Espinoza-Delgado, I., *et al.* (2010). Clinical Toxicities of Histone Deacetylase Inhibitors. *Pharmaceuticals* 3 (9), 2751–2767.

Sun, G.Y., Xu, J., Jensen, M.D. & Simonyi, A. (2004). Phospholipase A2 in the central nervous system: implications for neurodegenerative diseases. *Journal of lipid research* 45 (2), 205–213.

Sung, Y.M., Lee, T., Yoon, H., DiBattista, A.M., *et al.* (2013). Mercaptoacetamide-based class II HDAC inhibitor lowers Aβ levels and improves learning and memory in a mouse model of Alzheimer's disease. *Experimental neurology* 239, 192–201.

Tagliavini, F., Giaccone, G., Frangione, B. & Bugiani, O. (1988). Preamyloid deposits in the cerebral cortex of patients with Alzheimer's disease and nondemented individuals. *Neuroscience letters* 93 (2–3), 191–196.

Talbot, K., Young, R.A., Jolly-Tornetta, C., Lee, V.M., *et al.* (2000). A frontal variant of Alzheimer's disease exhibits decreased calcium-independent phospholipase A2 activity in the prefrontal cortex. *Neurochemistry international* 37 (1), 17–31.

Tanis, K.Q. & Duman, R.S. (2007). Intracellular signaling pathways pave roads to recovery for mood disorders. *Annals of medicine* 39 (7), 531–544.

Teng, F.Y.H. & Tang, B.L. (2006). Axonal regeneration in adult CNS neurons--signaling molecules and pathways. *Journal of Neurochemistry* 96 (6), 1501–1508.

Terry, R.D., Masliah, E., Salmon, D.P., Butters, N., *et al.* (1991). Physical basis of cognitive alterations in Alzheimer's disease: synapse loss is the major correlate of cognitive impairment. *Annals of neurology* 30 (4), 572–580.

Thirstrup, K., Sotty, F., Montezinho, L.C.P., Badolo, L., *et al.* (2016). Linking HSP90 target occupancy to HSP70 induction and efficacy in mouse brain. *Pharmacological research* 104, 197–205.

Tomlinson, B.E., Blessed, G. & Roth, M. (1968). Observations on the brains of non-demented old people. *Journal of the Neurological Sciences* 7 (2), 331–356.

Turenne, G.A. & Price, B.D. (2001). Glycogen synthase kinase3 beta phosphorylates serine 33 of p53 and activates p53's transcriptional activity. *BMC cell biology* 2, 12.

Turner, P.R., O'Connor, K., Tate, W.P. & Abraham, W.C. (2003). Roles of amyloid precursor protein and its fragments in regulating neural activity, plasticity and memory. *Progress in neurobiology* 70 (1), 1–32.

Ugarte, A., Gil-Bea, F., García-Barroso, C., Cedazo-Minguez, Á., *et al.* (2015). Decreased levels of guanosine 3′, 5′-monophosphate (cGMP) in cerebrospinal fluid (CSF) are associated with cognitive decline and amyloid pathology in Alzheimer's disease. *Neuropathology and Applied Neurobiology* 41 (4), 471–482.

Vassar, R., Bennett, B.D., Babu-Khan, S., Kahn, S., *et al.* (1999). Beta-secretase cleavage of Alzheimer's amyloid precursor protein by the transmembrane aspartic protease BACE. *Science* 286 (5440), 735–741.

Vieira, N.M., Elvers, I., Alexander, M.S., Lindblad-toh, K., *et al.* (2015). Jagged 1 Rescues the Duchenne Muscular Dystrophy Phenotype Article Jagged 1 Rescues the Duchenne Muscular Dystrophy Phenotype. *Cell* 163 (5), 1–10.

Wang, B., Wang, Z., Sun, L., Yang, L., *et al.* (2014a) The amyloid precursor protein controls adult hippocampal neurogenesis through GABAergic interneurons. *The Journal of neuroscience* 34 (40), 13314–13325.

Wang, H., Tan, M.-S., Lu, R.-C., Yu, J.-T., et al. (2014b) Heat shock proteins at the crossroads between cancer and Alzheimer's disease. *BioMed research international* 2014, 239164.

Wanucha, G. (2018). 6 Things We Know about Resilience in Alzheimer's Disease. Available from: http://depts.washington.edu/mbwc/news/article/6-things-we-know-about-resilience-in-alzheimers-disease

Weber, M., Wu, T., Hanson, J.E., Alam, N.M., *et al.* (2015). Cognitive Deficits, Changes in Synaptic Function, and Brain Pathology in a Mouse Model of Normal Aging. *eNeuro*. 2 (5),

Westerman, M.A., Cooper-Blacketer, D., Mariash, A., Kotilinek, L., *et al.* (2002). The Relationship between Aβ and Memory in the Tg2576 Mouse Model of Alzheimer's Disease. *The Journal of Neuroscience* 22 (5), 1858–1867.

Whitehouse, P.J., Price, D.L., Struble, R.G., Clark, A.W., *et al.* (1982). Alzheimer's disease and senile dementia: loss of neurons in the basal forebrain. *Science* 215 (4537), 1237–1239.

Whitmer, R.A., Sidney, S., Selby, J., Johnston, S.C., *et al.* (2005). Midlife cardiovascular risk factors and risk of dementia in late life. *Neurology* 64 (2), 277–281.

Wilson, R.S., Schneider, J.A., Bienias, J.L., Arnold, S.E., *et al.* (2003). Depressive symptoms, clinical AD, and cortical plaques and tangles in older persons. *Neurology* 61 (8), 1102–1107.

Winslow, B.T., Onysko, M.K., Stob, C.M. & Hazlewood, K.A. (2011). Treatment of Alzheimer disease. *American family physician* 83 (12), 1403–1412.

Wyszynski, M., Lin, J., Rao, A., Nigh, E., *et al.* (1997). Competitive binding of α-actinin and calmodulin to the NMDA receptor. *Nature* 385 (6615), 439–442.

Xu, W., Qiu, C., Gatz, M., Pedersen, N.L., *et al.* (2009). Mid- and late-life diabetes in relation to the risk of dementia: a population-based twin study. *Diabetes* 58 (1), 71–77.

Xu, Y., Zhang, H.-T. & O'Donnell, J.M. (2011). Phosphodiesterases in the Central Nervous System: Implications in Mood and Cognitive Disorders. *Handbook of experimental pharmacology* (204) 447–485.

Yang, Y., Turner, R.S. & Gaut, J.R. (1998). The chaperone BiP/GRP78 binds to amyloid precursor protein and decreases Abeta40 and Abeta42 secretion. *The Journal of biological chemistry* 273 (40), 25552–25555.

Yang, Z.-Z., Tschopp, O., Baudry, A., Dümmler, B., *et al.* (2004). Physiological functions of protein kinase B/Akt. *Biochemical Society transactions* 32 (2), 350–354.

Yiannopoulou, K.G. & Papageorgiou, S.G. (2013). Current and future treatments for Alzheimer's disease. *Therapeutic advances in neurological disorders* 6 (1), 19–33.

Yu, F., Rose, K.M., Burgener, S.C., Cunningham, C., *et al.* (2009). Cognitive training for early-stage Alzheimer's disease and dementia. *Journal of gerontological nursing* 35 (3), 23–29.

Yun, H.-M., Jin, P., Han, J.-Y., Lee, M.-S., *et al.* (2013). Acceleration of the Development of Alzheimer's Disease in Amyloid Beta-Infused Peroxiredoxin 6 Overexpression Transgenic Mice. *Molecular Neurobiology* 48 (3), 941–951.

Yun, M., Wu, J., Workman, J.L. & Li, B. (2011). Readers of histone modifications. *Cell research* 21 (4), 564–578.

Yuste, R. & Denk, W. (1995). Dendritic spines as basic functional units of neuronal integration. *Nature* 375 (6533), 682–684.

Zewail, A.M., Nawar, M., Vrtovec, B., Eastwood, C., *et al.* (2003). Intravenous milrinone in treatment of advanced congestive heart failure. *Texas Heart Institute journal* 30 (2), 109–113.

Zhang, L., Liu, C., Wu, J., Tao, J.-J., *et al.* (2014). Tubastatin A/ACY-1215 improves cognition in Alzheimer's disease transgenic mice. *Journal of Alzheimer's disease* 41 (4), 1193–1205.

Zhang, L., Sheng, S. & Qin, C. (2012). The Role of HDAC6 in Alzheimer's Disease. *Journal of Alzheimer's Disease* 33 (2), 283–295.

Zhang, Y., Thompson, R., Zhang, H. & Xu, H. (2011). APP processing in Alzheimer's disease. *Molecular Brain* 4 (1), 3.

Zhao, W.-N., Ghosh, B., Tyler, M., Lalonde, J., *et al.* (2018). Class I Histone Deacetylase Inhibition by Tianeptinaline Modulates Neuroplasticity and Enhances Memory. *ACS*

Chemical Neuroscience 9 (9), 2262–2273.

Zolotukhin, S., Byrne, B.J., Mason, E., Zolotukhin, I., *et al.* (1999). Recombinant adeno-associated virus purification using novel methods improves infectious titer and yield. *Gene Therapy* 6, 973–985.

Zucconi, E., Valadares, M.C., Vieira, N.M., Bueno, C.R., *et al.* (2010). Ringo: Discordance between the molecular and clinical manifestation in a Golden Retriever Muscular Dystrophy dog. *Neuromuscular Disorders* 20 (1), 64–70.

ANNEX

Cuadrado-Tejedor M, Garcia-Barroso C, Sánchez-Arias JA, Rabal O, Pérez-González M, Mederos S, Ugarte A, Franco R, Segura V, Perea G, Oyarzabal J, Garcia-Osta A. A First-in-Class Small-Molecule that Acts as a Dual Inhibitor of HDAC and PDE5 and that Rescues Hippocampal Synaptic Impairment in Alzheimer's Disease Mice. Neuropsychopharmacology. 2017, 42(2):524-539. http://doi.org/10.1038/npp.2016.163.

frontiers in Aging Neuroscience

BRIEF RESEARCH REPORT
published: 21 June 2019
doi: 10.3389/fnagi.2019.00149

Taking Advantage of the Selectivity of Histone Deacetylases and Phosphodiesterase Inhibitors to Design Better Therapeutic Strategies to Treat Alzheimer's Disease

*Mar Cuadrado-Tejedor[1,2,3†], Marta Pérez-González[1,2,3†], Cristina García-Muñoz[1], Damián Muruzabal[1], Carolina García-Barroso[1], Obdulia Rabal[4], Víctor Segura[3,5], Juan A. Sánchez-Arias[4], Julen Oyarzabal[4] and Ana Garcia-Osta[1,3]**

[1]*Neurobiology of Alzheimer's Disease, Neurosciences Program, Center for Applied Medical Research (CIMA), University of Navarra, Pamplona, Spain,* [2]*Department of Pathology, Anatomy and Physiology, School of Medicine, University of Navarra, Pamplona, Spain,* [3]*Health Research Institute of Navarra (IDISNA), Pamplona, Spain,* [4]*Small Molecule Discovery Platform, Molecular Therapeutics Program, Center for Applied Medical Research (CIMA), University of Navarra, Pamplona, Spain,* [5]*Bioinformatics Unit, Center for Applied Medical Research (CIMA), University of Navarra, Pamplona, Spain*

OPEN ACCESS

Edited by:
Patrizia Giannoni, University of Nîmes, France

Reviewed by:
Ana I. Duarte, University of Coimbra, Portugal
Boon-Seng Wong, Singapore Institute of Technology, Singapore

***Correspondence:**
Ana Garcia-Osta
agosta@unav.es

†These authors have contributed equally to this work

Received: *25 March 2019*
Accepted: *06 June 2019*
Published: *21 June 2019*

Citation:
Cuadrado-Tejedor M, Péerez-González M, García-Muñoz C, Muruzabal D, García-Barroso C, Rabal O, Segura V, Sánchez-Arias JA, Oyarzabal J and Garcia-Osta A (2019) Taking Advantage of the Selectivity of Histone Deacetylases and Phosphodiesterase Inhibitors to Design Better Therapeutic Strategies to Treat Alzheimer's Disease. Front. Aging Neurosci. 11:149. doi: 10.3389/fnagi.2019.00149

The discouraging results with therapies for Alzheimer's disease (AD) in clinical trials, highlights the urgent need to adopt new approaches. Like other complex diseases, it is becoming clear that AD therapies should focus on the simultaneous modulation of several targets implicated in the disease. Recently, using reference compounds and the first-in class CM-414, we demonstrated that the simultaneous inhibition of histone deacetylases [class I histone deacetylases (HDACs) and HDAC6] and phosphodiesterase 5 (PDE5) has a synergistic therapeutic effect in AD models. To identify the best inhibitory balance of HDAC isoforms and PDEs that provides a safe and efficient therapy to combat AD, we tested the compound CM-695 in the Tg2576 mouse model of this disease. CM-695 selectively inhibits HDAC6 over class I HDAC isoforms, which largely overcomes the toxicity associated with HDAC class 1 inhibition. Furthermore, CM-695 inhibits PDE9, which is expressed strongly in the brain and has been proposed as a therapeutic target for AD. Chronic treatment of aged Tg2576 mice with CM-695 ameliorates memory impairment and diminishes brain Aβ, although its therapeutic effect was no longer apparent 4 weeks after the treatment was interrupted. An increase in the presence of 78-KDa glucose regulated protein (GRP78) and heat shock protein 70 (Hsp70) chaperones may underlie the therapeutic effect of CM-695. In summary, chronic treatment with CM-695 appears to reverse the AD phenotype in a safe and effective manner. Taking into account that AD is a multifactorial disorder, the multimodal action of these compounds and the different events they affect may open new avenues to combat AD.

Keywords: Alzheimer's disease, multitarget therapy, histone deacetylase, phosphodiesterase, memory

INTRODUCTION

Alzheimer's disease (AD) is a multifactorial neurodegenerative disorder for which no effective treatment has yet been found, despite the effort and resources invested to date. One reason for this failure may be that most of the efforts to develop therapies have been directed towards single pathways and mainly, the amyloid pathology. However, the complex nature of this disease means that multiple events are likely to be implicated in its progression and thus, effective therapies must modulate several targets, as is now being considered with state-of-the-art treatments for many cancers and AIDS. Moreover, the focus in AD is now shifting from the pathways that directly decrease the amyloid pathology to address those that dampen the tau pathology or that effect synaptogenesis (Cummings et al., 2018).

We recently validated the efficacy of a novel multitarget therapy for AD that focused on the concomitant inhibition of histone deacetylases (HDACs) and a phosphodiesterase 5 (PDE5). The approach was validated using reference compounds (tadalafil and vorinostat), and with a new drug and novel chemical entity (NCE), CM-414, which displays moderate class I HDAC inhibition, and more potent HDAC6 and PDE5 inhibition (Cuadrado-Tejedor et al., 2015, 2017; Rabal et al., 2016). We demonstrated that chronic treatment of Tg2576 mice (a well-studied model of AD) with CM-414 diminished the accumulation Aβ and pTau in the brain, reversing the decrease in dendritic spine density on hippocampal neurons and the cognitive deficits in these mice. These effects were at least in part produced by inducing the expression of genes related to synaptic transmission. Interestingly, we demonstrated that these therapeutic effects persisted 1 month after the completion of a 4-week treatment period (Cuadrado-Tejedor et al., 2017).

CM-414 was designed taking into account that class I HDACs and HDAC6 (class IIb) are the HDACs most likely to be involved in AD-memory related dysfunction (Ding et al., 2008; Guan et al., 2009; Mahady et al., 2019). The inhibition of class I HDACs, and particularly that of HDAC2, seems to be essential to restore memory by remodeling chromatin and enhancing gene expression (Guan et al., 2009; Singh and Thakur, 2018). However, the inhibition of HDAC class I isoforms has also been associated with cytotoxicity (Subramanian et al., 2010), precluding their chronic use. Recently, a new chemical series of HDAC1 and 2 inhibitors designed to inhibit the HDAC-CoREST co-repressor complex were seen to have lower toxicity, while maintaining the beneficial effects in terms of synaptic plasticity (Fuller et al., 2019). By contrast, the inhibition (or reduction) of HDAC6, a cytoplasmic HDAC isoform that regulates microtubule behavior and stability *via* α-tubulin acetylation (Hubbert et al., 2002), seems to promote tau and Aβ clearance, thereby ameliorating the memory deficits in AD models (Cook et al., 2012; Sung et al., 2013; Zhang et al., 2014). Furthermore, inhibiting HDAC6 rescues the reduced mitochondrial axonal transport and mitochondrial length in hippocampal neurons treated with Aβ (Kim et al., 2012), as well as in pluripotent stem cells (iPSCs) from Amyotrophic Lateral Sclerosis (ALS) patients (Guo et al., 2017). In fact, due to its safety profile, HDAC6 is currently being considered as one of the most promising epigenetic targets in AD. Given the above, and despite the fact that CM-414 acts as a symptomatic and disease-modifying agent in AD mice models (Cuadrado-Tejedor et al., 2017), it is possible that some toxicity may be associated with the inhibition of the class I HDAC1, precluding its use in the chronic treatment of AD patients. Thus, in order to improve the safety profile of CM-414, we synthesized a new compound, CM-695, with higher selectivity for HDAC6 over class I HDACs.

PDE9 is a cyclic guanosine monophosphate (cGMP) specific PDE and it is the PDE most strongly expressed in the brain (Andreeva et al., 2001). In fact, when we compared the expression of PDE5 and PDE9 in the mouse hippocampus, we found that PDE9 is expressed 10 times more strongly than PDE5 (**Supplementary Figure S1**). Interestingly, the expression of PDE5 and PDE9 were increased in the cortex of AD patients compared to age-matched control subjects. Accordingly, levels of cGMP were decreased in the cerebrospinal fluid (CSF) of AD patients compared to that of healthy control individuals (Ugarte et al., 2015). By restoring cGMP levels through PDE5 and 9 inhibition, intracellular signaling pathways that are important in memory and learning could be stimulated. For example, an activation of the cAMP-responsive element binding protein (CREB) transcription factor can be observed, a factor known to be crucial for synapse formation and memory consolidation (García-Osta et al., 2012; Heckman et al., 2017). Since PDE9 has the highest affinity for cGMP of all the PDEs (Singh and Patra, 2014), it becomes an attractive target to increase the GMP in the brain. It was recently proposed that PDE9 inhibitors provide more protection against Aβ42 than PDE4 and PDE5 inhibitors in an *in vitro* model of AD (Cameron et al., 2017). Nevertheless, when specific PDE9 inhibitors (PF-04447943 and BI-409306) have been tested to treat AD in Phase II clinical trials, they both failed to meet their AD efficacy endpoints relative to the placebo (Schwam et al., 2014; Frölich et al., 2019). As indicated above, the complexity of the AD pathology means it is possible that the inhibition of a single enzyme alone will not produce therapeutic benefits in patients. Accordingly, we designed a new first-in class dual activity compound CM-695, that targets HDAC6 and PDE9 for inhibition, and with acceptable brain permeability, for it's *in vivo* efficacy in Tg2576 mice.

MATERIALS AND METHODS

Biological Activity *in vitro* and *in vivo*

Cells of the human neuroblastoma SH-SY5Y cell line were plated in 6-well plates and incubated at 37°C in a humid atmosphere with 5% CO_2 until reaching a confluence of 80%–90%. They were cultivated in Eagle's medium modified by Dulbecco (DMEM, Gibco BRL, Grand Island, NY, USA) supplemented with 1% non-essential amino acids solution (Gibco BRL, Grand Island, NY, USA), penicillin/streptomycin 100 U/ml (Gibco BRL, Grand Island, NY, USA) and 10% fetal bovine serum (Gibco BRL, Grand Island, NY, USA). Cells were incubated with different concentrations of CM-695 for 2 h. After incubation, medium was removed, washed with PBS and cells were lysed in a buffer containing SDS 2%, Tris-HCl (10 mM, pH 7.4), protease

inhibitors (Complete Protease Inhibitor Cocktail, Roche) and phosphatase inhibitors (0.1 mM Na_3VO_4, 1 mM NaF). The homogenates were sonicated for 2 min and centrifuged at 14,000× *g* for 15 min.

Protein concentration was determined using the Pierce™ BCA Protein Assay kit (Thermo Fisher Scientific, Waltham, MA, USA). For western blot analysis of acetylated histone 3 at lysine 9 (AcH3K9), pCREB and acetylated tubulin, protein samples (15–20 μg) were mixed with 6× Laemmli sample buffer and resolved onto SDS-polyacrylamide gels and transferred to nitrocellulose membrane. Membranes were blocked for 1 h with 5% milk in TBS and incubated overnight with the corresponding primary antibody: rabbit monoclonal anti-AcH3K9, rabbit monoclonal anti-pCREB (Ser129; 1:1,000, Cell Signaling Technology, Danvers, MA, USA), mouse monoclonal anti-Acetylated tubulin, mouse monoclonal anti-β-actin (1:50,000, Sigma-Aldrich, St. Luis, MO, USA).

Animals and Treatments

Transgenic mice (Tg2576) between 16 and 18 months of age and female gender were used. This strain expresses the human 695-aa isoform of the amyloid precursor protein (APP) carrying the Swedish (K670N/M671L) familial AD mutation driven by a hamster prion promoter (Hsiao et al., 1996). Mice were on an inbred C57BL/6/SJL genetic background. The Tg2576 AD mice strain accumulates Aβ peptide exponentially, in the brain, between 7 and 12 months of age, showing a hippocampal damage from the age of 9–10 months (Chapman et al., 1999; Westerman et al., 2002).

Animals were bred at "Centro de Investigación Médica Aplicada" (CIMA) in Pamplona, Spain. Animals were housed 4–5 per cage with free access to food and water and maintained in a temperature controlled environment on a 12 h light-dark cycle. All procedures were carried out in agreement with the European and Spanish regulations (2010/63/EU; RD1201/2005), and the study was approved by the Ethical Committee for the Animal Experimentation of the University of Navarra.

Tg2576 mice were treated six times a week for 4 weeks. They were administered intraperitoneally with CM-695 (40 mg/kg n = 10) or vehicle (10% DMSO, 10% Tween-20 in saline solution). The preparation of drug was performed daily to avoid precipitation due to their hydrophobic nature. Behavioral and biochemical studies were performed comparing transgenic mice to age-and strain-matched transgenic negative littermates (WT). The behavioral tests were always carried out during light time (from 9 am to 14 pm), in order to minimize the possible influence of circadian rhythms.

Behavioral Studies

Behavioral studies were carried out during light time (from 9 am to 2 pm). Protocols were approved by the Ethical Committee of the University of Navarra (in accordance with the European and Spanish Royal Decree 1201/2005).

Fear Conditioning Test

To evaluate the effects of drugs on cognitive function a fear-conditioning (FC) paradigm was used after 2 weeks of treatment with CM-695 (n = 11) or vehicle (n = 10). The FC is an hippocampus-dependent test to measure long-term memory consolidation by assessing the association between two stimuli, one conditioned (context) and another unconditioned (an electric shock; Maren, 2008). The conditioning procedure was carried out in a StartFear system (Panlab S.L., Barcelona, Spain) as described previously with slight modifications (Ricobaraza et al., 2012). During training phase mice received two footshocks (0.3 mA, 2 s) separated by an interval of 30 s. After 24 h mice were returned to the conditioning chamber and freezing behavior was recorded during 2 min.

Morris Water Maze Test (MWM)

During the 3rd week of treatment, Tg2576 mice treated with CM-695 (n = 11) or vehicle (n = 10) and non-transgenic littermates (n = 10) underwent spatial reference learning and memory testing in the Morris water maze (MWM) test (Morris, 1984) as previously described (Westerman et al., 2002). In this case, the hidden-platform training (with all visible cues present) was conducted during nine consecutive days (four trials per day) and memory retention was analyzed with three probe trials at the beginning of days 4th, 7th and 9th. Four animals per groups were sacrificed for hippocampal gene expression analysis 24 h after the last probe trial and the remaining animals were maintained to perform a reversal phase of MWM after a washout period of 4-weeks. In this phase, the platform was placed in the opposite quadrant of the tank and the hidden platform training during five consecutive days (four trials per day) was performed. All cues remained in their original positions. Memory retention was analyzed in a probe at day 6. Mice were monitored by a camera mounted in the ceiling directly above the pool, and all trials were recorded using an HVS water maze program for subsequent analysis of escape latencies and percent time spent in each quadrant of the pool during probe trials (analysis program WaterMaze3, Actimetrics, Evanston, IL, USA). All experimental procedures were performed blind to groups. Animals were euthanized 24 h after the last probe.

Determination of Aβ Levels

$A\beta_{42}$ pool containing intracellular and membrane-associated $A\beta_{42}$ levels were measured in the parieto-temporal cortical extracts by using a sensitive sandwich ELISA kit (Invitrogen, Camarillo, CA, USA). Tissue was homogenized in a buffer containing SDS 2%, Tris-HCl (10 mM, pH 7.4), protease inhibitors (Complete Protease Inhibitor Cocktail, Roche) and phosphatase inhibitors (0.1 mM Na_3VO_4, 1 mM NaF). The homogenates were sonicated for 2 min and centrifuged at 100,000× *g* for 1 h. Aliquots of supernatant were directly diluted and loaded onto ELISA plates in duplicate. The assays were performed according to the manufacturer's instructions.

Affymetrix Microarray Hybridization and Data Analysis

The hippocampi were dissected and RNA was extracted with TRIzol Reagent (Invitrogen, Carlsbad, CA, USA) and purified

with the RNeasy Mini-kit (Qiagen, Hilden, Germany). RNA integrity was confirmed on Agilent RNA Nano LabChips (Agilent Technologies, Santa Clara, CA, USA). The sense cDNA was prepared from 300 ng of total RNA using the Ambion® WT Expression Kit. The sense strand cDNA was then fragmented and biotinylated with the Affymetrix GeneChip® WT Terminal Labeling Kit (PN 900671). Labeled sense cDNA was hybridized to the Affymetrix Mouse Gene 2.0 ST microarray according to the manufacturer protocols and using GeneChip® Hybridization, Wash and Stain Kit. Genechips were scanned with the Affymetrix GeneChip® Scanner 3,000. Microarray data files were submitted to the GEO (Gene Expression Omnibus) database and are available under accession number GSE128422.

Both background correction and normalization were done using RMA (Robust Multichip Average) algorithm (Irizarry et al., 2003). Then, a filtering process was performed to eliminate low expression probe sets. Applying the criterion of an expression value greater than 16 in at least three samples for each experimental condition (hippocampi from mice treated with vehicle or CM-695, with three biological replicates for condition), 22,191 probe sets were selected. R/Bioconductor (Gentleman) was used for preprocessing and statistical analysis.

First, we applied one of the most widely used methods to find out the probe sets that showed significant differential expression between experimental conditions, LIMMA (Linear Models for Microarray Data; Wettenhall and Smyth, 2004). Genes were selected as significant using p-value < 0.01 as threshold. Using False Discovery Rate (FDR) method to correct for multiple hypotheses testing no significant results was obtained.

Additional network and functional analyses were analyzed through the use of IPA (QIAGEN Inc.[1]).

Quantitative Real-Time PCR

The RNA was treated with DNase at 37°C for 30 min and reverse-transcribed into cDNA using SuperScript® III Reverse Transcriptase (Invitrogen, Carlsbad, CA, USA). Quantitative real-time PCR (QRT-PCR) was performed to quantified gene expression. All the assays were done in triplicate using Power SYBR Green PCR Master Mix (Applied Biosystems, Warrington, UK) and the corresponding specific primers for heat shock protein family A (Hsp70) member 1 A/B (HSPA1A/B; Fw: 5′-AGCCTTCCAGAAGCAGAGC-3′; Rev: 5′-GGTCGTTGGCGATGATCT-3′), 78-KDa glucose regulated protein (GRP78; Fw: 5′-ACCAACTGCTGAATCTTTGGAAT-3′; Rev: 5′-GAGCTGTGCAGAAACTCCGGCG-3′) and for the internal control 36B4 (5′-AACATCTCCCCCTTCTCCTT-3′; 5′-GAAGGCCTTGACCTTTTCAG-3′). Real-time was carried out using an ABI Prism 7300 sequence detector (Applied Biosystems, Foster City, CA, USA) and data were analyzed using the Sequence Detection software v.3.0 (Applied Biosystems, Foster City, CA, USA). The relative gene expression was calculated with reference to the control group using the DDCT method (Livak and Schmittgen, 2001).

[1]https://www.qiagenbioinformatics.com/products/ingenuity-pathway-analysis/

Dendritic Spine Density Measurement by Golgi-Cox Staining

A modified Golgi-Cox method (Glaser and Van der Loos, 1981) was used to analyze dendritic spine density. Half-brains were incubated in Golgi-Cox solution (1% potassium dichromate, 1% mercury chloride, 0.8% potassium chromate) for 48 h at RT (protected from light). The solution was then renewed and tissue was maintained there for another 3 weeks. Thereafter, brains were maintained in 90° ethanol for 30 min until being processed in 200 μm-thick coronal slices using a vibratome. The slices were incubated in 70° ethanol, reduced in 16% ammonia for 1 h and fixed in 1% sodium thiosulfate for 7 min. They were then dehydrated in an increasing alcohol graduation and mounted with DPX mountant (VWR International, Leuven, Belgium).

Spine density was determined in the secondary apical dendrites of the pyramidal cells located within the CA1 region of the hippocampus (Megías et al., 2001). Each selected neuron was captured using a Nikon Eclipse E600 light microscope and images were recorded with a digital camera (Nikon DXM 1200F) at a resolution of 1,000–1,500 dots per inch (dpi). For each mouse ($n = 3$), three dendrites of nine different neurons were used for the analysis.

Data Analysis and Statistical Procedures

The data were analyzed with SPSS for Windows, version 15.0 (SPSS, Chicago, IL, USA) and unless otherwise indicated, the data are expressed as means ± standard error of the mean (SEM). Normal distribution of data was checked by the Shapiro–Wilks test.

In the MWM, latencies to find the platform were examined by two-way repeated measures analysis of variance (ANOVA) test (genotype × trial) to compare the cognitive status in WT mice and Tg2576 mice. Likewise, the treatments effect in spatial memory was examined also by a two-way repeated measures ANOVA test (treatment × trial) followed by *post hoc* Scheffe's analysis. When two groups were compared, Student's t-test was used, whereas when more than two experimental groups were compared, one-way ANOVA followed by *post hoc* Scheffe's test was used.

RESULTS

Biological Activity

The functional activity of the chemical probe CM-695 against its targets (HDAC class I, PDE9 and HDAC6) was assessed *in vitro*, in SH-SY5Y neuroblastoma cells. These cells were exposed to CM-695 for 2 h at concentrations ranging from 1 nM to 1 μM in order to determine its effect on histone acetylation (lysine 9 of histone 3, H3K9 mark), CREB-Ser133 phosphorylation and α-tubulin acetylation by western blot analysis. There was a significant increase in α-tubulin acetylation (4.47 ± 1.36 fold change vs. control, $^*p < 0.05$, **Figure 1D**) but not of AcH3K9 (0.81 ± 0.33 fold change vs. control, **Figure 1B**) in SH-SY5Y cells exposed to CM-695 (100 nM), consistent with its selective inhibition of HDAC6 (IC50 = 40 nM) as opposed to class I HDACs (IC50 = 593 and 3530 nM for HDAC1 and HDAC2, respectively). However, CM-695 had a

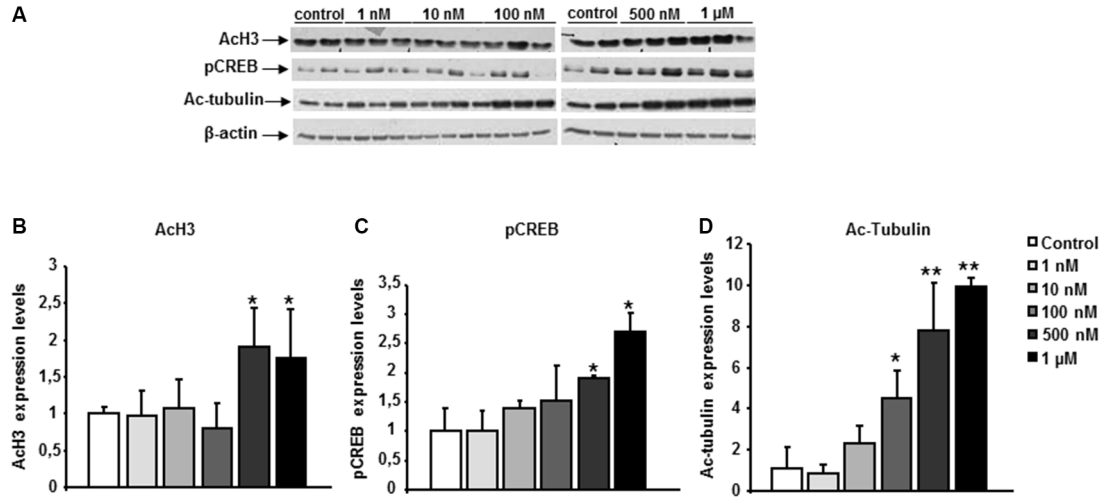

FIGURE 1 | CM-695 shows *in vitro* functional activities. **(A)** Representative bands of western blots showing histone 3 acetylation at lys 9 (AcH3K9), pCREB and Ac-Tubulin levels in SH-SY5Y cells treated with CM-695 at different concentrations (1 nM to 1 μM) for 2 h. **(B–D)** Histograms show the quantification of the immunochemically reactive bands in the western blot, $n = 3$ wells per condition, repeated in three different cultures. β-actin was used as a loading control. Data are represented as mean ± standard error of the mean (SEM) expressed as the fold change vs. vehicle; $^{*}p < 0.05$, $^{**}p < 0.01$.

significant effect on AcH3K9 at 500 nM (1.91 ± 0.56 fold change vs. control, $^{*}p < 0.05$, **Figures 1A,B**), although this effect was much stronger on tubulin acetylation (7.78 ± 2.36 fold change vs. control, $^{**}p < 0.01$, **Figures 1A,D**). In addition, at a concentration of 500 nM CM-695 significantly increased the levels of pCREB (1.91 ± 0.02 fold change vs, control, $^{*}p < 0.05$, **Figures 1A,C**), indicating this compound acts also against PDE9 (IC50 = 107 nM). These data confirmed the functional activity of this compound *in vitro* against its targets (HDAC6, PDE9 and HDAC class I).

CM-695 Ameliorates Memory Impairment in Aged Tg2576 Mice

Pharmacokinetic studies described for this compound indicated that CM-695 reached an acceptable brain concentration (around 100 nM/kg) 15 min after administering a dose of 40 mg/kg, concentrations that, according to the IC50, would ensure an effect on HDAC6 and PDE9. Furthermore, functional response in mouse brain was assessed *in vivo* in a group of animals to demonstrate the ability of the compound to inhibit HDAC and PDE9. Fifteen, 30 and 60 min after i.p. injection of 40 mg/Kg mice were sacrificed by cervical dislocation and their hippocampus were dissected. A western-blot was carried out to analyze pCREB and Ac-Tubulin in the hippocampus. As it shown in the **Supplementary Figure S2**, CM-695 increased pCREB levels at 15, 30 and 60 min. Regarding Ac-Tubulin, as basal levels of this protein are high in the brain of the animals, levels were slightly increased but no significant differences were appreciated. Likewise, a higher effect would probably be obtained with longer exposing times or in a chronic treatment. These data, demonstrated that CM-695 cross the BBB and reach the brain at a concentration which is enough to inhibit PDE9 (IC50 107 nm). Considering that HDAC6 IC50 is 40 nM and that a chronic treatment is achieved, an effect on Ac-Tubulin was assumed.

We analyzed the effects of administering CM-695 on the memory impairment in aged Tg2576 mice after a 2-week treatment (40 mg/kg, i.p. daily), assessing their performance in the fear conditioning test, a hippocampus-dependent learning task (**Supplementary Figure S3A**). Interestingly, the freezing response of Tg2576 animals was significantly ($^{*}p < 0.05$) stronger in those mice that received CM-695 (60.9% of freezing) than in those that received the vehicle alone (36.9% of freezing, **Figure 2A**). Moreover, 1 week later we evaluated the effects of CM-695 administration on learning in the MWM test (**Supplementary Figure S3B**). While the latency to find the platform was prolonged in Tg2576 mice relative to the WT mice, the escape latency was shorter when these Tg2576 mice received CM-695, although globally no significant differences were found between groups (**Figure 2B**). Interestingly, the Tg2576 mice remained significantly longer time in the target quadrant during the probe tests on days 4th (29.08 ± 4.6% vs. 18.91 ± 2.52%, $^{*}p < 0.05$), 7th (40.13 ± 5.50% vs. 24.61 ± 2.62%, $^{**}p < 0.01$) and 9th (32.18 ± 3.0% vs. 23.70 ± 2.45%, $^{*}p < 0.05$) when they received CM-695 (**Figure 2C**). To determine whether the effect of CM-695 persisted when the mice no longer received this compound, mice were re-trained in a reversal phase of the MWM test after a month wash-out, placing the platform in the opposite quadrant. The hidden platform training was carried out over 5 days (four trials per day) and it was followed by a memory retention test on day 6. No significant differences were found between the Tg2576 mice that received CM-695 or the vehicle alone in the hidden platform phase (**Figure 2D**) or in the probe trial (**Figure 2E**), indicating that none of the mice learned the platform location. Thus, it appears that the effect of CM-695 did not persist after the 4-week wash-out period.

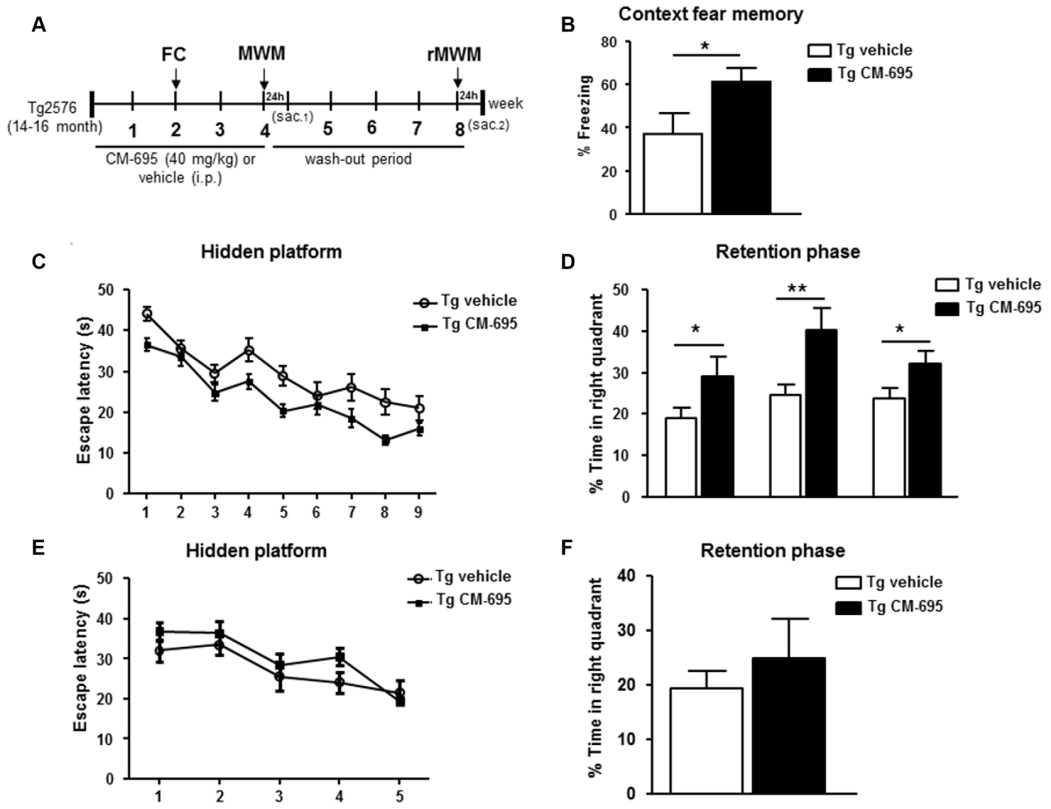

FIGURE 2 | Chronic treatment with CM-695 reversed learning deficits in aged Tg2576 mice. **(A)** Scheme showing timeline for treatment, behavioral tasks, and killing of mice. FC, fear conditioning; MWM, Morris water maze; rMWM, reversal MWM; Sac, sacrificed. **(B)** Freezing behavior from Tg2576 mice treated with vehicle (n = 10) or CM-695 (n = 11). Data represent the percentage of time of freezing during a 2 min test. **(C)** Escape latency of the hidden platform in the MWM test for the Tg2576 mice treated with vehicle (n = 10) or CM-695 (n = 11). **(D)** Percentage of time spent in correct quadrant during the probe test (days 4, 7, and 9). **(E)** Escape latency during the rMWM test for the Tg2576 mice treated with vehicle (n = 10) or CM-695 (n = 11) after the washout period. **(F)** Percentage of time spent in correct quadrant during the probe test after rMWM phase (day 6). In all figures results are expressed as mean ± SEM; $^{*}p < 0.05$, $^{**}p < 0.01$.

Taking all these results into account, it can be inferred that a chronic treatment with CM-695 ameliorated memory impairment in aged-Tg2576 mice although its effect was lost after a wash-out period of 4 weeks.

CM-695 Diminishes the Pathological Markers of AD in Aged-Tg2576 Mice

To determine the effects of CM-695 on amyloid pathology in aged-Tg2576 mice, ELISA was used to assess the $A\beta_{42}$ in parieto-temporal cortical extracts (see "Materials and Methods" section). The $A\beta_{42}$ levels were measured in two different groups of animals: one sacrificed at the end of the first MWM (after the 4th week of treatment, n = 4 per condition) and the other sacrificed at the end of the reversal-MWM (after the 4-week wash-out period in which the mice were not treated, n = 6–7 per condition). There was a significant decrease in $A\beta_{42}$ in the Tg2576 mice treated with CM-695 and sacrificed at the end of the treatment (7.70 ± 2.07, $^{**}p < 0.01$) relative to those that received the vehicle alone 17.8 ± 1.40, **Figure 3A**). Moreover, no $A\beta_{42}$ was detected in the WT littermates (data not shown). However, it was noteworthy that there was a significant decrease in the hippocampal $A\beta_{42}$ in the group of animals that was sacrificed after the 4-week wash-out period (13.33 ± 2.1, vs. 19.05 ± 2.69, $^{*}p < 0.05$, **Figure 3B**), although these differences (45% reduction) were not as strong as those observed prior to the wash-out period (56% reduction). These results suggest that a chronic treatment with CM-695 decreased amyloid pathology in elderly Tg2576 mice.

Given that Tg2576 mice display synaptic loss and dysfunction (Ricobaraza et al., 2012), we assessed whether the behavioral recovery induced by CM-695 was reflected by structural changes in dendritic spine density. Consistent with previous data, there was a significantly lower density of apical dendrites on CA1 pyramidal neurons in Tg2576 mice than in WT mice (**Supplementary Figure S4**). Taking into account the behavioral data obtained at the end of the treatment (**Figure 2**), we assumed that they could correlate with an increase in the density of dendritic spines in the treated animals, thus, we analyzed if the effect was maintained after 4 weeks without treatment as we observed for CM-414. However, when the mice were analyzed after the wash-out period, those that received CM-695 did not show any significant change in the density of spines on these neurons. It should be noted that there was a tendency to increase the density of spines that might account for the memory

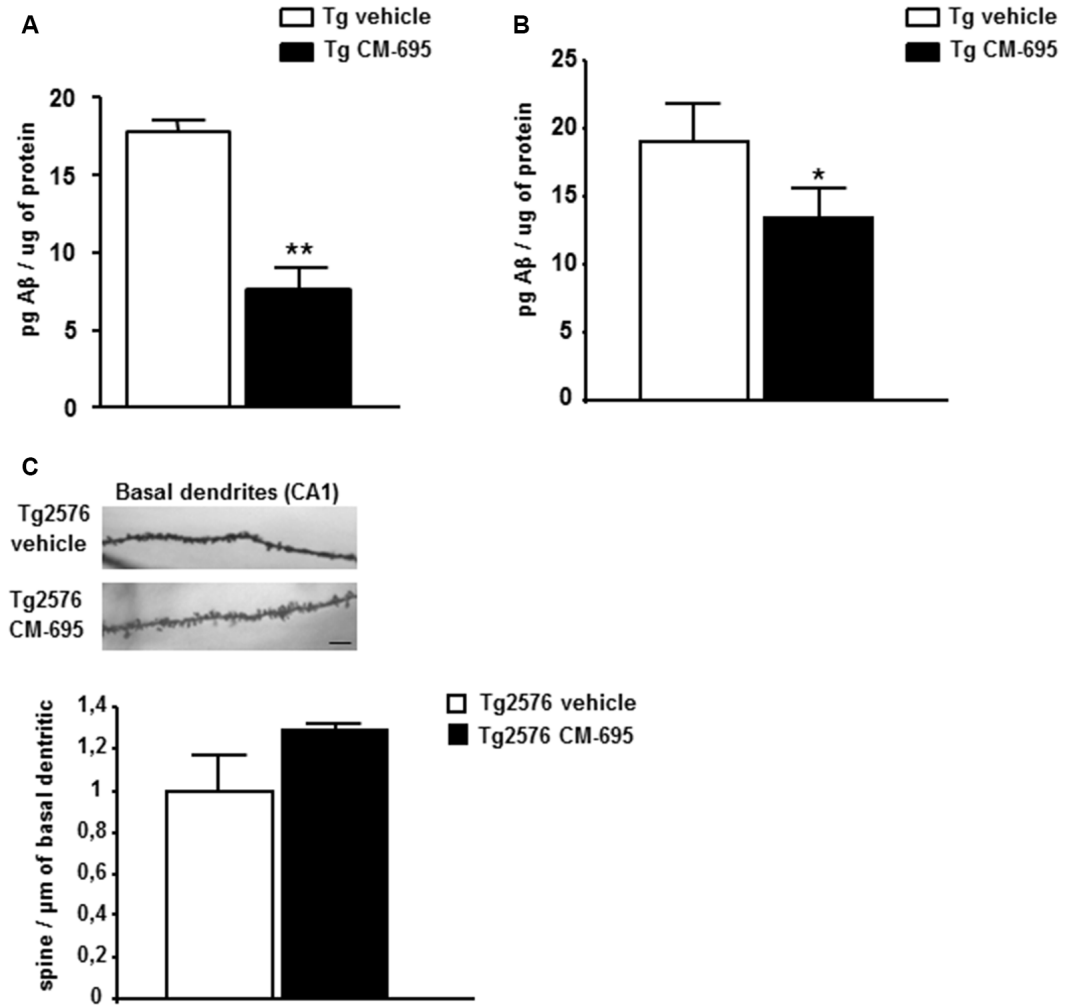

FIGURE 3 | Chronic treatment with CM-695 decreased amyloid levels but did not affect hippocampal dendritic spine density. $A\beta_{42}$ levels determined by ELISA in SDS hippocampal tissue extracts of Tg2576 mice treated with vehicle or CM-695 after 4 week of treatment ($n = 4$; **A**) or after a washout period of 4 weeks ($n = 6$–7). **(B)** $^{*}p < 0.05$, $^{**}p < 0.01$. **(C)** Representative Golgi staining images of the apical dendrites on CA1 hippocampal pyramidal neurons. Scale bar, 10 μm. The histograms represent the quantification of spine density of basal dendrites of hippocampal CA1 pyramidal neurons from Tg2576 mice treated with vehicle or CM-695 ($n = 34$–36 neurons from three animals per group).

improvement observed 4-weeks after treatment (**Figure 3C**). Nevertheless, after the wash-out period neither the effect on memory function nor the potential changes in dendritic spine density persisted.

To explore the mechanisms underlying the effect of CM-695 on amyloid pathology and on memory function, we analyzed the effects of CM-695 on gene expression in the hippocampus of Tg2576 mice compared to a group of transgenic animals receiving vehicle using Affymetrix microarrays. LIMMA was applied to find out the probe sets that showed significant differential expression between experimental conditions (Smyth, 2004). Genes were selected as significant using $p < 0.01$ as threshold. Differentially expressed genes were analyzed by using Ingenuity Pathways Analysis in order to gain information about the mechanistic approach of CM-695 therapeutic effect. Importantly, the Protein Ubiquitination Pathway (p-value = 6.76, E-05) and the Unfolded protein response (UPR, p-value = 3.1, E-05) were included among the top-ranked canonical pathways (**Figure 4A**) and more specifically, BIP (GRP78) and HSPA1A/B were among the genes overexpressed in the hippocampus of mice administered with CM-695 respect to the mice receiving vehicle (**Supplementary Figure S5**). In accordance, when differentially expressed genes were also categorized to diseases and biological functions "folding protein" (p-value and molecules) was significantly regulated (**Figure 4B**). Since chaperone activity plays a crucial role in proper protein folding activity, we analyzed the expression of GRP78 and HSPA1A/B by quantitative real time PCR. Accordingly to the results obtained in the array, a significant ($p < 0.01$) increase was observed in both GRP78 and HSPA1A/B mRNA levels in the hippocampus of CM-695 treated mice respect to mice receiving vehicle (**Figure 4C**). Next, we checked

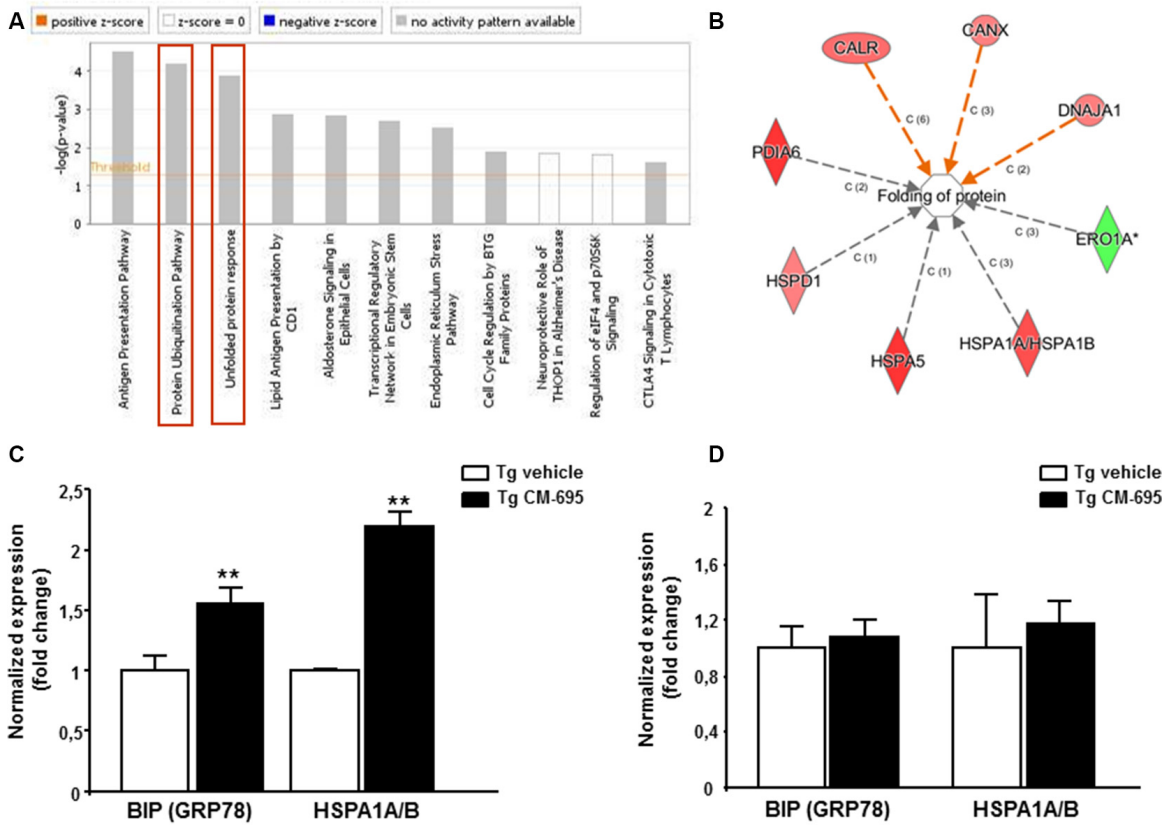

FIGURE 4 | Chronic treatment with CM-695 significantly increases chaperones: GRP78 and HSP70. **(A)** Ingenuity pathway analysis showing the most highly scoring canonical pathways (according to *p*-value). Horizontal orange line running through the bars is the threshold for *p*-value for these pathways. Color coding for positive and negative *z*-score and for pathways with no activity pattern available are shown in the figure. "Protein Ubiquitination Pathway" and the "Unfolded protein response" (remarked with a red box) were included among the top-ranked canonical pathways. **(B)** Network of differentially expressed genes categorized in Ingenuity by Disease and biological functions. **(C,D)** Quantitative RT-PCR (QRT-PCR) analysis of BIP (GRP78) and HSPA1A/B mRNA in the hippocampus of CM-695 treated mice vs. vehicle, 4 weeks after treatment (**C**, $n = 4$) and after the washout period respectively (**D**, $n = 6$–7). Bars represent the fold change (mean ± SEM) in gene expression normalized to vehicle-treated mice; $^{**}p < 0.01$.

if this effect in gene expression was maintained after the washout period. As depicted in **Figure 4D**, animals receiving CM-695 and sacrificed after a 4-weeks wash out period showed similar expression levels of GRP78 and HSPA1A/B to control group.

These results suggest that the increase in the levels of chaperones GRP78 and Hsp70, which are involved in protein folding, may underlie the improvement in AD symptoms observed after daily administration of the compound.

DISCUSSION

Given the high failure rate in AD drug development, with no new drug having been approved for this diseases since 2003 (Cummings et al., 2014), it is clearly necessary to change the way we approach the search for new AD targets to improve the results obtained in clinical trials. We have identified a NCE, CM-695, that has potential therapeutic effects in a well-established mouse model of AD. CM-695 is a potent HDAC6 and PDE9 inhibitor that, after chronic administration, ameliorates the cognitive impairment and amyloid pathology evident in aged-Tg2576 mice. An increase in the expression of the chaperones GRP78 and Hsp70, involved in protein folding, may underlie the improvement in AD symptoms observed after daily administration of the compound. The benefits obtained with this dual inhibitor are not maintained when the compound is no longer administered. Thus, CM-695 appears to be a safe and efficient disease-modifying agent for AD treatment, confirming that multi-target therapies may represent better options for the treatment of complex diseases.

HDACs are emerging targets for the treatment of AD (Yang et al., 2017). The inhibition of HDAC class I facilitates gene transcription and the formation of new synapses (Rumbaugh et al., 2015). The inhibition of HDAC class IIb (HDAC6), by targeting cytoplasmic proteins is involved in the clearance of misfolding proteins (Sung et al., 2013). The inhibition of both isoforms could be a promising and synergistic therapy to treat AD, which has been demonstrated by using pan-HDAC inhibitors. However, these compounds have unfavorable side effects when administered chronologically and at a dose

sufficient to reach the brain at appropriate concentrations. One strategy to reduce toxicity while maintaining effectiveness is to obtain new disease-modifying molecules maintaining HDAC inhibition combined with an additional function such as inhibition of PDEs, inhibition of glycogen synthase kinase 3β or antioxidant activity (De Simone and Milelli, 2019).

Based on the results obtained previously with different selectivity profiles of HDAC and PDE inhibitors (Rabal et al., 2016, 2018, 2019; Cuadrado-Tejedor et al., 2017; Sánchez-Arias et al., 2017), we designed a new series of PDE9 inhibitors that more specifically target HDAC6 over class I HDAC isoforms. This shift in specificity aimed to reduce the toxicity associated with class I inhibition which complicates the further therapeutic development of the new compound. Furthermore, since PDE inhibitors have pro-cognitive and neuroprotective effects, the inhibition of PDE9 was selected rather than PDE5 as its brain expression and affinity for cGMP is higher than that of other PDEs (**Supplementary Figure S1**, Andreeva et al., 2001; Singh and Patra, 2014). Among the new compounds designed, CM-695 was tested in AD model following the same guidelines used with CM-414 (Cuadrado-Tejedor et al., 2017), in order to compare the efficacy between the two compounds. The therapeutic effects obtained after chronic treatment with CM-695 were similar to those obtained with CM-414, except that the effect did not persist when the drug was no longer administered. Taking into account the differences in the inhibition profile of the two compounds, we confirm that the inhibition of class I HDACs, and more specifically HDAC2, plays an important role in maintaining memory function.

Interestingly, the effect of CM-695 on Aβ clearance is maintained, which may be mediated by the inhibition of HDAC6 (Boyault et al., 2007). One of the targets of HDAC6 is heat-shock protein 90 (Hsp90). As such, the inhibition of HDAC6 increases Hsp90 acetylation, releasing its client proteins like heat shock transcription factor 1 (HSF1), which in turn translocates to the nucleus and mediates the transcription of HSPA1A/B genes, and ultimately, Hsp70 (Wang et al., 2014). HSPA1A/B was among the genes overexpressed in the Affymetrix microarray analysis and validated by qRT-PCR in the hippocampus of mice administered CM-695. Significantly, a similar induction was induced by CM-695 in a model of thrombosis (Allende et al., 2017). Hsp70 fulfills a neuroprotective role in AD by decreasing the oligomerization and production of toxic Aβ isoforms, and by increasing its degradation (Magrané et al., 2004; Muchowski and Wacker, 2005; Kumar et al., 2007). Interestingly, Hsp70 upregulation by inhibiting Hsp90 was also proposed as a mechanism to normalize synaptic transmission in a transgenic model of tau aggregation (Thirstrup et al., 2016). These results suggest that the increase in Hsp70 expression observed at the end of treatment is at least partially responsible for the marked decrease in hippocampal Aβ levels observed. Together with PDE9 inhibition, this increase in Hsp70 may help restore learning ability. However, Hsp70 was no longer upregulated 4 weeks after the end of the treatment, causing a loss in Aβ clearance and a deterioration of the animals learning capacity. Considering the safe profile of CM-695, chronic treatment with no need for wash-out periods could be an option to consider for this NCE.

In conjunction, it seems that CM-695 is a safe and efficient disease-modifying agent to treat AD, confirming that multitarget therapies may provide good options to combat AD, as seen in other multifactorial diseases like cancer or AIDS.

DATA AVAILABILITY

The raw data supporting the conclusions of this manuscript will be made available by the authors, without undue reservation, to any qualified researcher.

ETHICS STATEMENT

All procedures were carried out in agreement with the European and Spanish regulations (2010/63/EU; RD1201/2005), and the study was approved by the Ethical Committee for the Animal Experimentation of the University of Navarra.

AUTHOR CONTRIBUTIONS

AG-O, MC-T and JO conceived the general framework of this study, designed experiments and discuss results. MP-G, CG-M, DM and CG-B performed the *in vitro* functional assays in cell culture, treatments, behavioral experiments and biochemical assays. JS-A performed biochemical experiments related to CM-695 compound *in vitro*. VS performed the bioinformatic analysis of the microarrays. OR and JO designed and characterized CM-695. AG-O and MC-T wrote the manuscript.

FUNDING

This work was supported by grants from FIS projects (11/02861 and 14/01244). We also thank the Foundation for Applied Medical Research, University of Navarra (Pamplona, Spain) as well as Fundación Fuentes Dutor for financial support and the Asociación de Amigos of University of Navarra for the grant to MP-G.

ACKNOWLEDGMENTS

We thank Maria Espelosin and Susana Ursua for their work in the animal facility and cell culture.

SUPPLEMENTARY MATERIAL

The Supplementary Material for this article can be found online at: https://www.frontiersin.org/articles/10.3389/fnagi.2019.00149/full#supplementary-material

REFERENCES

Allende, M., Molina, E., Lecumberri, R., Sánchez-Arias, J., Ugarte, A., Guruceaga, E., et al. (2017). Inducing heat shock protein 70 expression provides a robust anti-thrombotic effect with minimal bleeding risk. *Thromb. Haemost.* 117, 1722–1729. doi: 10.1160/th17-02-0108

Andreeva, S. G., Dikkes, P., Epstein, P. M., and Rosenberg, P. A. (2001). Expression of CGMP-specific phosphodiesterase 9A MRNA in the rat brain. *J. Neurosci.* 21, 9068–9076. doi: 10.1523/JNEUROSCI.21-22-09068.2001

Boyault, C., Zhang, Y., Fritah, S., Caron, C., Gilquin, B., So, H. K., et al. (2007). HDAC6 controls major cell response pathways to cytotoxic accumulation of protein aggregates. *Genes Dev.* 21, 2172–2181. doi: 10.1101/gad.436407

Cameron, R. T., Whiteley, E., Day, J. P., Parachikova, A. I., and Baillie, G. S. (2017). Selective inhibition of phosphodiesterases 4, 5 and 9 induces HSP20 phosphorylation and attenuates amyloid β 1–42-mediated cytotoxicity. *FEBS Open Bio* 7, 64–73. doi: 10.1002/2211-5463.12156

Chapman, P. F., White, G. L., Jones, M. W., Cooper-Blacketer, D., Marshall, V. J., Irizarry, M., et al. (1999). Impaired synaptic plasticity and learning in aged amyloid precursor protein transgenic mice. *Nat. Neurosci.* 2, 271–276. doi: 10.1038/6374

Cook, C., Gendron, T. F., Scheffel, K., Carlomagno, Y., Dunmore, J., DeTure, M., et al. (2012). Loss of HDAC6, a novel CHIP substrate, alleviates abnormal tau accumulation. *Hum. Mol. Genet.* 21, 2936–2945. doi: 10.1093/hmg/dds125

Cuadrado-Tejedor, M., Garcia-Barroso, C., Sanzhez-Arias, J., Mederos, S., Rabal, O., Ugarte, A., et al. (2015). Concomitant histone deacetylase and phosphodiesterase 5 inhibition synergistically prevents the disruption in synaptic plasticity and it reverses cognitive impairment in a mouse model of Alzheimer's disease. *Clin. Epigenetics* 7:108. doi: 10.1186/s13148-015-0142-9

Cuadrado-Tejedor, M., Garcia-Barroso, C., Sánchez-Arias, J. A., Rabal, O., Pérez-González, M., Mederos, S., et al. (2017). A first-in-class small-molecule that acts as a dual inhibitor of HDAC and PDE5 and that rescues hippocampal synaptic impairment in Alzheimer's disease mice. *Neuropsychopharmacology* 42, 524–539. doi: 10.1038/npp.2016.163

Cummings, J., Lee, G., Ritter, A., and Zhong, K. (2018). Alzheimer's disease drug development pipeline: 2018. *Alzheimers Dement.* 4, 195–214. doi: 10.1016/j.trci.2018.03.009

Cummings, J. L., Morstorf, T., and Zhong, K. (2014). Alzheimer's disease drug-development pipeline: few candidates, frequent failures. *Alzheimers Res. Ther.* 6:37. doi: 10.1186/alzrt269

De Simone, A., and Milelli, A. (2019). Histone deacetylase inhibitors as multitarget ligands: new players in Alzheimer's disease drug discovery? *ChemMedChem* 14, 1067–1073. doi: 10.1002/cmdc.201900174

Ding, H., Dolan, P. J., and Johnson, G. V. W. (2008). Histone deacetylase 6 interacts with the microtubule-associated protein tau. *J. Neurochem.* 106, 2119–2130. doi: 10.1111/j.1471-4159.2008.05564.x

Frölich, L., Wunderlich, G., Thamer, C., Roehrle, M., Garcia, M., and Dubois, B. (2019). Evaluation of the efficacy, safety and tolerability of orally administered BI 409306, a novel phosphodiesterase type 9 inhibitor, in two randomised controlled phase II studies in patients with prodromal and mild Alzheimer's disease. *Alzheimers Res. Ther.* 11:18. doi: 10.1186/s13195-019-0467-2

Fuller, N. O., Pirone, A., Lynch, B. A., Hewitt, M. C., Quinton, M. S., McKee, T. D., et al. (2019). CoREST complex-selective histone deacetylase inhibitors show prosynaptic effects and an improved safety profile to enable treatment of synaptopathies. *ACS Chem. Neurosci.* 10, 1729–1743. doi: 10.1021/acschemneuro.8b00620

García-Osta, A., Cuadrado-Tejedor, M., García-Barroso, C., Oyarzábal, J., and Franco, R. (2012). Phosphodiesterases as therapeutic targets for Alzheimer's disease. *ACS Chem. Neurosci.* 3, 832–844. doi: 10.1021/cn3000907

Glaser, E. M., and Van der Loos, H. (1981). Analysis of thick brain sections by obverse—reverse computer microscopy: application of a new, high clarity golgi—nissl stain. *J. Neurosci. Methods* 4, 117–125. doi: 10.1016/0165-0270(81)90045-5

Guan, J.-S., Haggarty, S. J., Giacometti, E., Dannenberg, J.-H., Joseph, N., Gao, J., et al. (2009). HDAC2 negatively regulates memory formation and synaptic plasticity. *Nature* 459, 55–60. doi: 10.1038/nature07925

Guo, W., Naujock, M., Fumagalli, L., Vandoorne, T., Baatsen, P., Boon, R., et al. (2017). HDAC6 inhibition reverses axonal transport defects in motor neurons derived from FUS-ALS patients. *Nat. Commun.* 8:861. doi: 10.1038/s41467-017-00911-y

Heckman, P. R. A., Blokland, A., and Prickaerts, J. (2017). "From age-related cognitive decline to Alzheimer's disease: a translational overview of the potential role for phosphodiesterases," in *Phosphodiesterases: CNS Functions and Diseases. Advances in Neurobiology*, (Vol. 17) eds H. T. Zhang, Y. Xu and J. O'Donnell (Cham: Springer), 135–168.

Hsiao, K., Chapman, P., Nilsen, S., Eckman, C., Harigaya, Y., Younkin, S., et al. (1996). Correlative memory deficits, aβ elevation, and amyloid plaques in transgenic mice. *Science* 274, 99–102. doi: 10.1126/science.274.5284.99

Hubbert, C., Guardiola, A., Shao, R., Kawaguchi, Y., Ito, A., Nixon, A., et al. (2002). HDAC6 is a microtubule-associated deacetylase. *Nature* 417, 455–458. doi: 10.1038/417455a

Irizarry, R. A., Bolstad, B. M., Collin, F., Cope, L. M., Hobbs, B., and Speed, T. P. (2003). Summaries of affymetrix GeneChip probe level data. *Nucleic Acids Res.* 31:e15. doi: 10.1093/nar/gng015

Kim, C., Choi, H., Jung, E. S., Lee, W., Oh, S., Jeon, N. L., et al. (2012). HDAC6 inhibitor blocks amyloid β-induced impairment of mitochondrial transport in hippocampal neurons. *PLoS One* 7:e42983. doi: 10.1371/journal.pone.0042983

Kumar, P., Ambasta, R. K., Veereshwarayya, V., Rosen, K. M., Kosik, K. S., Band, H., et al. (2007). CHIP and HSPs interact with β-APP in a proteasome-dependent manner and influence Aβ metabolism. *Hum. Mol. Genet.* 16, 848–864. doi: 10.1093/hmg/ddm030

Livak, K. J., and Schmittgen, T. D. (2001). Analysis of relative gene expression data using real-time quantitative PCR and the 2(-Delta Delta C(T)) Method. *Methods* 4, 402–408. doi: 10.1006/meth.2001.1262

Magrané, J., Smith, R. C., Walsh, K., and Querfurth, H. W. (2004). Heat shock protein 70 participates in the neuroprotective response to intracellularly expressed -amyloid in neurons. *J. Neurosci.* 24, 1700–1706. doi: 10.1523/JNEUROSCI.4330-03.2004

Mahady, L., Nadeem, M., Malek-Ahmadi, M., Chen, K., Perez, S. E., and Mufson, E. J. (2019). HDAC2 dysregulation in the nucleus basalis of meynert during the progression of Alzheimer's disease. *Neuropathol. Appl. Neurobiol.* 45, 380–397. doi: 10.1111/nan.12518

Maren, S. (2008). Pavlovian fear conditioning as a behavioral assay for hippocampus and amygdala function: cautions and caveats. *Eur. J. Neurosci.* 28, 1661–1666. doi: 10.1111/j.1460-9568.2008.06485.x

Megías, M., Emri, Z., Freund, T. F., and Gulyás, A. I. (2001). Total number and distribution of inhibitory and excitatory synapses on hippocampal CA1 pyramidal cells. *Neuroscience* 102, 527–540. doi: 10.1016/s0306-4522(00)00496-6

Morris, R. (1984). Developments of a water-maze procedure for studying spatial learning in the rat. *J. Neurosci. Methods* 11, 47–60. doi: 10.1016/0165-0270(84)90007-4

Muchowski, P. J., and Wacker, J. L. (2005). Modulation of neurodegeneration by molecular chaperones. *Nat. Rev. Neurosci.* 6, 11–22. doi: 10.1038/nrn1587

Rabal, O., Sánchez-Arias, J. A., Cuadrado-Tejedor, M., de Miguel, I., Pérez-González, M., García-Barroso, C., et al. (2016). Design, synthesis, and biological evaluation of first-in-class dual acting histone deacetylases (HDACs) and phosphodiesterase 5 (PDE5) inhibitors for the treatment of Alzheimer's disease. *J. Med. Chem.* 59, 8967–9004. doi: 10.1021/acs.jmedchem.6b00908

Rabal, O., Sánchez-Arias, J. A., Cuadrado-Tejedor, M., de Miguel, I., Pérez-González, M., García-Barroso, C., et al. (2018). Design, synthesis, biological evaluation and *in vivo* testing of dual phosphodiesterase 5 (PDE5) and histone deacetylase 6 (HDAC6)-selective inhibitors for the treatment of Alzheimer's disease. *Eur. J. Med. Chem.* 150, 506–524. doi: 10.1016/j.ejmech.2018.03.005

Rabal, O., Sánchez-Arias, J. A., Cuadrado-Tejedor, M., de Miguel, I., Pérez-González, M., García-Barroso, C., et al. (2019). Discovery of *in vivo* chemical probes for treating Alzheimer's disease: dual phosphodiesterase 5 (PDE5) and class I histone deacetylase selective inhibitors. *ACS Chem. Neurosci.* 10, 1765–1782. doi: 10.1021/acschemneuro.8b00648

Ricobaraza, A., Cuadrado-Tejedor, M., Marco, S., Pérez-Otaño, I., and García-Osta, A. (2012). Phenylbutyrate rescues dendritic spine loss associated with memory deficits in a mouse model of Alzheimer disease. *Hippocampus* 22, 1040–1050. doi: 10.1002/hipo.20883

Rumbaugh, G., Sillivan, S. E., Ozkan, E. D., Rojas, C. S., Hubbs, C. R., Aceti, M., et al. (2015). Pharmacological selectivity within class I histone deacetylases predicts effects on synaptic function and memory rescue. *Neuropsychopharmacology* 40, 2307–2316. doi: 10.1038/npp.2015.93

Sánchez-Arias, J. A., Rabal, O., Cuadrado-Tejedor, M., de Miguel, I., Pérez-González, M., Ugarte, A., et al. (2017). Impact of scaffold exploration on novel dual-acting histone deacetylases and phosphodiesterase 5 inhibitors for the treatment of Alzheimer's disease. *ACS Chem. Neurosci.* 8, 638–661. doi: 10.1021/acschemneuro.6b00370

Schwam, E. M., Nicholas, T., Chew, R., Billing, C. B., Davidson, W., Ambrose, D., et al. (2014). A multicenter, double-blind, placebo-controlled trial of the PDE9A inhibitor, PF-04447943, in Alzheimer's disease. *Curr. Alzheimer Res.* 11, 413–421. doi: 10.2174/1567205011666140505100858

Singh, N., and Patra, S. (2014). Phosphodiesterase 9: insights from protein structure and role in therapeutics. *Life Sci.* 106, 1–11. doi: 10.1016/j.lfs.2014.04.007

Singh, P., and Thakur, M. K. (2018). Histone deacetylase 2 inhibition attenuates downregulation of hippocampal plasticity gene expression during aging. *Mol. Neurobiol.* 55, 2432–2442. doi: 10.1007/s12035-017-0490-x

Smyth, G. K. (2004). Linear models and empirical bayes methods for assessing differential expression in microarray experiments. *Stat. Appl. Genet. Mol. Biol.* 3:3. doi: 10.2202/1544-6115.1027

Subramanian, S., Bates, S. E., Wright, J. J., Espinoza-Delgado, I., and Piekarz, R. L. (2010). Clinical toxicities of histone deacetylase inhibitors. *Pharmaceuticals* 3, 2751–2767. doi: 10.3390/ph3092751

Sung, Y. M., Lee, T., Yoon, H., DiBattista, A. M., Song, J. M., Sohn, Y., et al. (2013). Mercaptoacetamide-based class II HDAC inhibitor lowers Aβ levels and improves learning and memory in a mouse model of Alzheimer's disease. *Exp. Neurol.* 239, 192–201. doi: 10.1016/j.expneurol.2012.10.005

Thirstrup, K., Sotty, F., Pereira Montezinho, L. C., Badolo, L., Thougaard, A., Kristjánsson, M., et al. (2016). Linking HSP90 target occupancy to HSP70 induction and efficacy in mouse brain. *Pharmacol. Res.* 104, 197–205. doi: 10.1016/j.phrs.2015.12.028

Ugarte, A., Gil-Bea, F., García-Barroso, C., Cedazo-Minguez, Á., Javier Ramírez, M., Franco, R., et al. (2015). Decreased levels of guanosine 3′,5′-monophosphate (CGMP) in cerebrospinal fluid (CSF) are associated with cognitive decline and amyloid pathology in Alzheimer's disease. *Neuropathol. Appl. Neurobiol.* 41, 471–482. doi: 10.1111/nan.12203

Wang, H., Tan, M. S., Lu, R. C., Yu, J. T., and Tan, L. (2014). Heat shock proteins at the crossroads between cancer and Alzheimer's disease. *Biomed. Res. Int.* 2014:239164. doi: 10.1155/2014/239164

Westerman, M. A., Cooper-Blacketer, D., Mariash, A., Kotilinek, L., Kawarabayashi, T., Younkin, L. H., et al. (2002). The relationship between aβ and memory in the Tg2576 mouse model of Alzheimer's disease. *J. Neurosci.* 22, 1858–1867. doi: 10.1523/JNEUROSCI.22-05-01858.2002

Wettenhall, J. M., and Smyth, G. K. (2004). LimmaGUI: a graphical user interface for linear modeling of microarray data. *Bioinformatics* 20, 3705–3706. doi: 10.1093/bioinformatics/bth449

Yang, S.-S., Zhang, R., Wang, G., and Zhang, Y.-F. (2017). The development prospection of HDAC inhibitors as a potential therapeutic direction in Alzheimer's disease. *Transl. Neurodegener.* 6:19. doi: 10.1186/s40035-017-0089-1

Zhang, L., Liu, C., Wu, J., Tao, J.-J., Sui, X.-L., Yao, Z.-G., et al. (2014). Tubastatin A/ACY-1215 improves cognition in Alzheimer's disease transgenic mice. *J. Alzheimers Dis.* 41, 1193–1205. doi: 10.3233/jad-140066

Conflict of Interest Statement: The authors declare that the research was conducted in the absence of any commercial or financial relationships that could be construed as a potential conflict of interest.